Reviews

Spintronics and spintronics materials

V. A. Ivanov,[a]★ T. G. Aminov,[a] V. M. Novotortsev,[a] and V. T. Kalinnikov[b]

[a]N. S. Kurnakov Institute of General and Inorganic Chemistry, Russian Academy of Sciences, 31 Leninsky prosp., 119991 Moscow, Russian Federation. Fax: +7 (095) 954 1279. E-mail: vmnov@igic.ras.ru, aminov@igic.ras.ru, ivanov@ostrov.net
[b]I. V. Tananaev Institute of Chemistry and Technology of Rare Elements and Mineral Raw Materials, Kola Research Center of the Russian Academy of Sciences, 14 ul. Fersmana, 184209 Apatity, Murmansk Region, Russian Federation. Fax: +7 (815 55) 7 9414. E-mail: office@chemy.kolasc.net.ru

The review concerns the fundamentals of spintronics (spin-transport electronics). The material covers spin-spin interactions and spin relaxation in semiconductors as well as spin and spin injection related effects in the condensed matter. Examples of promising spintronic devices are given, requirements for spintronic materials are formulated, methods of synthesis of spintronic materials are described, and the physicochemical properties of some materials are characterized. Organic spintronic materials are briefly outlined and the state-of-the-art in the field of research on inhomogeneous magnetic semiconducting materials possessing high-temperature ferromagnetism is described. The emphasis is placed on the chemical bonding and electronic structure of magnetic impurities in semiconductors, consideration of the nature of ferromagnetism, and on the character of exchange interactions between localized spins in novel spintronic materials.

Key words: spintronics, spin-transport electronics, ferromagnetic semiconductors, dilute magnetic semiconductors, semimagnetic semiconductors, magnetic materials.

Introduction

Spintronics is a new, quickly developing field of science and technology, which deals with relationhips responsible for specific features of the spin interactions in metals, semiconductors doped with transition or rare-earth elements, and heterostructures that ensure unique properties of these materials.*

The main avenues of the development of spintronics are (i) fabrication of magnetic nanostructures including novel materials, thin films, heterostructures, and multifunctional materials; (ii) research on magnetism and spin control of magnetic nanostructures, theory of ferromagnetic exchange in dilute magnetic semiconductors (DMS), tunneling effects and spin injection, ans spin transport and detection of magnetism; (iii) magnetoelectronics and

* The term spintronics was proposed in 1998 in a joint press release of Bell Labs and Yale University (USA), which defined the problem of design of devices for information storage by manipulating atoms of matter using electron spin encoded bits. Researchers at the Defence Advanced Research Project Agency (DARPA, USA) defined spintronics as spin-transport electronics. Some other definitions of spintronics are as follows: this is (i) a science for which mutually consistent behavior of the electron charge and electron spin is of crucial importance;[1] (ii) "electron spin based electronics, in which information is transmitted by employing the electron spin rather than electron charge, which creates prerequisites for design of a new generation of devices that combine conventional microelectronics and spin-dependent effects";[2] (iii) a "science of manipulation of electric current in semiconductors and heterostructures by changing electron and nuclear spin orientationss in magnetic and electric fields";[3] and (iv) a "new branch of microelectronics where the electron spin and electron charge act as an active element for information storage and transmission, for integrated circuits and functional chips, multifunctional magneto-opto-electronic devices».

Published in Russian in *Izvestiya Akademii Nauk. Seriya Khimicheskaya,* No. 11, pp. 2255—2303, November, 2004.

1066-5285/04/5311-2357

devices employing the giant magnetoresistance (GMR) effect,[4,5] tunneling devices, semiconductor heterostructures for spin injection, spin transport and detection, and pulsed ferromagnetism; (iv) magneto-optical properties of dc magnetic semiconductor heterostructures and time-resolved experiments, optical spin injection and detection, optically induced ferromagnetism, ultrafast magneto-optic switches; and quantum information transmission; (v) pattern recognition; imaging and metrology including magnetic pattern recognition and anomalous Hall effect; and (vi) instrument engineering and applied studies.

Semiconductor spintronics is a science dealing with the coexistence of the charge and spin degrees of freedom in doped semiconductors and nanostructures, the nature of ferromagnetism in and methods of synthesis of these materials, and fabrication of devices employing the spin characteristics in semiconductors.

Magnetic semiconductors were obtained after the discovery of materials based on type III—V matrices (mainly (Ga,Mn)As) because they not only retain the semiconducting properties but acquire the ferromagnetic properties, being lightly doped with magnetic impurities. From this viewpoint the known magnetic semiconductors (chalcogenides of rare-earth metals, magnetic chalcospinels) would be well to call semiconducting magnets because these compounds (in the case of with stoichiometric compositions) are ferromagnets with intrinsic magnetic sublattices.

Synthesis of the type (III,Mn)V DMS, namely, (In,Mn)As alloys[6—8] and (In,Mn)As/(Ga,Al)Sb heterostructures[9] was basic to the breakthrough in technology of preparation of novel ferromagnetic semiconductors with high Curie temperatures (T_C).

At present, to distinguish between the DMS* which have mostly diamagnetic matrices and conventional magnetic semiconductors, the latter are called concentrated magnetic semiconductors (CMS). Doping them with other elements cannot cause significant changes in those intrinsic physicochemical characteristics of CMS that differ from the properties of the known semiconductors. At the same time, distinctions between the crystal lattices of CMS and the known semiconductors imposes severe restrictions on the possibility for CMS to be used in semiconductor devices.

It is assumed that spintronic devices will employ nonequilibrium spin density created in semiconductors, manipulation of spin orientations by external fields, and detection of the spin state thus formed.[10] In relation to relaxation processes, degradation mechanisms are of importance for spintronics (and microelectronics). However, spin currents induce a much lower degradation of integrated circuits compared to electric currents capable of inducing rearrangement of the atomic structure of integrated circuits at high current densities. Therefore, spintronic devices can act as counterparts or in some cases be used instead of conventional electronic devices.

If traditional electronics employs the charge degrees of freedom of substances, spintronics deals with the spin (magnetic) characteristics of materials. In contrast to electronic devices, spintronic devices employ the dependence of transfer of the current carriers on the electron spin orientation. A specific feature of spintronics is the joint action of the electron charge and electron spin; the smaller the object, the more pronounced the effect. A magnetic field induced electron spin-flip requires a much lower energy and occurs faster than the displacement of electron charges by an electric field. Therefore, one can expect that manipulation of spin states will permit in the future fabrication of ultrasmall logic elements and ultrafast computer chips of high information capacity and low power consumption. The subject of nanospintronics[11,12] is research on the behavior of spins in mesoscopic systems and on the indirect spin interactions in nanoparticles that has been poorly studied as yet. Engineering spintronics employs the spin degrees of freedom of the metals used in computer engineering (hard disks and MRAM chips for personal computers). At present, fabrication of semiconductor structures doped with magnetic impurities is placed on the agenda. The electronic structure of such materials is determined by the chemical bonds while the magnetic structure is governed by strong interactions between electrons of the transition metal or rare-earth metal (REM) impurity atoms.

Yet another aspect of computer engineering can also be related to spintronics. The case in point is that operation of computers in the binary number system requires two fast switchable states corresponding to "0" and "1" that must be stable in time and resistant to thermal fluctuations. These functions could be operated by an electron in a two-level system (*e.g.*, a diatomic molecule) by hopping between atoms. At present, hundreds and thousands of electrons per operation are "consumed" in electronic devices. Quantization of electron spin (with conventional "spin up" and "spin down" orientations) indicates that the spin is a natural logic cell with two states corresponding to "1" and "0". In this case, a logic operation can be encoded using a single electron. Therefore, the use of electron spin is much more beneficial compared to the electron charge.

Intensive basic research into the physical and chemical processes in solids with allowance for the spin degrees of freedom was carried out by researchers working in domestic institutes before introducing the term "spintronics" (see, *e.g.*, Refs. 13—31). Considerable advances have been

* In this review the terms "dilute magnetic semiconductors" and "high-temperature ferromagnetic semiconductors" cover novel magnetic semiconductors; the discovery of these materials gave rise to a new branch of science and technology, a new branch of electronics, that is, spintronics.

made in molecular design (including proteins and spin systems), design of molecule-based ferromagnets;[32] and investigations of the chemical, electrical, and magnetic properties of nanoclusters, nanotubes, and nanowires.[33] It was established that the spin dynamics is quickly responsive to the molecular dynamics of an elementary chemical act.[26] Spin chemistry emerged, which studies nuclear-spin related spintronic effects[27] and has some features in common with nuclear spintronics that is in the early stage of development.

The available reviews mainly concern new effects and applications of spintronic devices,[34,35] ferromagnetic alloys which have found some practical applications, and some novel materials with the spin degrees of freedom.[36—47] Some avenues of progress in spintronics have been elucidated.[48—55] Coexistence of the spin and charge, the ferromagnetic and semiconducting properties in the same material makes magnetic semiconductors of prime importance for spintronics applications; however, there is a lack of reviews covering the field. Here, we try to bridge the gap.

At first, we briefly outline the fundamentals of spintronics and consider spin-spin interactions and spin relaxation in semiconductors as well as spin-related and spin-injection related effects in condensed matter. We present examples of promising spintronic devices; formulate requirements for spintronic materials, and characterize the physicochemical properties of certain spintronic materials and relevant methods of synthesis. Organic spintronic materials are also touched upon and research in the field of inhomogeneous magnetic semiconducting materials exhibiting high-temperature ferromagnetism is discussed. Particular attention is paid to problems of the chemical bonding and electronic structure of magnetic impurities in semiconductors, the nature of ferromagnetism, and the character of exchange interactions between localized spins in the novel spintronic materials.

1. Band structure and spin interactions in spintronic materials

1.1. Band structure and impurity states

The nature of the charge carriers and spin carriers is closely related to the filled energy bands of semiconductors, namely, the valence band (this band is generally filled) and the conduction band (usually, this band is empty in *p*-type semiconductors) separated from the valence band by an energy gap (1.42 eV in GaAs, 2.26 eV in GaP, and 3.2 eV in GaN at 300 K). The electronic structure of semiconductors is governed by the chemical bonds. In semiconductors with the diamond, zinc blende or würtzite crystal structures these are the hybrid sp-bonds involving valence electrons, which are directed toward the vertices of a tetrahedron, being stronger than the s- and p-bonds.[56] For two atoms in the unit cell, the non-degenerate bonding (antibonding) combination of s-orbitals and the three-fold degenerate bonding (antibonding) combination of p-orbitals give rise to the valence band (conduction band). Among the bonding and antibonding states of the sp^3-orbitals in an A_nB_{VIII-n} type semiconductor (B is a pnictogen, chalcogen, halogen), the bonding p-orbitals of the anion sublattice are mainly near the top of a wide valence band, while the antibonding s-orbitals of the cation sublattice are near the bottom of the conduction band.

In semiconductors, the spin-orbit interaction (see below) removes the six-fold energy degeneration of the bonding combinations of the p-orbitals in the valence band, shifting doubly degenerate states with the total angular momentum $j = 1/2$ down from the heavy hole states with $j = 3/2$ by hundreds of meV (0.35 eV for GaAs). The four-fold degenerate energy states with $j = 3/2$ form the heavy hole band with the projections of the angular momentum $j_z = \pm(3/2)$ and the light hole band with the projections $j_z = \pm(1/2)$. The heavy hole band is of particular importance for the establishment of indirect exchange interaction between magnetic impurities in DMS and related isoelectronic systems.

The valence band is characterized by an enhanced electron density in the interatomic space, whereas in the conduction band the electron density is localized on atoms. The width of the energy gap between these bands is in fact determined by the bond dissociation energy or by the lowest energy required for an electron to go from the bound state to the conduction band. There are two types of charge carriers in semiconductors, called conduction electrons (electrons in the conduction band) and "holes" (missing electrons in the valence band). Holes also have spins, because all spins in the filled valence band are compensated and removal of an electron means the appearance of a spin (*vice versa*, removal of an electron causes the appearance of a positively charged hole). At low temperatures, the conductivity of semiconductors is mainly determined by the electrons and holes supplied by impurity atoms, defects, dislocations, *etc.*, having their impurity levels in the energy gap. The donor or acceptor character of an impurity is determined by its higher or lower ionization potential compared to the ionization potential of the replaced atom. In type III—V compounds, substitutional donor impurities for the anion sublattice are atoms of Group VI and VII elements and nitrogen atoms which have rather deep intrinsic s levels. A semiconductor with donor impurities is called an *n*-type semiconductor (here, electrons are current carriers), while a semiconductor with acceptor impurities is called a *p*-type semiconductor (positively charged holes are current carriers). In a non-degenerate impurity semiconductor, either donor electrons or acceptor holes are spatially localized near corresponding impurities. The radius of a cur-

rent carrier (or the radius of wave function localization) is given by the expression

$$r_0 = \varepsilon r_B(m/m^*) = (\varepsilon\hbar^2)/(m^*e^2),$$

where m^* is the effective mass of the current carrier, ε is the dielectric permeability of the material, r_B is the ground-state radius of hydrogen atom (so-called Bohr radius), m is the mass of electron, and $\hbar = h/(2\pi)$ (h is the Planck constant). Typical semiconductors are characterized by $\varepsilon = 10—20$, $m^* = 10^{-1}m$, and $r_0 = (100—200)r_B$; the last-mentioned parameter is much larger than the lattice constant $a \approx r_B$. This means that electrons in semiconductors (in contrast to, *e.g.*, transition metal oxides) cause weak lattice distortions and the impurity potentials can be considered as point potentials because the range of their action is much shorter than the radius of wave function localization. However, already at a low impurity concentration, $x \propto a^3/r_0^3$ per lattice site, the wave functions of current carriers are overlapped, thus forming an impurity band and the non-degenerate impurity semiconductor becomes a degenerate one.[57]

Impurity states in the electron energy spectrum of a semiconductor can be divided into shallow (hydrogen-like) and deep states depending on whose chemical properties (of the semiconductor matrix or the dopant, respectively) influence them to the greatest extent. Positions of shallow impurity levels are determined by the effective mass of the charge carrier and the dielectric constant of the semiconductor, *i.e.*, by the chemical nature of the matrix, and the properties of such impurities manifest themselves only as a weak distortion of the central cell (in addition to the charge). Shallow donor (acceptor) impurity levels lie near the bottom (top) of the conduction band (valence band) and can be correctly described by the effective mass theory. In type III—V compounds, Group I—III metals that are chemically similar to the replaced cations do not create deep levels in the forbidden energy band. On the contrary, positions of deep impurity levels are governed by the chemical nature of the impurities and specific features of their non-filled electron shells. In type III—V semiconductors, transition metal impurities in the cation sublattice almost without exception create deep levels.

In the theory of deep isoelectronic impurity levels in semiconductors the forbidden band is much narrower than the allowed bands[58] and the spherically symmetrical impurity potential gradually decreases at distances of the order of the lattice constant. In this case, creation is possible of virtual heavy hole states in the conduction band and of multiply charged levels with the formation of negatively charged impurity centers. The theory[58] of deep impurity levels established the principles of classification and the properties of the states localized on such levels.

In creating deep levels an important role is played by the states of the non-filled impurity electron shells.[59,60] Deep impurities cannot be described using the approaches suitable for the description of shallow impurities (Kohn—Lattinger and Koster—Slater models), according to which shallow levels are created as a result of potential scattering of the band carriers by the substitutional potential. Different symmetries of the valence band and the conduction band in the semiconductor predetermines their different contributions to the impurity states, which is ignored by the Koster—Slater model that implies equal involvement of carriers from the allowed bands in scattering by the impurity with a real symmetry. Deep levels are due to resonant scattering of the band electrons by the d levels of the non-filled shells.[61,62] For transition metal and REM impurities in semiconductors, an important role is also played by the inter-electron interaction.

1.2. Spin interaction in semiconductors

Spin interaction in semiconductors can be divided into several types.

Dipole-dipole interaction or spin-spin coupling is a direct interaction between the spin magnetic moments of electrons, which is proportional to the product of the magnetic moments and inversely proportional to the cube of the distance between them. Being proportional to $(v/c)^2$ (v is the speed of electron and c is the speed of light), the dipole-dipole coupling is too weak to play a significant role in semiconductors. The energy of the dipole-dipole interaction between two electrons occupying adjacent lattice sites is about 1K. The energy of the spin-spin coupling is comparable in order of magnitude with the low energy of the interaction between the spin magnetic moment of an electron and the anisotropy field. However, it is the weak spin-spin coupling that is of great importance for the useful properties of some magnetic semiconductors. In DMS the direct spin-spin coupling plays so insignificant role that the magnetization of DMS can easily be changed by applying experimentally attainable external magnetic fields. Relatively weak magnetic fields affect the characteristics of DMS to a greater extent compared to the parameters of normal magnetic semiconductors.

Spin-orbit interaction is the interaction between the spin magnetic moment of an electron and the magnetic moment of the orbital motion of the electron. The spin-orbit interaction is due to the fact that an electron traveling at speed $\vec{v}$ in an electric field of strength $\vec{E} = -\mathrm{grad}\varphi(r) = -(\vec{r}/r)\cdot(\partial\varphi/\partial r)$ (*e.g.*, in the field of an atomic nucleus with potential $\varphi(r)$), "sees" the magnetic field with the magnetic induction

$$\vec{B} = \frac{\vec{v}}{c} \times \vec{E} = \frac{1}{cm}\frac{1}{r}\frac{\partial\varphi}{\partial r}(\vec{r} \times m\vec{v}) \propto \vec{l}$$

(c is the speed of light) proportional to the angular momentum of the electron $\vec{l} = \vec{r}\times m\vec{v}$. In this magnetic field the electron with the magnetic moment $\vec{\mu} = g\mu_B\vec{s}$ ac-

quires an additional energy of the spin-orbit interaction $\vec{\mu}\vec{B} = \lambda\vec{l}\cdot\vec{s}$ (λ is the spin-orbit coupling constant). Due to the spin-orbit interaction, the spin of a moving electron or hole can be influenced by both static and alternating external electric fields. In semiconductors, the spin-orbit coupling is several orders of magnitude stronger than in atoms or metals; therefore, it can manifest itself even at thermal velocities of electrons. The spin-orbit coupling becomes stronger with an increase in the charge of atomic nucleus; its energy is 0.04 and 0.29 eV in Si and Ge semiconductors, respectively. Often, this interaction is responsible for spin relaxation and provides an interplay between the transport of current carriers and spin-related phenomena. The spin-orbit interaction relates the spin coordinates of an electron to its spatial coordinates and produces an effective intracrystalline magnetic field (magnetic anisotropy field), because the orbital motion of a particle is related to the crystallographic directions. A particular case of the spin-orbit interaction for two-dimensional systems with asymmetrical potential was reported.[20] Such a potential is induced in the channel of a silicon field-effect transistor. In this case, the shape of the potential can be manipulated by applying a voltage to the transistor´s base, thus varying the strength of the spin-orbit coupling. Strain produced in the crystal lattice of supported DMS layers also affects the spin-orbit coupling. Depending on the type of the strain produced, that is, compression or tension, the DMS magnetization (ferromagnetic easy magnetization axis) lies either in the plane of the ferromagnetic layer or is parallel to the growth direction of this layer, *i.e.*, the magnetic anisotropy field in DMS also depends on the lattice distortion.

Exchange interaction is a part of inter-electron Coulomb interaction, which depends on permutation of two electrons following the Pauli exclusion principle: $-J\vec{s}_1\cdot\vec{s}_2$. Such a "quantum force", which depends on the mutual spin orientation, originates from different orbital motions of two electrons that tend to form electronic configurations either with distant electrons (probability for both electrons to be in close proximity to each other is low) or with close located electrons (here, this probability is high). In this case, the total spin of the electron pair, $\vec{S} = \vec{s}_1 + \vec{s}_2$, equals either 1 (spin triplet) or 0 (spin singlet). The exchange energy (integral) J equals a halved energy difference between these two electronic configurations. The intensity of the exchange interaction is somewhat weaker than the halved strength of electrostatic Coulomb interaction. If the electron shell of an atom contains several electrons (d and f shells of transition metal atoms and rare-earth elements), the Coulomb repulsion between them is minimum in the case of aligned spins, *i.e.*, the exchange integral is positive, $J_H > 0$ (intra-atomic Hund exchange). In this case the electron configurations tend to have the maximum possible total spin (the first Hund rule). For the same reason in an isolated atom the spins of the s and d electrons of the atomic shell are also aligned. The appearance of a magnetic impurity makes the situation in the non-magnetic metal more complicated, namely, the spin orientation of the s conduction electron can be parallel or antiparallel to the spin orientation of the d impurity electron. The result depends on the intra-atomic repulsion between the d electrons, which is characterized by the Anderson—Hubbard parameter U, and on position of the impurity level in the energy band of the metal; creation of uncompensated magnetic moment is facilitated at a low density of conduction electrons and low degree of bond covalency.[63] For covalent bonding to occur, the energetically favorable situation must involve orbital motion of electrons with the maximum electron density in the region between positively charged nuclei ($J < 0$), so covalent bonding produces a spin singlet. As the bond covalency in M^{3+}—An—M^{3+} and M^{4+}—An—M^{4+} (An is an anion) increases in the order of anions F^-, O^{2-}, S^{2-}, Se^{2-}, the exchange integral J also increases. Mutual spin orientation and, eventually, ferromagnetism are governed by the exchange interaction of the atoms of the metal impurity M^{n+}, which, however, is not responsible for the total spin orientation with respect to the crystallographic axes. Degeneration of the total magnetization of the crystal relative to crystallographic axes is partially removed by the spin-orbit interaction. Combined with the Pauli exclusion principle, the kinetic energy of electrons tends to destroy the spin order; the temperature at which the material no longer possesses ferromagnetic properties is said to be the Curie temperature. In semiconductors, direct exchange interaction between delocalized electrons or holes plays an insignificant role owing to the low density of charge carriers and abrupt (exponential) weakening of the exchange interaction with distance. The exclusions are a group of CMS with rather low Curie temperatures and the semiconductor—ferromagnetic interfaces that are of importance for spin injection phenomena. In some cases, an exchange interaction between localized d or f electrons and conduction electrons (sd-interaction characterized by the exchange parameter J_{sd}) or valence holes (pd-interaction characterized by the exchange parameter J_{pd}) is phenomenologically introduced for magnetic semiconductors.[64] Owing to peculiarities of the electron density distribution over the semiconductor energy bands, electrons move along magnetic cations, whereas holes move along non-magnetic anions. Therefore, ferromagnetic exchange between the localized electrons and conduction electrons must be stronger than their antiferromagnetic exchange interaction with holes in the valence band: $J_{sd} > |J_{pd}|$. Without dwelling on specific features of the structure of chemical bonds between impurities and the semiconductor matrix, note that, phenomenologically, these exchange interactions in magnetic

semiconductors are treated as contact interactions centered on magnetic atoms.

Indirect spin interactions. In the crystal, direct spin interaction between distant atomic cores (electronic configurations), *e.g.*, magnetic impurity ions in semiconductor is negligible. The spin interaction between such ions occurs *via* disturbance of electron states in the atoms shared by these ions.

If itinerant electrons are localized on, *e.g.*, non-magnetic anions (F^-, O^{2-}, S^{2-}, Se^{2-}, *etc.*), being involved in the chemical bonding between identical magnetic ions M (M^{3+}—An—M^{3+} and M^{4+}—An—M^{4+} ions in perovskites $LaMO_3$ and $CaMO_3$ or Cr^{3+}—F^-—Cr^{3+} ions in CrF_3), the orbitals of electrons localized on the magnetic ions are overlapped. In this case, an electron can be transferred from one ion to another ion with the kinetic energy t. In the case of semiconductors doped with magnetic impurities the hopping integral t appears due to the direct overlap of the impurity orbitals (wave functions). Having arrived at the filled orbital of another ion, an electron with antiparallel spin orientation acquires an additional energy of electrostatic repulsion, $U \gg t$, and the energy of electron pair is governed by competition between the kinetic energy of electron transfer and the repulsion energy between electrons in the same orbital:

$$E = 2\alpha t + \alpha^2 U$$

(α is the overlap of the orbitals of localized electrons). Minimization gives the energy necessary for spin disordering, $E_{\uparrow\downarrow} = -(t^2/U)$. In particular, two localized electrons are stabilized with antiparallel spin orientations and the antiferromagnetic exchange integral is

$$J_{\uparrow\downarrow} = -(4t^2/U) < 0.$$

This indirect exchange interaction is called (kinetic) superexchange, or Anderson superexchange.

If the atom of a main group element is replaced by an atom of other main group element with a different valence (*e.g.* $La^{3+} \rightarrow A^{2+}$ in $(La,A^{2+})MnO_3$), the magnetic manganese ions become mixed-valence ions. Electrons of the Mn atoms are now delocalized and can move between distant magnetic ions through the anion, *e.g.*, as follows: $Mn^{3+} \rightarrow O^{2-} \rightarrow Mn^{4+}$ and $Mn^{4+} \leftarrow O^{2-} \leftarrow Mn^{3+}$.[65] Such a "hopping" electron with a given spin orientation avoids tunneling toward a site occupied by an electron with antiparallel spin orientation, due to strong repulsion U, which is important in the case of antiferromagnetic superexchange. Then, competition between a low kinetic energy of electron tunneling between cations (t) and a strong Hund intra-atomic ferromagnetic exchange between localized and delocalized electrons ($J_H > 0$) stabilizes aligned cation spins. Indeed, an electron can execute free motion between ions, thus reducing the total energy of the system, only if the spins of all ions are aligned. This type of ferromagnetic ordering of cations with $T_C \propto t$ is due to two transitions involving the non-magnetic anion and is therefore called double exchange.[65] In fact, the double exchange interaction exchanges different valence states ($Mn^{3+} \rightleftharpoons Mn^{4+}$ in $(La,A^{2+})MnO_3$); therefore, it occurs in mixed-valence compounds. The mechanism of double exchange was repeatedly refined.[66,67] Sometimes, this type of magnetic exchange between two different-valence ions is called Zener (ferromagnetic) exchange, though it was proposed earlier by Fröhlich and Nabarro for nuclear ferromagnetism.[68] Long before Zener, mutual biasing of the localized and delocalized (itinerant) electrons was pointed out by Vonsovsky[69—71] who considered indirect exchange of establishment of ferromagnetism of localized electrons involving itinerant electrons in the case where all non-magnetic ions in the crystal lattice are replaced by atoms of transition metals or rare-earth elements (sd-model) and, similarly to Zener,[65] calculated changes in the conductivity on transition to the ferromagnetic phase. The phenomenological sd-model was also used by Zener.[72] The Zener exchange[65] is a particular case for double exchange studied earlier by Vonsovsky,[70,71] namely, the limiting case of a very strong Hund intra-atomic exchange $J_H \gg t$. Because of this, it would be more correct to call the double exchange mechanism[70—72] the Vonsovsky—Zener mechanism. This mechanism was extended to ferromagnetic semiconductors with the magnetic sublattice and to antiferromagnetic semiconductors.[73—75] The superexchange and double exchange mechanisms were used to describe a number of magnetic semiconductors with intrinsic magnetic ion lattices (*i.e*, concentrated magnetic conductors).[64]

Superexchange responsible for antiferromagnetism occurs between magnetic ions with different spin orientations and equal charges and removes the energy degeneracy of the two-electron virtual state with high energy U. Superexchange induces antiferromagnetism in semiconductor transition metal compounds with relatively low Neel temperatures $T_N \approx t^2/U$. Double exchange responsible for ferromagnetism occurs between differently charged ions involving delocalized electrons and removes the energy degeneracy of real states due to transition *via* a virtual anion state. Therefore, the double exchange mechanism is inapplicable to the description of ferromagnetism in semiconductors doped with magnetic impurities with integer valences. In spite of the fundamental difference between mixed-valence CMS and integer-valence DMS the latter are often studied using the double exchange mechanism (see., *e.g.*, Refs 76—79).

Some authors postulate the existence of two exchange contact interactions between the impurity d electrons and itinerant s and p electrons. Because of the density distribution of the delocalized carriers over the conduction band and the valence band this exchange must be ferro-

magnetic in character in the conduction band ($J_{sd} > 0$) and antiferromagnetic in character in the valence band ($J_{pd} < 0$). The fitting character of these interactions led to discrepancies between the estimates of the exchange interaction J_{pd} in the best studied DMS, (Ga,Mn)As. They ranged from −4.5 (see Ref. 80), −3.3 (see Ref. 81), and 2.5 eV (see Ref. 82) to much smaller values, −1.2 (see Ref. 83), −1.0 (see Ref. 84), and −0.6 eV (see Ref. 86) (negative sign corresponds to antiferromagnetic exchange interaction of the d and p electron spins). The scatter in the data depends on which methods were used to calculate J_{pd} from experimental data on (Ga,Mn)As in different phenomenological models or which "first-principle" numerical methods were employed ("first principles" based on density functional were analyzed in Ref. 86). The difference between estimates of the magnitude and sign of the parameter of ferromagnetic exchange interaction between localized d electrons and delocalized s conduction electrons ($J_{sd} \approx 10^{-1}$ eV) is much smaller.

An unjustified use of the double exchange mechanism led[77] to prediction of high T_C only in *p*-type DMS, which contradicts facts, namely, high-temperature ferromagnetism in some *n*-type magnetic semiconductors, *e.g.* (Ga,Mn)N, and high-temperature magnetic semiconductors similar to $(CdGe,Mn)P_2$. Recent cyclotron resonance experiments* with DMS in magnetic fields of up to 500 T, carried out taking *p*-type $In_{1-x}Mn_xAs$ films ($0 < x < 2.5$) grown by molecular beam epitaxy on GaAs substrates as examples, indicated the absence of double exchange in DMS.

When considering magnetic impurities in semiconductors, it is of great importance to allow for the tunneling energy V of the impurity d electron to the band of itinerant carriers and back to another impurity atom. The parameter V is related to the degree of hybridization of the localized and delocalized electrons, being in fact a measure of covalency of the bond between them, *i.e.*, the hybridization parameter is the one-electron energy. The magnitude of the hybridization parameter of the d impurity electrons and itinerant *p*-holes ($V_{pd} > 1$ eV) in DMS and HTFS is comparable with the width of the heavy hole band. It is important that tunneling occurs with conservation of the spin projection. If we introduce the density of states of itinerant electrons $\rho(\varepsilon) = \Delta N/\Delta\varepsilon$, where ΔN is the number of electron states in the energy interval $\Delta\varepsilon$, the quantity $\rho(\varepsilon)V$ gives the proportion of the conduction electrons in the energy interval $(\varepsilon, \varepsilon + \Delta\varepsilon)$, which are polarized by the electrons with the same spin projection localized on the impurity. Double tunneling from the impurity to the band and from the band to another impurity (as follows: $d_1 \Rightarrow p \Rightarrow d_2$) in DMS and HTFS governs coupling between distant impurities with the transfer energy proportional to ρV^2 (dependence on the distance is omitted), which is of importance for occurrence of kinematic exchange interaction.

Hyperfine coupling between electron and nuclear spins is, similarly to the spin-orbit coupling, relativistic in nature. In the case of semiconductors it provides an additional, as compared to metals, possibility of manipulation of electron spin by not only external magnetic field but also the field of atomic nuclei present in the semiconductor lattice. Overhauser[87,88] described interaction between the electron and nuclear spins in condensed matter starting from contact interaction between them in isolated atoms (Fermi hyperfine interaction). It can be written in the form

$$A\vec{S}\sum_i \vec{I}_i\delta(\vec{r} - \vec{r}_i) \equiv g\mu_B\vec{B}_n\vec{S},$$

where $\delta(\vec{r})$ is the Dirac delta function, summation is performed over positions $\vec{r}_i$ of all atomic nuclei with the spins $\vec{I}_i$, g is the gyromagnetic ratio for electron, and A is the hyperfine coupling (HFC) constant. This interaction is equivalent to the existence of a long-lived strong magnetic field $\vec{B}_n$ (Overhauser field) exerted on the electron spin $\vec{S}$ by the spin-polarized nuclei distributed over some domain in the material. Semiconductors are characterized by rather long nuclear spin relaxation times (10^2—10^3 s at helium temperatures), which much exceed the electron spin relaxation time (~10^{-7} s). This means that nuclear depolarization is a slower process compared to electronic depolarization. The Overhauser field can be very strong, its magnitude depends on the type of atoms (*via* the HFC constant A) and on the degree of nuclear spin polarization.[89—93] For GaAs semiconductor, the HFC constant is negative and the Overhauser field $\vec{B}_n$ tends to polarize electron spins in the same way as nuclear spins, reaching a value of 5.3 T at 100% nuclear polarization.

In connection with importance of the hyperfine coupling between the electron and nuclear spins, nuclear spintronics can be considered as a separate branch.* The nuclear spin can be used instead of electron spin. In principle, it is possible to fabricate a device in which information is transmitted to nuclei by light *via* electrons. The information capacity of such a nuclear memory will be many orders of magnitude higher than and faster than conventional semiconductor-based memory. Electronics, photonics, and magnetism can give rise to spin photonics in order to design devices operating at teraHertz frequencies.

* Y. H. Matsuda, G. A. Khodaparas, M. A. Zudov, J. Kono, Y. Sun, F. V. Kyrychenko, G. D. Sanders, C. J. Stanton, N. Miura, S. Ikeda, Y. Hashimoto, S. Katsumoto, H. Munekata, http://arXiv.org/cond-mat/0404635.

* I. D. Vagner, *Nuclear Spintronics: Quantum Hall and Nano-Systems*, http://arXiv.org/cond-mat/0403087.

1.3. Spin relaxation mechanisms

The most important problem in studies of spin phenomena in the condensed matter is electron spin relaxation (in other words, spin decoherence) generally interpreted as a result of the action of fluctuating magnetic fields.[10] Usually, these are the effective fields originating from the spin-orbit and exchange interactions. The fluctuating magnetic fields are characterized by their amplitudes (more exactly, root-mean-square amplitudes) and correlation times, τ_c (during the time interval τ_c the field can be considered constant). In some cases, it is convenient to use the mean frequency, ω, of spin precession in the fluctuating field instead of the field amplitude. Then spin relaxation can be imagined as follows. An electron spin precesses about a certain random direction of the effective magnetic field with the characteristic frequency ω over the characteristic time τ_c. Then, both the direction and magnitude of the magnetic field are changed and the spin now precesses about a new direction. Finally, after a number of random changes the electron "forgets" the initial direction of spin orientation. Real fate of the electron spin in the semiconductor is governed by the dimensionless parameter $\omega\tau_c$, *i.e.*, the characteristic angle of rotation of the precessing spin and the correlation time.

Usually, the angle of precession is small ($\omega\tau_c \ll 1$) and the spin orientation experiences a slow angular diffusion. During the time interval τ the electron will be involved in τ/τ_c independent random changes (the angle of precession squared in each step is $(\omega\tau_c)^2$) and the total angle of precession squared equals $(\omega\tau_c)^2 t/\tau_c$. The spin relaxation time, τ_s, is defined as the time taken for the angle of precession squared to reach a value of the order of a unity, $\tau_s \propto 1/(\omega^2\tau_c)$.

Otherwise, at $\omega\tau_c \gg 1$, the electron spin will execute many rotations about the magnetic field direction during the correlation time. The time-averaged (over the time interval of the order of $1/\omega$) spin projection perpendicular to the magnetic field direction completely disappears, whereas the spin projection on the magnetic field direction is retained. After the time τ_c, the magnetic field direction will be changed and the initial spin polarization will vanish. Thus, in this case one has $\tau_s \propto \tau_c$, *i.e.*, the spin relaxation time is of the same order of magnitude as the spin correlation time.

Different mechanisms are responsible for creation of the fluctuating magnetic fields governing the spin relaxation. The Dyakonov—Perel mechanism[94—96] relating the effective magnetic field to the momentum-dependent spin splitting of the conduction band dominates in the case of mobile carriers in the semiconductors based on type III—V and II—VI compounds and two-dimensional electrons in quantum wells. This and other mechanisms involving the motion of electrons are inapplicable to electrons localized on donor sites or in quantum dots and the spin relaxation times are very long. The problem of spin depolarization is of crucial importance for realization of spin-based quantum computers.

The hole spin relaxation times are much shorter than the electron spin relaxation times and spin exchange between electrons and holes enhances decoherence of both types of carriers. Therefore, creation of spin coherence requires the absence of holes, as is the case of *n*-type semiconductors.

In the absence of holes spin decoherence is mainly due to the spin-orbit coupling that is relativistic in nature. Namely, an electron moving in the electric field of a crystal "senses" a part of the field as magnetic field; as a consequence, the electron spin begins precession about the field direction. Initially excited spin-polarized electrons are characterized by a scatter of velocities and therefore each of them precesses in its own fashion. Two electrons with initially equal spin projections can change them after a short time. As the degree of spin disordering increases, the total spin polarization on the average decreases and the spin coherence vanishes. Experiments with novel magnetic semiconductors showed that the spin coherence times can be much longer than the observation times, thus providing conditions for efficient operation of spintronic devices in the future.

1.4. Basic spin effects

Pioneering experiments[97] on manipulation of electron spin orientation by external electromagnetic fields were concerned with observation of depolarization of mercury vapor luminescence by applying a transverse magnetic field (here, terrestrial magnetic field). The mechanism of the effect observed[98] involves precession of atomic electron spins about the direction of the magnetic field. On exposure to continuous irradiation the average spin projection on the direction of observation, which determines the degree of circular polarization of luminescence, decreases owing to precession. As a result, the degree of polarization decreases as the transverse magnetic field increases. Measurements of the dependence of luminescence depolarization on the magnetic field allows both the spin relaxation time and the recombination time to be determined. Later, detailed studies of optical pumping of atoms were carried out.[99,100] At present, depolarization of atomic luminescence by transverse magnetic field has been efficiently used in experiments on spin orientation in semiconductors.

There is a number of effects following from interrelation between spins and charge transfer.[10] One of them (Mott effect) is related to the fact that spin-orbit coupling produces asymmetry of electron scattering by a charged center relative to the plane passing through the momentum vector and the direction of spin orientation. This effect induces an additional electric current with the den-

sity $\vec{j} = -\beta\vec{E}\times\vec{S} - \delta rot\vec{S}$, where $\vec{S}$ is the spin density vector, $\vec{E}$ is the electric field strength of, *e.g.* light wave, and the coefficients β and δ are proportional to the spin-orbit coupling constant. The first term describes the so-called anomalous Hall effect and the second term describes the additional electric current that is due to the spin-orbit coupling and nonuniform spin density distribution,[101,102] which was confirmed experimentally.[103] The reverse effect is also possible, namely, electric current can induce spin orientation near the surface of the sample.[104] In gyrotropic semiconductors (here, the crystal lattice has no center of inversion), electric current can also be induced by a uniform nonequilibrium spin density distribution; this was predicted theoretically[105,106] and then confirmed experimentally.[107]

Optical polarization of electron spins in semiconducting materials (*e.g.*, silicon[108]) is in principle similar to optical pumping in atomic physics and differs from the latter in that in semiconductors we deal with spin-polarized conduction electrons rather than bound electrons in the atom.

The polarization of nonequilibrium spin-polarized electrons can be transferred with ease to atomic nuclei in the crystal lattice. Long-lived nuclear spin polarization creates a very strong effective magnetic field, which in turn affects the electron spins (rather than the orbital motion of electrons). Owing to hyperfine coupling, spin-polarized electrons and the lattice of oriented nuclear spins form a tightly bound system. Using circular polarization of luminescence,[109,110] in this system one can observe such nonlinear phenomena as slow undamped oscillations and hysteresis.[111] Interband optical pumping experiments[108] permitted attainment of 32% nuclear polarization, which provided[112] an internal magnetic field of 1.7 T. An improved technique[113] involves nuclear spin polarization by creating nonequilibrium spins in the electron subsystem, which transfers its spin polarization to the nuclear subsystem during relaxation to the thermodynamic equilibrium state.

This technique is much more efficient than spin polarization of nuclei by external magnetic fields H. In the latter case the degree of nuclear spin polarization $\propto \mu_I H/k_B T_I$ is expressed through world constants, *viz.*, the Boltzmann constant k_B and nuclear magneton μ_I. Though the nuclear magneton is small compared to the Bohr magneton, nuclear spin polarization is possible even in weak fields due to low temperature T_I of the nuclear spin system. This effect and a strong feedback between the electron and nuclear spin systems in the semiconductor[114] can also be employed in spintronics. However, low initial temperatures (liquid helium) and the lack of isotopically pure materials preclude practical implementation of these physical effects. Note also a report on the effect of nuclear spins on the low-temperature magnetotransport.[115]

In the ferromagnetic tunneling contact, or the magnetic tunneling transition, the height of the potential barrier is different for electrons with different spin orientations, thus providing different tunneling probabilities. Therefore, the contact barrier will pass electrons with preferable spin orientation. Spin injection from a ferromagnetic tip into GaAs *via* electron tunneling was first demonstrated[116] before the term "spintronics" was proposed. Magnetic tunneling transitions are of paramount importance for fabrication of highly sensitive field transducers and memory devices. Recently, experiments on spin injection into DMS have been carried out.

Spin-dependent resistance in ferromagnetic metals was also studied[117,118] long before the emergence of spintronics. It was shown that at sufficiently low temperatures the electrons whose magnetic moments are parallel and antiparallel to the magnetization direction of a ferromagnetic are not mixed in scattering processes. Then, the total conductivity can be represented by the sum of independent and unequal contributions of two different orientations of electron spins. This concept was generalized[119–121] to explain different magnetoresistance effects.

In the novel DMS the temperature dependence of resistivity, $\rho(T)$, is nonmonotonic at the magnetic impurity concentration corresponding to the highest T_C. Below T_C, one has $d\rho/dT > 0$ (*cf.* $d\rho/dT < 0$ above T_C). The resistivity of magnetic materials also depends on an external magnetic field. At a specified temperature, the resistivity can be reduced by applying a magnetic field, the greatest resistivity drop being near T_C. This phenomenon is often observed in the DMS and magnetic metals. It is due to the spin-dependent scattering of charge carriers by spin fluctuations owing to exchange interaction. This scattering is most pronounced near T_C where the magnetic correlation length is comparable with the Fermi carrier wavelength.[122] As the magnetic field increases, additional ordering of localized spins occurs, thus suppressing the spin-dependent scattering and being responsible for negative magnetoresistance.

Ferromagnetic materials (Sn,Mn)Te,[123] $(GeTe)_{1-x}(MnTe)_x$ [124] and (Pb,Sn,Mn)Te [125] have not received wide acceptance because of the Curie temperatures and of the properties of type IV—VI matrices that are of limited use in electronics.

1.5. Spin injection

Operation of "spin memory" devices, "spin transistor", and "spin quantum computer" requires spin injection-polarized electrons, rather long spin relaxation times in electron transport processes, and detection of the spin state of an electron. One must create quantum state of electrons with specified spin orientation, retain the state during the operation of the device, and then read the

electron state at the output. Seemingly, a natural solution to the problem of spin injection into semiconductors was to use ferromagnetic injectors made of Fe, Co, of Ni. Spin polarization of current in the ferromagnetic containing free carriers is due to the difference between the density of states of electrons with spin orientations "up" and "down" and to subsequent difference between the conductivities of the systems of electrons with antiparallel spin orientations. This spin injection technique was successfully employed in the ferromagnetic metal/superconductor system. Spin injection from a ferromagnetic into normal metal was first proposed theoretically[126] and experimentally observed nearly a decade later.[127]

However, attempts to realize this approach for the ferromagnetic metal/semiconductor system failed. First experiments on spin injection of electrons from ferromagnetic Ni into GaAs failed owing to low quality of heterostructures though researchers did observe a substantial change in the coercive force on exposure of the structure to a weak luminous flux with an intensity of only 5 mW cm^{-2}.[128] In the case of electron injection into a semiconductor through a ferromagnetic metal/semiconductor contact, electrons in the semiconductor have nonequilibrium spins that contain information on the electron spins in the ferromagnetic; *i.e.*, spins of electrons in the semiconductor can act as, *e.g.*, detectrors of the state of the magnetic film. In turn, the orientation of electron spins in semiconductors can be detected both optically and electrically. The magnetic properties of the ferromagnets placed in contact with semiconductors in heterostructures can also be controlled.* To date, the highest efficiency of spin injection from ferromagnetic metal into a semiconductor (up to 30%) was achieved only in experiments with a scanning tunneling microscope.[129—131] A reason for low efficiency of spin injection through the metal/semiconductor interface (~1%)[132] is a large conductivity difference between these materials.[133]

The efficiency of spin injection can be enhanced using the Schottky barriers (electrostatic barriers formed at the metal/semiconductor interface due to defect formation) which can act as tunneling barriers, thus weakening the effect of the difference between the electrochemical potentials of the ferromagnetic metal and semiconductor on the transport of spin-polarized electrons through the interface. This allowed an efficiency of 2% in the spin injection from a Fe contact into a GaAs/(In,Ga)As light-emitting diode to be achieved at room temperature.[134]

Efficient solution to the problem requires that the injector be a ferromagnetic semiconductor or a semiconductor placed in an external magnetic field. Then, the spin polarization of electrons can be as high as nearly 100% owing to the exchange interaction between the conduction electrons and the magnetic impurity.[135]

First, it was proposed to use manganese-doped type II—VI semiconductors whose conductivity is comparable with the conductivity of the non-magnetic semiconductor containing injected spin-polarized electrons. The spin polarization efficiency was 50% for the (Zn,Mn)Se/GaAs contact,[136] more than 50% for (Cd,Mn)Te/CdTe,[137] and 86% for spin injection from a paramagnetic semiconductor $Be_xMn_yZn_{1-x-y}Se$ into a quantum well light-emitting diode AlGaAs/GaAs.[138] Recombination of spin-polarized charge carriers causes emission of circularly polarized light; by measuring the degree of polarization of luminescence it is possible to estimate the efficiency of spin injection. Severe problems posed when using type II—VI magnetic semiconductors for injection are due to the necessity of operation at low temperatures (<10 K) because these materials are paramagnetics and an increase in temperature causes a dramatic decrease in their magnetization at a specified external magnetic field.*

Clearly, efficient spin injection reqiures ferromagnetic semiconductors that could inject, transfer, and easily orient the spin-polarized carriers in the semiconductor heterostructures. Therefore, the most promising candidates for spin injectors are high-T_C ferromagnetic semiconductors that are technologically compatible with normal semiconductors. Among possible candidates are the DMS based on type III—V matrices, the Geissler alloys X_2YZ (X and Y are transition elements and Z are Group III—V elements), and semimetallic and half-metallic ferromagnetic oxides.

After the synthesis of novel DMS, experiments on electron injection from a ferromagnetic injector layer into normal semiconductors were carried out.[139,140] Spin-polarized holes were injected from a ferromagnetic (Ga,Mn)As electrode into a non-magnetic GaAs electrode.[139] In spite of difficulties originated from the quality of the material and the presence of defects served as electron scattering centers, researchers did measure the spin polarization of the material. The efficiency of spin injection from a *p*-type ferromagnetic (Ga,Mn)As (T_C = 110 K) into a photoluminescent diode with non-magnetic quantum well InGaAs/GaAs was 1%.[139] Highly efficient (82±10%) spin injection from (Ga,Mn)As (T_C = 120 K) into an (Al,Ga)As light-emitting diode at 4.6 K was demonstrated.[141] At present, search has been carried out for novel ferromagnetic semiconductors with higher T_C, which could serve as room-temperature spin injectors at weak or zero external magnetic fields. In spite of the problems faced by the crystal growth and doping techniques, high-T_C ferromagnetism in semiconductors per-

* V. L. Korenev, *VI Ross. konf. po fizike poluprovodnikov* [*VI All-Russia Conference on Physics of Semiconductors*] (*St.-Petersburg, October 27—31, 2003*), Sankt-Petersburg, 2003.

* A. A. Toropov, http://link.edu.ioffe.ru/winter/2001/main/toporov.

mits optimistical expectations of fabrication of spin devices operating at room temperature. (The problem of spin transport in microelectronic devices has been the subject of a review.*)

Most spin injection experiments involve passage of electric current from a ferromagnetic into a semiconductor through a tunneling barrier. High degree of spin polarization can be achieved using a magnetic tunnel transistor.[142,143] At present, spins are injected into semiconductors by passing spin-polarized electric current from the magnetic semiconductor under the action of voltage applied. This is the principle of the operation of a spin filter. However, the process is hampered by interference at the ferromagnetic/semiconductor interface. If we change the sign of the voltage, the ferromagnetic will pass only those electrons whose spins are aligned with the magnetization vector of the ferromagnetic semiconductor rather than all non-polarized electrons flowing from the normal semiconductor. Electrons with antiparallel spin orientations will not pass through the interface and thus will accumulate in the semiconductor. This pure electronic technique was implemented in the experiments on spin injection using a GaAs layer 500 nm thick placed in contact with a ferromagnetic semiconductor MnAs ($T_C \approx 600$ K) layer 25 nm thick at $T = 7.5$ K.[144] The highest efficiency of accumulation of spin-polarized electrons was achieved at a voltage of 1.5 V. This is several times higher than the efficiency of spin injection from ferromagnetic semiconductor into normal semiconductor. The degree of spin polarization was determined from magneto-optical measurements. Thus, spin injection into semiconductors was realized using electric current from normal semiconductor to ferromagnetic semiconductor.**

Spin injection of current carriers is closely related to two practically important problems, namely, how long are the distances appropriate for the spin excitation transfer and at which rates can the spin states be switched on and off. It was proposed to create a nonequilibrium spin system in semiconductors by passing electric current through a ferromagnetic contact.[145] If an electron leaved from the ferromagnetic by tunneling, it must retain the spin orientation in the semiconductor at a distance of the order of the spin diffusion length $\sqrt{D\tau_s}$, where D is the diffusion coefficient and τ_s is the spin relaxation time. At the ferromagnetic/semiconductor interface, potential barriers to electrons with the spins oriented parallel and antiparallel to the magnetization of the ferromagnetic become different owing to the exchange interaction. For this reason, any deviation from the spin equilibrium (due to electric current through the interface or to exposure to light) will cause injection of spins into the semiconductor. In this case the nonequilibrium spin orientation will be retained at distances of the order of the spin diffusion length $\sqrt{D\tau_s}$.

Macroscopic spin transfer was first demonstrated taking *n*-type GaAs semiconductor as an example.[146] A laser pulse excited coherent precession of electron spins and then electrons were transferred along the crystal over distances longer than 100 μm nearly without loss of spin polarization by applying an electric field. These distances are much longer than the characteristic sizes necessary for modern microelectronics. Coherent precession of electron spins was excited by a 150 fs laser pulse, *i.e.*, spins could be manipulated thousands of times during the spin relaxation time. Since modern electronics widely employs heterostructures, the results obtained are also of importance in relation to spintronics. *n*-Type semiconductors GaAs also exhibit retention of optically induced spin polarization of electrons with long (longer than 100 ns) spin relaxation times.[147] After relaxation of electron spins on nuclear spins the relaxation time of GaAs was extended to 300 ns.[148]

Electric voltage induced spin injection from GaAs semiconductor layer into a ZnSe heterostructure layer through a p—n-junction at 5 K was also reported.[149] (Until now, it was assumed that electrons passed through the p—n-junction always lose their spin orientations due to scattering.) Ordered groups of electron spins that were transferred by the applied electric field also sustain their spin polarizations for a rather long time at room temperature. The total transferred spin retains its characteristics as the spin reservoir both in the first semiconductor and in the adjacent semiconductor layer. Applying an external electric field makes possible the reversal of spin current. Because spins were manipulated by electric rather than magnetic field, the effect detected points to considerable promises for fabrication of multifunctional electronic devices (*e.g.*, spin transistors) in which logic functions are combined with memory functions. Such devices could be simultaneously manipulated by both electric and magnetic field, thus completely employing the electron charge and electron spin degrees of freedom.

2. Spintronic facilities and devices

An attractive feature of many devices employing the spin-dependent properties of materials is their similarity to classical valves, diodes, transistors, *etc.*, used in integrated circuits. The operation of the novel devices can be understood with ease based on analogy between the electron spin flip-flop for the materials with different polarization of electron spins and a conventional p—n-junction for *p*-type and *n*-type semiconductors. It is also possible to design combined ferromagnetic semiconductor

* A. S. Borukhovich, N. A. Viglin, and V. V. Osipov, Electronic journal "*Issledovano v Rossii*" [*Studied in Russia*], http://zhurnal.ape.relarn.ru/articles/2001/.

** A. V. Ivanov, *Scientific.ru*, 11.04.04, http://www.scientific.ru.

devices using the advantages of microcircuitry. Consider spintronic-related effects and spintronic devices in more detail.

Time-resolved optical experiments. Time-resolved optical experiments[150] with picosecond temporal resolution revealed a marked spin precession as well as the electron and hole spin relaxation. The method provides a unique possibility to observe fine details of various spin-related processes in semiconductors.

Electric-field controlled ferromagnetism. A characteristic feature of novel magnetic semiconductors based on type III—V matrices and isoelectronic materials is the dependence of T_C on the concentration of charge carriers. The density of charge carriers can be changed by doping, by applying an electric field, or by irradiation with light. A ferromagnetic DMS (In,Mn)As changes its magnetic properties on applying an electric field (see Refs 150—153). As a positive potential was applied to the grounded layer of (In,Mn)As (T_C = 30 K in the absence of external fields), the electric field inside the layer caused a decrease in the hole density and disappearance of ferromagnetism in the layer. *Vice versa*, at negative potentials applied or at zero potentials, ferromagnetism restored. Electric field induced changes in the magnetization of small domains of samples in the vicinity of electrodes were detected from changes in the Hall resistance. The Hall effect in magnetic materials is the sum of the normal Hall effect induced by the action of the Lorentz force on the charge moving in the magnetic field and the anomalous Hall effect due to the magnetization induced asymmetric scattering of current carriers

$$R_{\text{Hall}} = (R_0/d)H + (R_M/d)M.$$

Here, R_0 is the normal Hall coefficient, H is the magnetic field strength, R_M is the anomalous Hall coefficient, and M is the magnetization perpendicular to the layer of thickness d. In magnetic materials, the anomalous Hall effect is much stronger than the normal Hall effect, which allows the sample magnetization to be determined by measuring the transport properties. At present, these laboratory experiments are of academic interest for elucidation of the nature of ferromagnetism because the electric voltage applied was 125 V. One could decrease the thickness of the active layer, but at d = 5 nm ferromagnetism in (Ga,Mn)As disappeared. Ferromagnetism in $Ge_{1-x}Mn_x$ can be manipulated at much lower voltages (~1 V) and higher temperatures (~50 K).[154] These experiments can appear to be basic to design of a new type of recording devices.

Non-magnetic spin manipulation in strained semiconductors. Direct measurements of coherent electron spin precession in zero magnetic field as the electrons drifted in response to an applied electric field were reported.[155] Ultrafast optical spectroscopy was employed to study the electron spin dynamics in the strained GaAs and InGaAs epitaxial layers. A spin splitting arising from strain in the semiconductor films was observed. The method permits electrical control over electron spins with allowance for strain produced in the crystal lattice. The strain induced shift of the spin resonance frequency can be as high as nearly 30 MHz.

Spin polarization of electrons by electric field. A possibility of creation of spin-polarized electron beams, which can find practical application in spintronics, was reported.[156] The authors considered the spin-orbit interaction in the presence of current flowing in the plane of oriented two-dimensional electron gas with the Hamiltonian[20] (orientation is due to, *e.g.*, asymmetry of the quantum well). Evaluation of the effect for a typical case of GaAs/AlGaAs heterostructure with an electron concentration of $5 \cdot 10^{11}$ cm^{-2} and an electron mobility of 10^4 cm^2 (V s)$^{-1}$ and an electric field applied of 10 V cm^{-1} showed that a total of 10^8 electrons per cm^2 become oriented. Though this relative polarization is very small, the effect observed allows the degree of polarization to be controlled by applying an electric field.

Datta—Das spin transistor. Almost all studies concerning spintronic devices mention the so-called Datta—Das transistor,[157] that is, a ballistic (without scattering) field-effect transistor as a future spintronic device. Unlike a conventional field-effect transistor, here the emitter is a source of spin-polarized electrons and the collector is a spin filter; depending on the base voltage, the current can be switched on or off. At a nonzero voltage, the emitter injects electrons with oriented spins that precess during the time-of-flight of an electron to the collector. Spin precession is due to the spin-orbit coupling and the voltage applied, which for the moving electrons is transformed into the effective magnetic field (Bychkov—Rashba effect[20,158]). Since the magnetic collector detects electrons with a particular spin orientation, the electric current is an oscillating function of the voltage applied to the circuit. The device proposed was called an electronic analog of electro-optic modulator.

Various improvements of the spin transistor, related to the mutual orientation of the magnetization vectors of the emitter and collector can also be imagined. However, conventional spin-independent electron scattering in the transistor causes mixing of the spin states due to the spin-orbit coupling. Thus, successful operation of the spin transistor is only possible in the ballistic regime; however, in this case the device loses its advantages over conventional ballistic transistor.

The spin transistor was "improved"[159,160] with allowance for the so-called Dresselhaus correction to the spin-orbit coupling for three-dimensional systems, whose crystal lattices are asymmetrical with respect to inversion of the spatial coordinates. In this case, coherent carrier transport between coupled channels creates an additional spin

precession and at the same Rashba and Dresselhaus constants in the spin-orbit coupling scattering becomes spin-independent, so the spin transistor can now operate in the non-ballistic regime.

Though fabrication of spin transistors faces some problems such as stray magnetic fields and low efficiency of spin injection, the results of recent experiments show that these difficulties can be avoided using novel DMS.

Spin-dependent light-emitting diode. A spin diode and a bipolar transistor have been reported.[161] The materials used were a semimagnetic *n*-type semiconductor Be—Mn—Zn—Se with 100% spin polarization at 30 K in a magnetic field of 2 T [162] and a dilute magnetic semiconductor *p*-$Ga_{1-x}Mn_xAs$ with $T_C > 100$ K and 98% spin polarization at room temperature and a Zeeman splitting of 100 meV. These devices seem to be promising for magnetic sensors, non-volatile memory devices, and reprogrammable logic devices. The aim of current research is to achieve technological integration of optical and magnetic characteristics. Opto-electronics employs a light-emitting diode in which the electron-hole recombination causes spontaneous emission of light (silicon light-emitting diode[163]). Magnetoresistive transducers that employ electron spin polarization have also been reported.

Spin valve based on organic semiconductor. Compared to traditional materials such as Si, organic semiconductors are easier to produce and their resistivity can also be changed by doping. The first organic semiconductor spin valve[164] is based on an organic semiconductor made from Al and 8-hydroxyquinoline (100 nm thick) sandwiched in between ferromagnetic layers (Co and La—Sr—Mg-based alloy). This organic material is processable because it is used in some light-emitting diodes and TV displays. As the orientation of the electrode magnetizations changed from antiparallel to parallel, the electric current increased by 40%, thus exhibiting a GMR effect. This organic spin valve operates at temperatures between −262 °C and −40 °C and can be arranged on a chip with a surface area of 1/3 square inch.

Spin-valve luminescent transistor[165] modulates the luminescence intensity in the near IR region depending on the magnetic field applied. High sensitivity to magnetic field (200% optical signal modulation on a change in the magnetic field by tens of Gauss) and a relatively small size (900×900 μm^2) of this transistor offer prospects for remote detection and imaging of magnetic fields and for fabrication of magnetic memory devices with optical data output channel. Similarly to a conventional transistor, the new device comprises a nano-assembled collector, an emitter, and a base. The collector is a p—i—n-junction grown by molecular beam epitaxy on GaAs substrates. The *p*-type impurity content in the AlGaAs layer is an order of magnitude higher than the *n*-type impurity concentration; therefore, this is a hole-rich heterostructure. By increasing the *n*-type impurity concentration it is possible to extend the lifetime of the incoming electrons and thus to enhance the efficiency of electron-hole optical recombination at the center of the transition (GaAs layer 10 nm thick) and, hence, the intensity luminescence. The transistor´s base comprises two NiFe and Co magnetic layers 5 nm thick obtained by high-temperature vacuum deposition and forms a Schottky contact with the collector. The emitter (Al layer 6 nm thick) was deposited on an insulating Al_2O_3 layer 100 nm thick, which separates the emitter and the base. As a voltage is applied, electrons move from the emitter to the collector and recombine with the excess holes, thus emitting photons that are detected. The problem is of what happens to the electron current as it passes through two ferromagnetic layers. If the NiFe and Co layers are magnetized in parallel, the spin-polarized electrons moving from the emitter pass through the base to the collector without scattering. Antiparallel magnetization of the NiFe and Co layers causes a decrease in the electron current and a 200% decrease in the luminescence intensity (experimentally observed). This device combines a spin-valve transistor and an optical output.

Spin photocurrents. Numerous results of studies on the spin photocurrents (also known as circular photogalvanic effect) were reported in a review.*

Detection of spin-polarized electric current in semiconductor layers irradiated with circularly polarized light was reported.[166] The effect originates from a specific property of the materials with the quantum wells formed by the "sandwich' of different semiconductors. Namely, electrons with antiparallel spin orientations acquire differently directed velocities owing to asymmetry of the crystal lattice. Then circularly polarized laser radiation directed perpendicular to the quantum well plane results in a spin-polarized electron beam. By changing the light polarization it is possible to reverse the spin current. This effect can be used for fabrication of circularly polarized light driven spin logic switches.

Theoretically, the spin current can be generated by two-beam laser irradiation of the electron system in the semiconductor.[167] Using interference of the laser beams, one can not only produce electron spin polarization and spatial orientation of electron spins but also generate the electron spin current without electric voltage.

All-optical magnetic resonance. Nearly five decades experimental NMR techniques have employed radio-frequency electromagnetic fields for orientation of the magnetic moments of atomic nuclei. With allowance for the electron spin degrees of freedom the NMR technique can be improved as follows. One laser excites the electron spins whose magnetic moments cause orientation of the spins of the nearest nuclei owing to the hyperfine cou-

* S. Ganichev and W. Prettl, http://arXiv.org/cond-mat/0304268.

pling. During the process, the nuclei are controlled by the second laser beam. This method was first demonstrated taking GaAs semiconductor as an example.[113] This basically new alternative to conventional NMR considerably enhances the resolution of the technique, because light can be focused much better than the radiofrequency electromagnetic fields. All-optical NMR provides the possibility of coherent manipulation of individual nuclear spins, being a step toward establishment of optical control over spin-polarized nuclei in solids.[168]

Microwave radiation in spintronics. A magnetic multilayer nanoscale heterostructure can transform electric current into high-frequency magnetic waves, *i.e.*, nanomagnets can serve as sources of the spin-polarized current driven microwave radiation.[169] Experiments were carried out with a copper nanorod with elliptic cross-section (principal axes 130 and 70 nm long) in which a layer of "thick" (40 nm) Co ferromagnetic film with the magnetization directed perpendicular to the axis of the cylinder and a layer of thin Co magnetic film (3 nm thick) were separated by a short distance. A weak dc current (~1 mA) was passed along the nanorod axis. After passage through the thick magnetic layer, electrons were found to be spin polarized and the spin polarization was transferred to the thin Co layer. As a result, the magnetization of the thin layer began precession and emission in the microwave range. A microwave detector integrated with the circuit detected this emission whose frequency varied over a wide range up to ~18 GHz depending on the electric current strength and the external magnetic field applied. Earlier, the spin precession dynamics in the microwave region was studied by exposing the material to microwave radiation. The reverse effect, namely, microwave emission generated by the nanomagnet magnetization precession was studied.[169] The results obtained permitted evaluation of the intensity of oscillations at different frequencies as function of the electric current and magnetic field and comparison of the estimates with the results of calculations. Technological applications require that the threshold current density (10^7 A cm^{-2}) be reduced to 10^5—10^6 A cm^{-2} while the power of the output signal be increased, although being forty times higher than room-temperature noise. This effect can be employed in spintronic nanodevices for generation of microwave emission and in various oscillators.

On spin currents. In contrast to the electron charge, the electron spin can be transferred with a low energy loss. For instance, the spin relaxation time in semiconductor GaAs is 100 ps (three orders of magnitude longer than the hole lifetime). Therefore, a topical problem in spintronics is to study the laws of spin motion. It was proposed[170] that an electric field applied to a semiconductor will produce a flow of electron spins due to the spin-orbit coupling and topological effects. The direction of the spin current is determined following a rule according to which the electric field strength, spin orientation, and spin current density vectors must be mutually perpendicular. Seemingly, the voltage applied to the semiconductor to control the dissipation-free motion of electron spins (spintronics) can be used instead of using voltage for electron transfer (electronics).

However, strictly speaking, the electron spin is not conserved in the presence of spin-orbit coupling. Therefore, one must critically look at calculations of the spin currents. Switching on the electric field disturbs symmetry of the system relative to inversion of the spatial coordinates. Therefore, in the case of time reversal both the direction of current and the spin orientation change, *i.e.*, the spin current is conserved. The conductivity and electric field strength appeared in the Ohm law remain unchanged on time reversal, which eventually causes unavoidable release of the Joule heat. On the contrary, the spin conductivity relating the spin current density to the electric field strength appears to be[170] dissipation-free as in, *e.g.*, the superconductor. However, the spin currents derived cannot serve as transport currents, *i.e.*, they cannot be used for spin tansport and spin injection into materials. Indeed, persistent spin currents in the semiconductors, whose crystal lattices have no center of inversion (*e.g.*, GaAs and GaP with zinc blende structures), must also exist in the thermodynamic equilibrium state without external electric fields. Thus, although being dissipation-free, the spin currents proposed[170] appear to be pure background currents. Rigorous calculations showed that the background spin currents do not contribute to spin transfer both in the two-dimensional[143,171] and in one-dimensional[172] cases.*

Giant planar Hall effect. In the normal Hall effect the current flowing through a planar conductor is deviated by the magnetic field applied perpendicularly to both the direction of the current and the plane of the conductor. As a result, the resistivity of the sample along some directions decreases. This type of the magnetoresistance anisotropy is observed in magnetic metals, being rather weak. The anisotropy effect observed in the experiments[173] with the dilute magnetic semiconductor (Ga,Mn)As at 45 K was found to be four orders of magnitude stronger than in ferromagnetic metals. This effect called giant planar Hall effect can favor the development of improved versions of magnetic resonance spectroscopy, fabrication of magnetic transducers and, probably, elements of solid-state quantum computers based on DMS.

Supergiant magnetoresistance effect. In ballistic magnetoresistance the size of a sensor can be reduced to the size of a cluster of ferromagnetic atoms connected by two wires. Here, the term "ballistic" means that the size of the sensor is less than the scattering length of electrons; because of this, the electron trajectories are straight lines.

* A. V. Ivanov, *Scientific.ru*, 16.04.04, http://www.scientific.ru.

Hence, electron scattering is due to the magnetic effects rather than collisions with the atoms of the sensor or with impurities in the transducer. This significantly enhances the sensitivity of information reading process. Spin-polarized electrons moving through the transducer are scattered stronger or weaker (which implies a larger or smaller resistance) depending on the magnetization of the atoms of the electrode material. The ballistic magnetoresistance of nickel nanocontacts was studied experimentally.[174] The sensor is so small (of the order of a few nanometers) that the spin of an electron passing through the contact does not "sense" the spin of the second electrode. But if the latter differs from the spin of the electrode material, the effect of giant magnetoresistance is produces. An enormously high change in the magnetoresistance, up to 3150% (room-temperature effects reach 100% for GMR and up to 1300% for colossal magnetoresistance) was detected. This is the strongest room-temperature spin-dependent magnetoresistance effect ever observed in spintronic devices. Since the size of the transducer is small, the information storage density can be increased to terabytes per square inch.

Tunneling magnetoresistance. A low-temperature study[175] of the tunneling magnetoresistance of a three-layer heterostructure (Ga,Mn)As/GaAs/(Ga,Mn)As at 0.39 K revealed a 290% effect at nearly zero base voltage. The spin polarization was determined from the combined Hanle effect[98] and magneto-optical Kerr effect measurements.

Magnetoresistance measurements of a magnetic tunnel junction $Ga_{1-x}Mn_xAs$ (x = 0.04, 50 nm)/AlAs/$Ga_{1-x}Mn_xAs$ (x = 0.033, 50 nm)[176] with an AlAs layer less than 1.6 nm thick revealed a spin polarization of 75% in $Ga_{1-x}Mn_xAs$ at 8 K. This spin polarization of the DMS is comparable with that of the manganite La—Sr—Mn—O, being greater than those of the classical ferromagnets Fe and Co (<50%), Ni (~30%) and lower than that of the metallic ferromagnetic CrO_2 (~80%) only.

Spin precession and magnetization of nanoscale objects. Information storage in memory devices is based on reversal of the magnetization vector of a certain domain of a magnetic compound involving local magnetic fields. An increase in the recording density in a memory device faces the problem of induction of a controllable magnetic field in a small spatial domain of the compound. The use of magnetic fields produced by local currents requires unrealistically heavy electric currents for the magnetization reversal of the small volume elements of the compound. In this connection, a promising way is to employ spin driven manipulation of the micromagnetization of domains. A number of studies were concerned with the possibility of the magnetization reversal of a small domain of a magnetic substance by spin-polarized electron beam. The magnetic field of such an electron beam is too weak to cause the magnetization reversal, and the dipole interaction between the electron spins and the magnetic moments of atoms is also weak. Here, utilization of the exchange interaction between the beam electrons and electrons of the atoms of the material can appear to be efficient.

Experimentally,[177] spin-polarized photoemission electron beams from GaAs were generated using circularly polarized light and then passed through the suspended Fe, Co, and Ni magnetic films a few nanometers thick, whose magnetizations were perpendicular to the direction of the spin polarization of the beams. A spin filter detected coherent precession of the magnetic moments of electrons in the beam. The reverse effect of the spin-polarized electron beam on precession of the magnetization of a small domain in the ferromagnetic films became pronounced with decreasing the size of the domain. Both the direct and reverse effects can be used for information recording and reading. A switching frequency of tens of gigaHertz seems to be attainable.

Quantum dot spin filter. Spin orientation can be achieved by using the spin-orbit interaction between spins and the crystal lattice of the material, whih allows the design of the spin device to be significantly simplified. For instance, in a spin filter[178] operating without using external magnetic fields, non-polarized electrons are passed through a T-shaped quasi-one-dimensional channel. Partial spin selection of electrons near the channel intersection is due to the spin-orbit interaction. The process can be controlled using an external electrode. When the incident electron energy is in resonance with the quantum dot states at the intersection, the efficiency of spin selection for the trasmitted electrons approaches 100%.

Interest in the spin effects in quantum dots is due to the expected long spin relaxation times. Indeed, here the relaxation mechanism is related either to phonons or to hyperfine interactions between electron and nuclear spins. Transport of electrons through quantum dots must be spin-dependent owing to the Pauli exclusion principle. If the quantum dot contacts the spin-polarized reservoir, one can manipulate the spins of the incident electrons or the spins of the electrons passing out, which changes the electric current flowing through the quantum dot. Hence, the spin state of the quantum dot can be encoded by using an external electron added. *Vice versa*, the spin state of the quantum dot can be probed or changed by adding an electron or by applying an external magnetic field. Such a unique single-charge or single-spin control can play an important role in the future solid-state quantum computers in which the quantum system with two discernible states, capable of storing a bit of information, comprises specially created spin states.[179] It is also of interest to employ electron spins in quantum dots for fabrication of functional elements for quantum computers.[180]

Carbon nanotubes and dilute magnetic semiconductors. Carbon nanotubes are mechanically stable and can resist

the elevated temperatures and electric currents of density up to 10^9 A cm^{-2} (*cf.* ~10^5 A cm^{-2} for normal metals). The first field-effect transistor based on a nanotube with metallic contacts[181] was of low quality owing to the chemical incompatibility of the materials. Electric contacts of the carbon nanotube with the semiconductor material were found to be much more promising and and technologically integrable. For instance, a single-walled carbon nanotube was attached to the GaAs/AlAs and (Ga,Mn)As heterostructures grown by molecular beam epitaxy on GaAs substrates.[182] In fact, a nanotriode was fabricated, in which a dilute magnetic semiconductor, *p*-type $Ga_{0.95}Mn_{0.05}As$ only 20—50 nm thick, acts as an emitter and a collector, the *n*-type GaAs semiconductor layer 20 nm thick being a base. The emitter—collector distance was of the order of 1 μm. The technique permits fabrication of (i) field-emission p—n—p-transistors using carbon nanotubes in which the emitter, collector, and base are chemically compatible semiconductors and (ii) nanolasers with semiconductor cavities made of doped carbon nanotube. Great prospects are offered for fabrication of hybrid devices comprised of nanotubes and semiconductors in traditional semiconductor chips, which is convenient for studies of spin-polarized transport from DMS to nanotubes.

Atomic nuclei and spintronics. The field produced by the magnetic moments of atomic nuclei (Overhauser field) governs the effective Zeeman spin splitting of electronic states and eventually the spin polarization of a nanoscale object. A new mechanism was proposed[183] of manipulation of electron spins in nanostructures by using a spatially nonuniform distribution of the atoms of isotopes with nonzero nuclear spins. Polarization of the nuclear spins in a small domain of a semiconductor material creates a local potential attracting electrons with a particular spin orientation and repulsing electrons with antiparallel spin orientation. As a result, the polarized nuclear spins produce an effective magnetic field, which can create bound electron, whose energies are up to a few meV in semiconductor nanoscale objects of size greater than 200 Å. Such spin-dependent potentials can form a new type of spin nanostructures, namely, spin quantum dots, spin quantum wells, *etc.*, in real time using coherent polarization or depolarization of nuclear spins. Thus it makes possible spin engineering of nanoscale objects with polarized nuclear spins. Here, the magnetic field of atomic nuclei strongly influences the electron spins, resulting in magnetization of the nanoscale objects, although the Overhauser field does not manifest itself due to small nuclear magnetic moments.

Manipulation of nuclear spins. Compared to magnetic fields, electric fields are much easier to induce and control. Therefore, electric-field controlled manipulation of nuclear spins is desired. The first step in this direction was reported in Ref. 184. First, a laser pulse polarizes electron spins in an $Al_xGa_{1-x}As$ quantum well. A disk of polarized electrons of radius 2000 nm and 20 nm thick, formed in the quantum well can be transferred with nanometric accuracy by varying the voltage applied. The atomic nuclei confined within the domain filled with the polarized electrons will also be polarized, being aligned with the electron spins. As a result, position of a small domain comprised of ten polarized nuclei can be exactly located and changed by applying an electric voltage. Such thin layers of polarized nuclei can appear to be the main element of storage/memory devices based on nuclear spins.

Quantum computer and nuclear spins. The idea of quantum computing[185] has been the subject of keen discussion since 1986.[186] It was proposed[185,186] to employ operations with the states of a quantum system, each of them being a superposition of states in contrast to the classical system. However, a boom of projects of quantum computers began after a lecture and publications by P. Shor[187] who proposed an algorithm for factoring large *n*-digit numbers into their prime components. The amount of operations needed to solve the problem using modern computers grows as an exponential function of the size of the number. It is complexity (nonsolvability) of this problem for modern computers that is employed in encrypting information in cryptographic systems. A quantum computer needs n^3 operations to solve the problem, with the speedup coefficient that can be very large at large *n*. At the same time there are algorithms executed on traditional computers, which do not accelerate on quantum computers. Shor´s algorithm seems to provide an example of the phenomenon where the complexity class of a task changes basically depending on which physical princilpes underlie computations. When using a traditional computer, the task belongs to the same class, whereas the quantum nature of qubits (a quantum bit, or qubit, is the smallest amount of information in quantum computing) in the quantum computer significantly accelerates the process of computation. Having intrinsic parallellism in large-scale computations, the quantum computer can decode almost any message. The use of quantum logic cells for information recording, storage, and writing will provide in the future fabrication of quantum memory devices capable of self-correcting errors and suitable for eternal information storage.

To date, a number of projects of quantum computers was proposed,[188] based on different matrix materials including liquids (helium) and solids. To realize a solid-state quantum computer, one would employ the experience of microelectronic technology. Then, quantum computers could be similar to microchips. The goal of most studies in this field is to integrate modern microelectronics technologies with quantum computing ideas with spintronics underlying research efforts. It is of great importance that materials for quantum computers based on ferromagnetic semiconductors don´t need have high T_C.

In solid-state quantum computers information can also be encoded by nuclear spins because they interact with the environment weaker than do the electron spins and therefore retain their state for a longer time. In addtion, small magnetic moment of a nucleus can be more readily reoriented by external magnetic fields compared to the magnetic moment of an electron. If one treats the nuclear spins I of a donor impurity in the semiconductor as qubits, the atomic nuclei of the semiconductor must have $I = 0$ to prevent possible spin-spin interaction. This excludes all type III—V semiconductors from being candidates for the matrix material because none chemical element has stable isotopes with $I = 0$ in this case. To this end, silicon seems to be the most appropriate element because methods of preparation of isotopically pure ^{28}Si ($I = 0$) have been best developed compared to other technologies and considerable experience in fabrication of nanoscale objects has been accumulated. The only shallow donor in Si is the ^{31}P isotope (spin $I = 1/2$). At a low ^{31}P concentration and $T = 1.5$ K, the electron spin relaxation time in the Si—^{31}P system is of the order of 10^3 s while the ^{31}P spin relaxation time exceeds ten hours. Seemingly, at temperatures about 1 mK the ^{31}P spin relaxation time limited by the interaction with phonons only will be of the order of 10^{18} s, which makes this system unbeatable for quantum computing.[189] Low temperatures favor computations involving nuclear spins because it excludes the ionization of donors. Then, the conduction electrons are accumulated near the donor nuclei, thus providing a sufficiently strong HFC between the electron and nuclear spins. On this basis it was proposed to use the ^{31}P nuclear spins injected into a single crystal of isotopically pure silicon as qubits for the quantum computer.[190] Qubits were manipulated by using static magnetic and electric fields and a radio-frequency magnetic field. At $T \approx 0.1$ K, a silicon plate was placed in a constant magnetic field $B_0 \geq 2$ T, in which nearly 100% of electron spins were polarized; the nuclear spins were ordered *via* the hyperfine exchange interaction with the electron spins. The results obtained were quite unpretending, namely, one- or two-qubit spin interactions. The authors of Ref. 191 improved the ideas[190] using electron spin resonance in epitaxial Si/Ge heterostructures with the electron energy bands dependent on the composition of the material.

Possible alternatives. Though such DMS as (GaMn)As, (GaMn)P, and (GaMn)N have sufficiently high T_C, they also have defect structures and are crystallochemically incompatible with silicon. At the same time silicon is a nonmagnetic substance and attempts at doping of silicon with magnetic impurities led to destruction of the crystal structure, the multiphase composition of the sample, and reduction of conductivity.

Potentially, an alternative to DMS is provided by transition metal monosilicides. For instance, compounds $Fe_{1-x}Mn_xSi$ and $Fe_{1-y}Co_ySi$ based on the narrow-gap insulator FeSi, in which iron atoms are replaced by Mn or Co atoms in the whole range of concentrations, were reported more than two decades ago.[192] Recently, detailed studies of the magnetotransport properties of these substances have begun in relation to spintronics demands.[193] At $x < 0.8$, the alloy $Fe_{1-x}Mn_xSi$ remains a p-type paramagnetic down to 1.7 K. Compound $Fe_{1-y}Co_ySi$ is characterized by elelctronic conductivity, being at $y < 0.3$ a helicoid magnetic with a long-period structure and a highest transition temperature of 53 K. Metallic magnetic $Fe_{1-y}Co_ySi$ with $T_C = 53$ K and the best studied DMS (Ga,Mn)As with $T_C = 110$ K are strongly different in current carrier density ($1.5 \cdot 10^{20}$ for (Ga,Mn)As and $4.4 \cdot 10^{21}$—$1.3 \cdot 10^{22}$ cm^{-3} for $Fe_{1-y}Co_ySi$) and in effective masses of current carriers ($0.5m_e$ and $0.08m_e$ respectively for the heavy and light holes in (GaMn)As and $30m_e$ for $Fe_{1-y}Co_ySi$). Nevertheless, $Fe_{1-y}Co_ySi$ and (GaMn)As have similar magnetizations and the magnetic field affects the electric properties of $Fe_{1-y}Co_ySi$ and (GaMn)As in a similar fashion. The Co-enriched material $Fe_{1-y}Co_ySi$ retains the crystal structure of the FeSi matrix, thus providing yet another route to preparation of spintronic materials.

3. Magnetic spintronic materials

3.1. Requirements for spintronic materials

Being an interdisciplinary field of science and technology, spintronics has been the subject of intensive studies carried out in a continuously increasing number of research laboratories. At present, computer hard disks, reading heads, and MRAM chips are produced based on ferromagnetic metallic alloys belonging to the first generation of spintronic materials. More than 90% of hard disks contain platinum. It is the properties of the Co—Pt alloy that make possible production of hard disks with information capacity greater than 20 Gb. If the thermal stability of the properties is important, computer disks are produced from magnetic materials based on the Sm—Co alloy. The major drawback of this type of hard disks is high cost of samarium and cobalt, which hampers wide use of these alloys. GMR reading heads are produced using films of Fe—Ni magnetic alloys with specified compositions, characterized by the saturation induction which is two to four times greater than that of the widely used ferromagnetic alloy permalloy. The major drawback of these spintronic materials is that they are metals.

Most ferromagnetic materials are metals. First of all, these are elemental ferromagnets (nine elements including three 3d-metals, namely, Fe, Co, and Ni and six 4f-metals, that is, Gd, Dy, Tb, Ho, Er, and Tm) and a large number of metallic alloys and compounds. Most non-metallic magnetic materials are antiferromagnets or ferrimagnets. A ferrimagnet (antiferromagnet) is a material with antiparallel spin orientations of the magnetic

ions in different magnetic sublattices and different (equal) magnetic moments of the sublattices, which provides a nonzero (zero) total magnetization in the magnetically ordered state. Ferrimagnets (*e.g.*, magnetite Fe_3O_4) have long been known, whereas actually experimental studies of antiferromagnetism began in 1938 taking MnO as an example.[194] Usually, ferrimagnets have the crystal structure of spinel AB_2O_4 in which spins of the magnetic ions in the tetrahedral (*A*) and octahedral (*B*) cation sites have antiparallel orientations. Non-metallic properties of magnetite $FeFe_2^{2+/3+}O_4$ and, hence, retention of the band gap both below and above the Vervey charge phase transition temperature ($T_V \approx 120$ K), and a ferrimagnetic—metal phase transition at 865 K are due to strong exchange and Coulomb interactions between electrons in the non-filled atomic shells of the Fe ions.[195] Interest in magnetite as a spintronic material increased after experiments[196] that revealed a giant negative magnetoresistance effect in nanocontacts at room temperature. Magnetic hysteresis permits the use of magnetite for production of memory elements and switches in spintronic devices. In this connection mention may be made of the synthesis of the first dilute ferrimagnetic semiconductor $[ZnGa_2O_4]_{1-x}[Fe_3O_4]_x$ * based on the semiconductor spinel $ZnGa_2O_4$ with a band gap of 4.1 eV[197] and $T_C \approx 200$ K at $x = 0.15$.

In spite of practical use of the first-generation spintronic materials mentioned above, they possess no useful semiconducting properties employed in microelectronics. They can hardly be doped and cannot be used for signal enhancement in semiconductor devices. The magnetic properties of these materials are preset by the magnetic sublattice characterized by ordered arrangement of the magnetic ions.

At present, the key problem in spintronics is the lack of novel ferromagnetic materials possessing a necessary combination of the semiconductor, magnetic, and optical properties. As mentioned above, magnetic semiconductors (inlcuding novel materials) exhibit interesting effects that underlie a number of spintronic devices proposed. However, until now wide use of these devices is hampered by the lack of magnetic semiconductors suitable for retention of the necessary operating properties at temperatures somewhat exceeding room temperature. Efforts into the development of spintronics on the basis of traditional semiconductor matrices appear to be inefficient since most of these materials are ferromagnets at very low temperatures or non-magnetic at all. And since the operating temperatures of, *e.g.* the surface components in computers can be as high as 50 °C, the production of cooling systems would make computers bigger and more expensive.

The present-day demands for the Curie temperatures, T_C, of ferromagnetic spintronic materials are similar to the earlier requirements for the operating temperatures of materials for solid-state electronics. For instance, the operating temperatures of germanium transistors were at most 70 °C. Because of the lack of methods for the surface passivation the operating characteristics of these transistors were unstable, especially at elevated temperatures, and transistors *per se* were non-durable. Only replacement of germanium by a new semiconductor, silicon, after elaboration of methods for the synthesis of ultrapure Si (to 10^{-6} at.% of impurities) allowed the operating temperature of transistors to be increased to 120—150 °C at stable characteristics. Elaboration of planar technology permitted a reliable protection of the surface of the silicon crystal against the action of external medium by a thin SiO_2 film; then, chips were fabricated, which marked a revolution in microelectronics.

There are at least three criteria that must be met by the most promising spintronic semiconducting materials[198]:

1) ferromagnetic properties of these materials containing both *n*- and *p*-type mobile current carriers must be retained at the operating temperatures of semiconductor devices (above room temperature);

2) among technologically important are relatively simple and inexpensive synthetic routes to spintronic materials and methods of integration of items with conventional semiconductor circuits;

3) it is desired that ferromagnetic semiconductors not only possess the necessary magnetic properties but also retain the structure and physicochemical properties of the starting semiconductor matrices without deterioration of their useful characteristics.

The use of the complex growth techniques and high-level experimental methods for the synthesis of spintronic materials is expensive. Ferromagnetic semiconductors for spintronics applications are as a rule synthesized using expensive vacuum deposition techniques including molecular beam epitaxy, laser irradiation, and ion implantation. At the same time traditionally the most widely used method for the preparation of chemical compounds is relatively fast and cheap synthesis of samples with controlled compositions and structure from high-purity powders. Versatility of these methods makes them perfect for the synthesis of substances with specified properties and characteristics. Production of cheap spintronic materials requires a close collaboration of physicists, chemists, materials scientists, and engineers and integration of the principles of spintronics with technology of novel ferromagnetic semiconductors.

3.2. Concentrated magnetic semiconductors

Design of a material exhibiting the properties of a ferromagnet and a semiconductor (coexistence of the spin and charge degrees of freedom) is an age-long dream.

* A. S. Risbud and R. Seshadri, http://arXiv.org/cond-mat/0404147.

However, the first ferromagnetic semiconductor $CrBr_3$ with $T_C = 37$ K was synthesized as long as 1960.[199] The second generation of spintronic materials is represented by ferromagnetic semiconductors.

The family of concentrated magnetic semiconductors (CMS) comprises europium and lead chalcogenides, chromium-chalcogenide spinels (*e.g.*, $CdCr_2Se_4$, $CuCr_2S_4$), and a number of transition metal oxides (manganites) and pnictides[57] in which the magnetic ions have own magnetic sublattices.

In EuO and europium chalcogenides EuX (X = S, Se, Te)[200—202] the internal magnetic field of the Eu^{2+} ions can produce a giant Zeeman splitting of the spin subbands (nearly 0.5 eV for EuS).[200,201] In the mean field approximation, the energy of the total spin splitting between two subbands in the electron spectrum is given by the expression $E = g\mu_B H + 2J\vec{s}\langle\vec{S}\rangle$, where the first term is the Zeeman spin splitting due to the external magnetic field H and the second term describes the magnetic interaction between the spin $\vec{s}$ of the conduction electron and the averaged magnetization $\vec{S}$ of magnetic ions, which is "sensed" by the electron owing to the magnetic exchange interaction J. The second term is much larger than the first one. It is the interaction described by the second term that is the reason for giant changes in the energies between the band electrons with antiparallel spin orientations. Because of this, magnetic insulators are efficient spin filters in, *e.g.*, metal/magnetic insulator/metal heterostructures.[203] However, europium chalcogenides are of limited use owing to low T_C that are much lower than room temperature.

The Curie temperatures of chalcospinels are somewhat higher, namely, 84.5 K for $CdCr_2S_4$, 106 K for $HgCr_2Se_4$, and 130 K for $CdCr_2Se_4$. The Curie temperatures of semiconducting materials $CuCr_2Se_{4-x}Br_x$ exceed room temperature but the materials are unstable in air. Of interest are also the families of multicomponent semiconductor solid solutions based on ferromagnetic compound $CuCr_2S_4$ ($T_C = 367$ K) and antiferromagnets $Cu_{0.5}M_{0.5}Cr_2S_4$ (M = In, Ga, Al) or ferrimagnets $CoCr_2S_4$ and $MnCr_2S_4$, which possess above-room-temperature ferromagnetism.[57] But, having retained some properties of the ferromagnetic matrix $CuCr_2S_4$ with *p*-type conductivity, they are still far from meeting purity requirements for electronic materials.

A number of transition metal compounds with ferromagnetic or ferrimagnetic order, namely, magnetite Fe_3O_4 (see above),[204] CrO_2,[205] Geissler alloys X_2YZ (see Section 1.5),[206] and pnictides MnAs,[207] MnSb,[208] CrAs,[209] and CrSb[210] are also attractive for spintronics applications. These materials are called semimetals and half-metals.

Unfortunately, the properties of the Geissler alloys are unstable and vary over a wide range depending on the stoichiometry. Only Ni_2MnGa has a Curie temperature exceeding room temperature and exhibits a good hysteresis.[211] Other compounds exhibit a non-classical temperature dependence of magnetization and their properties cannot be described using the available models. Ferromagnetism in Geissler alloys disappears on disordering of magnetic ions. Synthesis of thin films of these materials on semiconductor substrates is also a complicated task. The exclusion is Ni_2MnSb with $T_C \approx 730$ K, which was studied in order to reveal tunneling effects.[212]

A number of complex oxides possess ferromagnetism with relatively low Curie temperatures. These are $BiMnO_3$ ($T_C = 105$ K),[213] $GeCuO_3$ ($T_C = 26$ K),[214] $YTiO_3$ ($T_C = 29$ K),[215] and EuO ($T_C = 79$ K).[216] Recently,[217] it was found that CuO doped with Mn (3.5—15 at.%) also exhibits ferromagnetism with $T_C = 80$ K. Transition metal and rare-earth element oxides, fluorides, and phosphides are poorly compatible with the semiconductor technologies in physicochemical parameters. The properties of these and other semimetals are briefly outlined in Ref. 218.

At present, only one oxide, CrO_2, simultaneously possesses metallic properties and ferromagnetism. Though this compound is widely used in recording devices, until recently its electronic structure was poorly studied and band structure calculations predicted semimetalic properties.[219] Chromium dioxide is a saturated ferromagnet (one spin subband is completely filled, whereas the other is empty), at least at low temperatures. Experimental photoemission studies show that at room temperature 80% of spins in CrO_2 remain polarized. Because of this CrO_2 is of paramount interest as a material for spintronic devices.[220] Chromium dioxide ($T_C = 400$ K) crystallizes in the rutile structure and has an integer magnetic moment of 2 μ_B per Cr ion. This material is obtained in the form of a single-crystalline film epitaxially grown on rutile substrates;[221] textured CrO_2can be grown on sapphire (Al_2O_3) substrates.[222] It is unknown whether is it possible to obtain CrO_2 in the form of a textured or epitaxial thin film on GaAs or Si. The material exhibits complex magnetotransport properties.[205,223] The dependence of the Hall resistance on the magnetic field differs from that characteristic of the ferromagnetic metal in the temperature range from helium temperatures to 100 K and has both the hole and electron contributions. Consideration in the framework of the two-band model shows that CrO_2 has highly mobile holes that move coherently with more abundant but less mobile electrons, *i.e.*, the band structure of the material appears to be more complex than that predicted by calculations. However, all spin-polarization related kinetic characteristics[224] and the results obtained by tunneling spectroscopy[225] indicate that at low temperatures all carriers in CrO_2 are spin polarized. Thus, CrO_2 can be a candidate for being a source of spins or a spin detector in spintronic devices.

Manganites based on antiferromagnetic matrices $AMnO_3$ (A is REE) doped with Ca, Sr, Ba, *etc.*, are also

of interest as spintronic materials. Applied value of these materials is due to the possibility of fabrication of high-quality thin films and to colossal negative magnetoresistance of some heavily doped manganites at room temperature. These materials possess specific properties. Namely, being heavily doped, a number of them are ferromagnets with $T_C \approx 350$ K; however, they undergo structural transitions depending on the degree of doping and on the magnitude of external magnetic field. But manganites are poorly integrable with semiconductor microelectronic devices owing to differences in crystallochemical parameters.

Compared to perovskites $AMnO_3$, ferromagnetic semimetallic transition metal oxides having the double perovskite structure $A_2BB'O_6$ (A is an alkali-earth metal ion and B and B′ are transition metals) and possessing room-temperature magnetoresistance effects can appear to be more attractive for spintronics. For instance, the Curie temperature of Sr_2FeMoO_6 is 420 K,[226] whereas that of Sr_2CrReO_6 is 635 K.[227] Sr_2CrReO_6 films fabricated by magnetron sputtering on $SrTiO_3$ substrates exhibit a T_C of 620 K.[228] A homogeneous polycrystalline material Sr_2FeMoO_6 (T_C = 416 K) has a magnetoresistance effect of 45% at 5 K (H = 9 T) and of 6.5% at room temperature (H = 0.3 T).[229] Doping with Al permits an increase in the magnetoresistance of $Sr_2Fe_{1-x}Al_xMoO_6$ (x = 0.15) to nearly 60% at 5 K (H = 1 T) and improvement of electron transport properties.[230]

Differences between the crystal structures of normal semiconductors GaAs and Si and the CMS or semimetals and half-metals prevent the latter from being integrated into semiconductor heterostructures for spintronics applications.

3.3. Semimagnetic semiconductors

In spite of the fact that CMS possess a number of interesting spin-related properties, these materials do not meet requirements imposed by semiconductor engineering. Spintronics applications require thick films, layers, and quantum dots that retain the useful physicochemical properties of semiconductors. Therefore, it is important to synthesize and study such magnetic semiconductors that are compatible with tetrahedrally coordinated semiconductors and mechanically stable against structural distortions. Of considerable interest are magnetic semiconductors based on type $A^{II}B^{VI}$ and $A^{IV}B^{VI}$ (A^{II} = Zn, Cd, Hg; A^{IV} = Pb, Sn; B^{VI} = S, Se, Te) matrices, namely, CdMnSe, CdMnTe, PbSnMnTe, *etc.*, in which the transition metal ions Fe^{2+}, Co^{2+}, or Mn^{2+} randomly replace the A-elements in the lattice sites. For instance, doping with manganese (compound $Zn^{2+}{}_{1-x}Mn^{2+}{}_xSe$) introduces into the matrix only randomly distributed spins S = 5/2, leaving the charge carrier density in the semiconductor unchanged. These semiconductors are sometimes called semimagnetic semiconductors because their magnetization can be readily changed by applying external magnetic fields but the materials retain the characteristics of the semiconductor matrix. Considerable attention was paid ro $Cd_{1-x}Mn_xTe$ with a high solubility of Mn (up to 77%). Many properties of these materials are due to the exchange interaction between the d-electrons responsible for the local magnetic moments and the conduction electrons or holes in the valence band. Owing to predominant antiferromagnetic exchange interaction between magnetic ions most $A^{II}B^{VI}$-based semimagnetic semiconductors appeared to be weak ferromagnets with $T_C < 10$ K,[231–233] antiferromagnets, paramagnetics, or even spin glasses (see reviews[135,234]) depending on the concentration of magnetic ions.

Spin glasses are materials characterized by relatively stable arrangement of randomly oriented spins, which is established at temperatures below the so-called glass transition temperature. Metallic spin glasses were discovered in the experiments on light doping of noble metals with transition metals. Here, an indirect magnetic exchange interaction between spins of the localized transition metal ions occurs involving the conduction electrons (so-called Ruderman—Kittel—Kasuya—Yosida, or RKKY interaction[235–237]) with the energy

$$H = -J_{RKKY}\vec{S}_1\vec{S}_2 = \\ = -9\pi\frac{(nJ)^2}{\varepsilon_F}\frac{2k_FR\cos(2k_FR) - \sin(2k_FR)}{(2k_FR)^4}\vec{S}_1\vec{S}_2,$$

where J_{RKKY} is the constant of the RKKY spin-spin interaction, J is the parameter of the exchange interaction between a shared charge carrier (conduction electron in the case of spin glasses) and a localized electron (in the vicinity of an ion the spin orientations of the conduction electrons are parallel to the spin orientation of the magnetic ion), k_F is the Fermi wave vector related to the volume density of free carriers n ($k_F \propto n^{1/3}$), $R \propto 1/x^{1/3}$ is the distance between two spins, $\vec{S}_1$ and $\vec{S}_2$, of the magnetic atoms with the concentration x, and $\varepsilon_F = (\hbar k_F)^2/(2m)$ is the Fermi energy.[238] At high current carrier density and low concentration of magnetic atoms, one has $k_FR \gg 1$ and the RKKY interaction becomes oscillating in character and weakens with the spin-spin separation

$$H \propto -\frac{J^2}{\varepsilon_F}\frac{\cos(2k_FR)}{(2k_FR)^3} \sim x\cdot\sqrt[3]{n},$$

i.e., in the spin glass state the interaction between spins of different pairs of the transition element atoms can be both ferromagnetic and antiferromagnetic. The oscillating character of indirect RKKY exchange interaction provides a correct explanation for magnetism of rare-earth metals. And *vice versa*, at high concentrations of spin carriers (magnetic impurities) and low charge carrier densities

one gets $k_F R \ll 1$, the indirect magnetic RKKY exchange always being ferromagnetic in character, *i.e.*, no spin glass state is formed and one deals with the Vonsovsky—Zener double exchange. In this case the concentration dependence of the RKKY interaction has the form $J_{RKKY} \sim n \cdot \sqrt[3]{x}$. Though, in principle, memory elements can be based on spin glasses, the glass transition temperatures of these materials are low. The RKKY interaction manifests itself provided that the exchange parameter is smaller than the Fermi energy ($J \ll \varepsilon_F$) or the band gap, which holds for metals and spin glasses but not for novel magnetic semiconductors (here, $J \gg \varepsilon_F$). Then, the RKKY interaction is inefficient near the critical temperatures of magnetic disordering because in these regions damping of free electrons simulated by de Broglie planar waves is significant. Despite the fact that the RKKY interaction was theoretically proposed nearly five decades ago, direct experimental confirmation of the existence of this interaction was obtained only recently. The RKKY spin polarization of conduction electrons was first detected[239] in the GMR measurements of heterostructures containing REE (Dy, Gd, Nd) layers. Spin glasses also exhibit a giant Zeeman splitting and can be used for fabrication of ferromagnetic—normal semiconductor contacts and other hybrid systems possessing ferromagnetic and semiconducting properties.[240—242]

Strong exchange interactions in the doped type II—VI paramagnetic materials also favor high spin polarization of carriers in external magnetic fields. Indeed, though a strong exchange interaction between the Mn 3d states and the semiconductor states causes no ferromagnetic ordering of the Mn moments, an external magnetic field polarizes the manganese spins; the intrinsic magnetic field of the Mn spins causes a giant spin splitting. For instance, the spin splitting in (BeZn,Mn)Se is 400 mRy,[138,243] being five orders of magnitude larger than the characteristic Zeeman energy of elementary magnetic moment in 1T magnetic field. A combination of strong exchange interaction between the Mn 3d states and the carriers in the semiconductor matrix with very low temperatures (or even absence) of magnetic phase transitions makes semimagnetic semiconductors based on type II—VI and IV—VI matrices very interesting objects suitable for studies of exchange interactions. This class of materials is also appropriate for fabrication of spin injection devices. Doped materials based on type IV—VI matrices also exhibit low-T_C ferromagnetism, but these materials and their heterostructures including widely used semiconductors can hardly be synthesized.

Passage to type II—VI binary compounds (hosts for semimagnetic semiconductors) is illustrated in Scheme 1 (second line): atoms of Group IVa elements are replaced by their second neighbors on the left and on the right in the Mendeleev periodic system. Synthesis of spintronic materials based on the isoelectronic type I—III—VI_2 matrix (lowest line), *e.g.*, $CuGaTe_2$ with well-studied phase diagram is also of interest.

Scheme 1

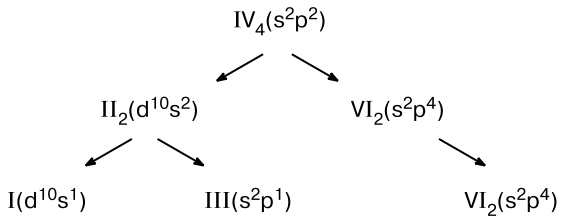

Although semimagnetic semiconductors based on type II—VI matrices can also serve as spin filters or for spin transport,[138] their use as sources of polarized spins in spintronic semiconductor devices is inefficient.

Seemingly, an epitaxially growth semimagnetic semiconductor (Zn,Mn)Te confirms this conclusion because the highest T_C is reached at a *p*-type carrier density of $1.53 \cdot 10^{19}$ cm^{-3}, being only 2.4 K.[244] But the discovery of ferromagnetism in the DMS (Zn,Cr)Te [245] shows some promise of the future of these materials in spintronics. Detailed magnetization and magneto-optical response measurements of (Zn,Cr)Te at a Cr concentration, *x*, of 0.2 revealed a Curie temperature of 300±10 K.[246] Interest in the magnetic semiconductors based on type II—VI matrices also renewed after the discovery of high-temperature ferromagnetism in transition-metal doped ZnO. But most of these materials are inhomogeneous so far (see Section 3.7).

Note that doping of the starting Group IV material with transition metals can also give rise to ferromagnetism. For instance, oriented $Mn_xGe_{1-x}(001)$ films on Ge and GaAs(001) substrates were grown at 70 °C.[154] These temperatures of the substrates rule out the formation of $Mn_{11}Ge_8$ clusters with high T_C similar to room temperature; these clusters are formed at substrate temperatures of 300—350 °C. Mn_xGe_{1-x} materials were characterized by semiconductor *p*-type conductivity with a carrier density of about 10^{19}—10^{20} cm^{-3} at the Mn concentration, *x*, lying in the range $0.006 < x < 0.035$ and exhibited ferromagnetic properties with $25 < T_C < 116$ K depending on the impurity content. Ferromagnetism in $Co_{0.12}Mn_{0.03}Ge_{0.85}$ epitaxial film ($T_C \approx 270$ K) is also of interest.[247]

3.4. Dilute magnetic semiconductors

Type III—V semiconductors with the zinc blende or würtzite lattices are in great request on the market of lasers operating in the IR and visible regions, reading devices (GaAs), and magnetic sensors (InAs). Broad forbidden bands in the energy spectrum make these materi-

als transparent in corresponding optical ranges. Excellent electric and optical characteristics of GaAs and InP provide a high switching rate and low power consumption. Passage from the semiconductors based on Group IVa elements to type III—V binary compounds (matrices for DMS) and to isoelectronic type II—IV—V_2 ternary compounds (high-temperature ferromagnetic semiconductors) is shown in Scheme 2.

Scheme 2

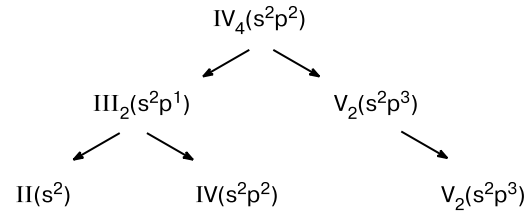

Following the CMS, semimetals, half-metals, and semimagnetic semiconductors, the DMS synthesized in the 1990s serve as the basis for next-generation spintronic materials. In these compounds certain atoms of Group III elements of the semiconductor matrix (InAs, InP, GaAs, GaP or GaN) are randomly replaced by transition metal atoms with non-filled 3d-electron shells. It is important that DMS retain the crystal structure of the semiconductor matrix, being isoelectronic to silicon (see Scheme 2). A distinctive feature of this class of magnetic semiconductors is that their Curie temperatures and other magnetic properties depend on the dopant concentration or current carrier density.

Search for and studies of the ferromagnetic compounds based on type III—V matrices were initiated by the discovery of ferromagnetism in (In,Mn)As (T_C = 7.5 K).[8] More recently, a T_C of 350 K was reached in InAs:Mn quantum dot layers[248] and the Curie temperature of (In,Mn)As thin films was raised to 35 K [9,249—252] and then to 60 K (x = 0.063).[253] InP with ion implanted Mn^+ is characterized by $T_C \approx 90$ K.[254]

One can overcome the thermodynamic limit of manganese solubility in the type III—V semiconductor matrix using low-temperature molecular beam epitaxy (T < 523 K; the phase diagram is presented in Ref. 140). Usually, molecular beam epitaxy imvolves Ga, Mn, In, Al, and As targets. (Ga,Mn)As epitaxial films are grown on GaAs(001) substrates at growth rates of 0.6—0.8 μm h^{-1}. Prior to epitaxy, the buffer (Ga,Mn)As, GaAs or (Al,Ga)As layers are built up. To relieve strain in the material synthesized, in some cases a thick (In,Ga)As layer (~1 μm) is used, with the lattice constant greater than that of (Ga,Mn)As. Usually, the Mn content in $Ga_{1-x}Mn_xAs$ films is determined from the lattice constant using a calibration curve. If a monophase material (Ga,Mn)As is grown at $T \approx$ 473—523 K, the Mn impurities replace atoms in the Ga sublattice. This was established by EXAFS [255] and is consistent with the linear dependence of the lattice constant on the Mn content (Vegard law): $a = 0.566(1 - x) + 0.598x$ (nm).[256] The lattice constant depends on the synthesis conditions (As pressure, annealing temperature) because another relation, $a = 0.5654(1 - x) + 0.5901x$ (nm), was obtained in another study.[257] If the substrate temperature or the Mn concentration are high, yet another phase, metallic ferromagnetic MnAs, is formed on the surface of (Ga,Mn)As samples. A (Ga,Mn)As sample with zinc blende structure, which was synthesized in 1998, exhibited a record (at that time) T_C = 110 K[43,81,258] at a hole density of 10^{20} cm^{-3} and a resistivity of the order of 10 mOhm cm, which is four orders of magnitude higher than the copper resistivity at 300 K (2.24 μOhm cm); *i.e.*, (Ga,Mn)As is a "bad" metal. Thus, the DMS conductivity is similar in order of magnitude to the conductivity of non-magnetic semiconductors. This is a great advantage of the DMS and HTFS over metals when used for spin injection applications.

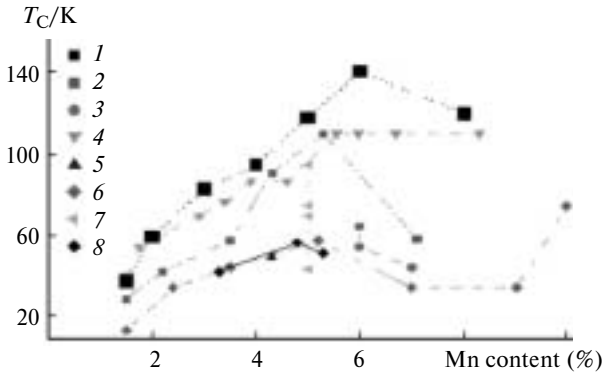

Fig. 1. Curie temperature (T_C) plotted *vs.* Mn content (at.%) in (Ga,Mn)As. Experimental data were taken from the following references:

Curve	*1*	*2*	*3*	*4*	*5*	*6*	*7*	*8*
Reference	*	81	260	261	262	257	263	264

At first, (Ga,Mn)As exhibited mostly nonmonotonic dependences of T_C (see Fig. 1) and of the density of free holes on the dopant concentration. The magnetization of samples was also not in proportion to the Mn content. Annealed samples grown by low-temperature molecular beam epitaxy exhibited a more monotonic dependence $T_C(x)$. Interestingly, the Curie temperature of compound $(In_{0.5}Ga_{0.5})_{0.93}Mn_{0.07}As$ (~110 K)[259] is the same as that of $Ga_{0.945}Mn_{0.055}As$.[81]

At present, $Ga_{1-x}Mn_xAs$ materials with $x \leq$ 9—10 at.% and heterostructures of corresponding composition[255—257,265—283,**] are the best studied DMS. Manga-

* B. Gallagher, http://ep2ds14.fzu.cz/ms/level2.nott.php.

** D. Chiba, Y. Sato, T. Kita, F. Matsukura, and H. Ohno, http://arXiv.org/cond-mat/0403500.

nese atoms not only replace Ga atoms during the formation of GaMnAs alloy but can also occupy interstitial sites in poorly annealed samples,[284,285] though GaAs samples grown at high temperatures have a stoichiometric composition. However, GaMnAs is obtained at relatively low temperatures. In this case a fraction of As atoms can occupy Ga sites, thus forming so-called antisites As_{Ga} which, in addition to the manganese interstitial defects, act as donors compensating the holes supplied by the Mn ions in gallium positions and thus reduce T_C. Besides, the magnetic moments of the interstitial Mn ions tend to form antiferromagnetic bonds with substitutional impurities, thus reducing the average magnetic moment per Mn atom in (Ga,Mn)As. The Mn interstitial defects in (Ga,Mn)As films can be removed by coating the material with As layer followed by annealing at 473 K for 2 h.* Being a substitutional impurity with respect to Ga, manganese is an acceptor and accepts an electron from the valence band of the GaAs matrix in order to saturate its own bonds, thus supplying a delocalized hole into the matrix. Deuteration causes saturation of all manganese bonds and abruptly decreases the density of delocalized holes, leaving the Mn content unchanged. This approach can be used to suppress ferromagnetism in ferromagnetic $Ga_{0.963}Mn_{0.037}As$ film 320 nm thick with T_C = 70 K.[286] Ferromagnetic (In,Ga,Mn)As films were grown on InP substrates (001) by molecular beam epitaxy.[287,288].

Using low-temperature molecular beam epitaxy, a manganese concentration of 6—9 at.% can be attained in $Ga_{1-x}Mn_xAs$ film; a specific multilayer technique (digital alloys)[252] allow a Mn content of up to 14 at.% to be achieved. At higher Mn concentrations, the second phase is formed with the crystal structure different from the zinc blende structure. Multiphase composition and reduction of lattice symmetry to hexagonal (NiAs type) or orthorhombic (MnP type) dramatically deteriorates the optoelectronic properties of the material.

DMS are also synthesized from organometallic compounds using vapor phase epitaxy. (Ga,Mn)As films thus grown contain up to 4 at.% of Mn but also include nanoclusters formed at high growth temperatures (673—873 K) that are necessary for decomposition of the compounds mentioned.[289,290]

The Curie temperatures of dilute magnetic semiconductor (Ga,Mn)As reported in different studies are plotted *vs.* manganese content in Fig. 1. At this writing a "three-layer" system (Ga,Mn)As/GaAs/(Ga,Mn)As exhibited T_C = 160 K [291] while Mn-doped GaAs/Be-doped *p*-type AlGaAs heterostructures (the so-called δ-doping, or digital alloy) were reported to have T_C = 172 K.[292]

A (Ga,Fe)As alloy with *n*-type conductivity and Fe content up to 10 at.% was obtained[293] by molecular beam epitaxy on GaAs substrate in the temperature range from 533 to 623 K. The lattice constant of the doped material decreased with increasing the Fe concentration because the Fe—As bond is shorter than the Ga—As bond. At lower temperatures, gallium atoms are replaced by iron atoms in the zinc blende lattice sites and the (Ga,Fe)As films become paramagnetic. At higher temperatures, Fe clusters and Fe—As complexes possessing ferromagnetic properties[294] are formed.

Molecular beam epitaxy was also used for the synthesis of (Ga,Cr)As with Cr concentration up to 10 at.%. A number of samples exhibited no ferromagnetism; at the same time a T_C of nearly 45 K was reported. Similarly to (Ga,Fe)As, these materials can be inhomogeneous.

It should be noted that (In,Mn)As, (Ga,Mn)As, and (Ga,Mn)P samples with the highest T_C have a high hole density (~10^{20} cm^{-3}) and their characteristics are typical of ferromagnetic materials. For instance, a domain structure (stripes of width 1.5 μm) was observed at 5 K in ferromagnetic $Ga_{0.957}Mn_{0.043}As$ film grown on $Ga_{0.84}In_{0.16}As$ substrate.[295] Rectangular magnetization hysteresis loops also favor normal ferromagnetism in DMS. As the temperature increases, the magnetization and coercive force of the materials decrease, the magnetizations of DMS and isoelectronic HTFS being not proportional to the dopant (magnetic ion) concentration.

Recently, above-room-temperature ferromagnetism in dilute magnetic semiconductor DMS (Ga,Mn)P with the zinc blende structure was reported. Ion-implantation doping of *p*-type GaP:C (carrier density ~10^{20} cm^{-3}) with manganese to ~6 at.% of Mn followed by annealing at 700 °C allowed T_C = 270 K to be achieved.[296] Using molecular beam epitaxy, one can obtain a DMS (Ga,Mn)P with T_C = 330 K.[297,298] According to theory (see below), a $T_C(x)$ dependence should also be expected for (Ga,Mn)P-type DMS and HTFS.

Owing to weakened spin-orbit coupling in the type III—N semiconductors compared to type III—As semiconductors, doped nitrides are expected to have longer spin relaxation times and spin coherence lengths compared to arsenides. First attempts to detect ferromagnetism in würtzite-type (Ga,Mn)N crystallites grown at high temperatures (~1200 °C) have failed.[299] Using different regimes of Mn diffusion at 523—1073 K in epitaxial GaN films grown on sapphire substrates, (Ga,Mn)N samples with T_C = 220—370 K were prepared.[300,301] The samples obtained by ion implantation were characterized by lower T_C.[302] (Ga,Mn)N samples with *n*-type conductivity and Mn content of 6—9 at.% were also obtained by molecular beam epitaxy at 853—993 K.[303] Measurements of the temperature dependence of magnetization carried out up to 750 K and extrapolation of this dependence to

* M. Adell, V. Stanciu, J. Kanski, L. Ilver, J. Sadowski, J. Z. Domagala, P. Svedlindh, F. Terki, and C. Hernandez, http://arXiv.org/cond-mat/0406584.

zero revealed T_C = 940 K. However, the results obtained in this study and in other studies (T_C > 900 K in (Ga,Mn)N) require verification because no ferromagnetic manganese compounds with gallium or nitrogen, possessing so high T_C have been reported so far. At the same time, a ferromagnetic Mn—Ga alloy is characterized by $T_C \approx 750$ K.[304]

n-Type (Ga,Mn)N was reported to have T_C = 320 K.[305] Room-temperature anomalous Hall effect measurements confirmed that manganese-doped gallium nitrides and phosphides are homogeneous ferromagnets. However, EXAFS data and a study[306] point to *p*-type conductivity of the HTFS (Ga,Mn)N and to the presence of some amount of manganese clusters in the samples, which increases with the Mn concentration. Studies of (Ga,Mn)N are important for establishment of the nature of ferromagnetism in DMS because (Ga,Mn)N is a high-T_C material with *n*-type conductivity, whereas other high-T_C DMS, *e.g.*, (Ga,Mn)As and (Ga,Mn)P have a *p*-type conductivity.

Gallium nitride containing implanted Fe [307] and Ni [308] exhibits ferromagnetism with $T_C \approx 200$ and 50 K, respectively. (Ga,Fe)N films grown by molecular beam epitaxy are characterized by T_C < 100 K.[309] Of interest is a DMS (Ga,Cr)N with T_C > 400 K, prepared[310] by molecular beam epitaxy at 973 K on sapphire substrate. A (Ga,Cr)N sample was characterized[311] by T_C = 280 K, *n*-type conductivity with a carrier density of $9 \cdot 10^{18}$ cm^{-3}, a mobility of 150 cm^2 (V s)$^{-1}$, and a magnetic moment of 1.1 μ_B per Cr ion.

Characteristics of DMS also depend on the annealing conditions.[263,271,312] Materials belonging to the (III,Mn)V family possess new spintronics-related properties of doped semiconductors, such as injection of long-lived spins, carrier induced and optically controlled ferromagnetism (see a review[44]), and electric current driven magnetization reversal of the heterostructures.[313]

Yet another material is aluminum nitride AlN, which is used in opto-electronic devices that operate in the green, blue, and UV regions of the optical spectrum. Chromium-doped AlN also exhibits interesting optical properties. In addition, doping of this material with chromium occurs at higher temperatures compared to the doping of other type III—V matrices with manganese, which favors the synthesis. Pioneering results[314] included the synthesis of $Al_{1-x}Cr_xN$ films with chromium content up to x = 0.357 and Curie temperatures exceeding 340 K. (Al,N)Cr films (T_C > 600 K) obtained by the same molecular beam epitaxy technique were studied.[315] Here, the expected magnetic moment of the Cr^{3+} ion occupying an Al vacancy is 3 μ_B. The measured magnetic moments were equal to 1.0 μ_B per Cr atom at 300 K and 1.2 μ_B per Cr atom at 10 K. From here it follows that at room temperature only 33% of Cr^{3+} ions are magnetoactive, while at low temperatures the proportion of such ions in the doped AlN is 40%. The presence of magnetic phases CrO_2 or Cr_2O_3 in the (Al,N)Cr films grown cannot be ruled out.

$Al_{1-x}Cr_xN$ thin films ($0.02 < x < 0.1$) on sapphire substrates were synthesized.* At 300 and 50 K, the magnetic moments of Cr^{3+} ions were respectively 0.62 and 0.71 μ_B per Cr atom. At x = 0.027, ferromagnetism with T_C > 900 K was observed, probably, T_C approaching 1000 K.

Indium nitride InN possesses useful spintronics-related transport properties, *e.g.*, a high carrier drift velocity. Epitaxial (In,Cr)N films were grown on a sapphire substrate at 623—723 K using a buffer GaN layer to smooth out differences between the lattice constants of the substrate and the film grown. X-Ray analysis revealed a monophase single-crystalline structure, while photoluminescence measurements confirmed the existence of a band gap of width 0.78 eV, as in the starting InN matrix. SQUID magnetic measurements of the (In,Cr)N fields revealed a nearly room-temperature Curie point of the material. Noteworthy is that Hall effect measurements in (In,Cr)N revealed *n*-type conductivity with an electron concentration of ~10^{20} cm^{-3}.**

Among type III—V semiconductor matrices, InSb has the narrowest band gap (0.17 eV) and the highest electron mobility. This material is used for fabrication of sensitive Hall sensors; therefore, interest in the preparation of InSb-based DMS is quite understandable. (In,Mn)Sb epitaxial films obtained[316] by molecular beam epitaxy exhibited ferromagnetism with T_C = 20 K (samples with *p*-type conductivity and a hole density of $1.1 \cdot 10^{20}$ cm^{-3}), whereas the samples with *n*-type conductivity and an electron density of $8.6 \cdot 10^{18}$ cm^{-3} were found to be paramagnetics.

3.5. High-temperature ferromagnetic semiconductors

At present, DMS based on type III—V matrices have been studied in most detail. High degree of spin polarization and the possibilities of optical or electric control of the magnetic properties and of integration with semiconductor circuits make the DMS quite attractive from technological viewpoint. However, fabrication of DMS using molecular beam epitaxy technique can produce antistructural, interstitial, and other uncontrollable defects that deteriorate the transport properties of materials. To date, defects in the (III,Mn)V systems are removed by prolonged controlled annealing. This allows the hole mobility to be enhanced to, *e.g.*, 10 cm^2 (V s)$^{-1}$ in (Ga,Mn)As. Most of DMS compounds are ferromagnetic *p*-type semiconductors with spin-polarized holes, which leads to lower carrier mobilities and shorter spin relax-

* D. Kumar, J. Antifakos, M. G. Blamire, and Z. H. Barber, http://arXiv.org/cond-mat/0404436 (unpublished results).

** R. Rajaram, R F. C. Farrow, G. Solomon, J. S. Harris, and S. S. P. Parkin, *Opening Event of the IBM-Stanford Spintronic Science and Applications Center* (April 26, 2004), 2004.

ation times compared to those of the *n*-type materials. Yet another drawback of the DMS materials is that some of them must be synthesized using Ga, which is incompatible with the most widely used material for microelectronics, silicon, and toxic arsenic. Nevertheless, spintronic DMS materials are expected to be of great promise because, theoretically, their Curie temperatures can lie above room temperature. Digital alloys (δ-doping) have higher T_C compared to homogeneous DMS.

Other semiconductors, namely, type II—IV—V_2 and type I—III—VI_2 compounds crystallizing in the chalcopyrite structure,[200] are also of interest. Chalcopyrites $ZnGeP_2$ and $CdGeAs_2$ possess unusual nonlinear optical properties and can be used for fabrication of optical modulators and frequency converters. Compound $ZnSnAs_2$ is also a candidate for optical applications in the far IR region. The lattice constants of wide-gap chalcopyrites $ZnGeN_2$ and $ZnSiN_2$ are similar to those of GaN and SiC. Because of this, ferromagnets based on these hosts would favor fabrication of hybrids of magnetic sensors or switches with lasers operating in the blue/green/UV regions of the optical spectrum, light-emitting diodes, and microwave electronic devices based on GaN and SiC. A matter of no small consequence is that the width of the forbidden band in $ZnGe_xSi_{1-x}N_2$ is a linear function of the germanium content and varies over a wide range, from 3.2 eV (x = 1) to 4.46 eV (x = 0). Yet another advantage of the type II—IV—V_2 and I—III—VI_2 compounds as hosts for novel ferromagnetic semiconductors is facilitation of *p*-type doping with high carrier mobility in these ternary compounds.

The synthesis of ferromagnetic semiconductors $CdGeP_2$:Mn (averaged Mn/Cd ratio of 20%) with T_C = 320 K [317] and $ZnGeP_2$:Mn with T_C = 350 K [318] marked the emergence of novel spintronic materials, namely, high-temperature ferromagnetic semiconductors (HTFS). Similarly to semimagnetic or dilute semiconductors, in the HTFS the atoms of the semiconductor host are randomly replaced by transition metal and, probably, REE impurities. Compounds $A^{II}B^{IV}C^{V}_2$ are electronic analogs of compounds $A^{III}B^{V}$ because the average valence of A^{II} and B^{IV} in HTFS equals the valence of the element A^{III} in DMS. Here, the density of itinerant holes (charge carrier density) is an order of magnitude lower than the Mn impurity content (density of localized spins). Analysis of the properties of HTFS based on type II—IV—V_2 and I—III—VI_2 compounds shows that, compared to DMS, the Mn^{2+} impurity in HTFS can replace both the atoms of Group II or I elements and the atoms of Group IV or III elements, thus playing the role of acceptors and donors of mobile holes. This was confirmed by measuring the EPR spectra of $(ZnGe,Mn)P_2$ [319,320] that revealed two types of substituted manganese sites, Mn_{Zn} and Mn_{Ge}.

Recently, high-temperature ferromagnets $ZnGeP_2$:Mn (T_C = 312 K),[321] $ZnSnAs_2$:Mn (T_C = 329 K)[322] and $ZnSiGeN_2$:Mn ($T_C \approx$ 300 K)[323,324] were discovered. Studies of the transport properties of epitaxial HTFS with composition $ZnSiGeN_2$:Mn (5 at.% Mn; $T_C \approx$ 300 K), grown on sapphire substrate, revealed *n*-type conductivity.[324] Compared to DMS, HTFS are characterized by higher mobility of both *p*- and *n*-type carriers. Completely substituted chalcopyrites $MnGeP_2$ and $MnGeAs_2$ possess ferromagnetism with T_C = 320 and 340 K, respectively,[325] and are of academic interest because their semiconductor characteristics differ from those of the starting materials $ZnGeAs_2$ and $ZnGeP_2$.

High-temperature ferromagnetic semiconductors $(CdGe,Mn)P_2$ and $(ZnGe,Mn)P_2$ were obtained[317—320,326] by Mn deposition on pre-synthesized single-crystalline substrates $CdGeP_2$ and $ZnGeP_2$, respectively, at nearly 673 K followed by manganese diffusion into the interior of the samples. The HTFS thus obtained contained no MnP phase. A study[327] of $(ZnGe,Mn)P_2$ showed that the manganese diffusion profile reflects inhomogeneity of the sample with a metallic surface layer covering $(ZnGe,Mn)P_2$. Layer-by-layer etching revealed ferromagnetism in both phases (the surface phase and the internal phase).

A 8 mm×8 mm single crystal and polycrystals of $(ZnGe,Mn)P_2$ were synthesized starting from Zn, Ge, Mn_3P_2, and P in quartz ampules by stepwise heating to 1400 K followed by slow cooling. A single-crystalline sample with a Mn concentration, x, of 0.03 and polycrystalline samples with x = 0.045, 0.056, and 0.2 (calculated for the composition $Zn_{1-x}Mn_xGeP_2$) were obtained. The samples with x = 0.056 and 0.2 were characterized by T_C = 312 K and exhibited antiferromagnetism at temperatures below 47 K.

HTFS samples of composition $(ZnGe,Mn)P_2$ with a Mn content, x, of 0.08 and 0.15 were synthesized according to Ref. 321 and then studied.[328] Measurements of the ^{55}Mn and ^{31}P NMR spectra of the samples with x = 0.15 at temperatures above and below $T_C \approx$ 300 K showed that more than 90% of Mn atoms are clustered to form an impurity phase MnP with cluster sizes of the order of 10 nm.

At present, intensive theoretical and experimental research[198] on novel HTFS has been carried out. Single crystals and polycrystals of $(CdGe,Mn)As_2$ were first obtained using pre-synthesized $CdAs_2$, Mn powder, Ge, and As.[329] Single crystals of $(CdGe,Mn)As_2$ containing 0.5 wt.% Mn, were grown using a vertical modification of Bridgeman technique followed by heat treatment. Thermal e.m.f. measurements at 300 K revealed a *p*-type conductivity of the materials containing less than 6 wt.% of Mn and X-ray phase analysis confirmed that Cd and Ge atoms in the lattice sites are replaced by Mn atoms.

(CdGe,Mn)As_2 samples containing 1, 3, and 6 wt.% of Mn appeared to be novel HTFS with $T_C \approx 355$ K.[329]

Considerable attention has also been paid to the preparation of HTFS based on carborund SiC, which is used in high-temperature high-power electronics. Carborund has more than seventy polymorphs, some of them being structurally similar to würtzite. The 6H polymorph has a broad forbidden energy band (3 eV), *p*-type conductivity, good transport properties, and can be doped. By ion implantation of Ni, Fe, or Mn (up to ~5 at.%) followed by annealing of the 6H-SiC polymorph of carborund one can obtain ferromagnets with T_C = 50 (6H-SiC:Ni), 250 (6H-SiC:Mn), and 270 K (6H-SiC:Fe)* with a hole density of ~10^{17} cm^{-3} and a coercive force of 150 and 50 Oe (at 10 K) for the last-mentioned two samples.[330]

3.6. Organic spintronic materials

At present, spintronics employs "sandwiches" that are sputtered or grown on thick substrates. But at long distances travelled by electrons passing through one layer to another layer the electron spins lose their orientation. This significantly deteriorates the current-switching properties of devices. A decrease in the layer thickness to a few atoms must favor solution to this problem. At present, it is possible to fabricate thin layers of organic conductors and even superconductors on the surface of a polymer matrix. This is an ancestor of conducting organic strips in electronic circuits. Organometallic compounds possess a variety of properties and have definite chemical compositions. One can influence the molecules in the conducting layer, which permits control of the electrical properties. For instance, a quasi-two-dimensional material based on bis-ethylenedithiotetrathiofulvalene (BEDT-TTF) molecules has the same chemical composition but can be a conductor, antiferromagnet, or a superconductor depending on the mutual arrangement of molecules in layers or on the layer thickness (see Ref. 30 and references cited therein).

A new class of ferromagnetic spintronic materials, namely, organic ferromagnets were discovered at the end of the 20th century. Among them, crystals with structures comprised of alternating conducting layers based on the BEDT-TTF molecules and insulating layers (oxalates of magnetic ions Fe^{3+}, Cr^{3+}) can be pointed out. This class of materials opens the possibility of electric current driven control by changing the spin orientation in the magnetic field. A possible practical application of such crystals are devices for molecular and spin electronics. Organic ferromagnets also comprise molecular ferromagnets based on organic paramagnetic molecules (stable radicals and polyradicals and high-spin carbene molecules) or paramagnetic complexes with magnetic ions encapsulated in a ligand shell comprised of organic molecules. To fabricate spintronic materials with different structures and spin densities, molecules and organometallic complexes containing ten to twenty and more electron spins per particle and a magnetic moment of up to several tens of Bohr magnetons are synthesized. Molecular ferromagnets have some drawbacks, namely, a low spin density and a large proportion of chemical "garbage" and therefore weak exchange interaction and low T_C (3—30 K). But molecular ferromagnets are of great interest as promising high-tech materials; interest in them has even increased in connection with the development of spintronics. Recent information on the preparation of high-temperature molecule-based ferromagnets with T_C = 315—330 K stimulated this interest. Unfortunately, unambiguous structural characterization of these substances has not been reported so far.* Among organic spintronic materials, mention may also be made of recently synthesized magnetic plastic based on vanadium tetracyanoethanide.[331] This material possesses magnetic properties at high temperatures (above boiling point of water) and can therefore be used in spintronic devices without using a cooling system.

A current-*vs*.-voltage curve of a benzene-1,4-dithiol molecule connecting two gold contacts was studied.[332] In the future such nanostructures fabricated from molecular wires based on organic molecules connecting transition-metal nanocontacts will make it possible to realize spin-dependent transport through organic molecules, thus opening the field of molecular spintronics.[333]

3.7. Inhomogeneous magnetic materials

Monophase magnetic materials are best for efficient spin injection into semiconductors. However, inhomogeneous materials with high T_C of the magnetic component can also be useful in spintronics, especially for magneto-optical applications.

An example is provided by the semiconducting materials TiO_2:Co [334,335] with the anatase structure, which sometimes possess room-temperature ferromagnetism. Magneto-optical and magnetic measurements[336] revealed a large hysteresis at room temperature. However, the scatter of magnetization depending on the method of preparation of the sample indicates the presence of Co or an unknown compound of the system Co—Ti—O in the anatase matrix. The results of the temperature measurements of resistance[337,338] indicate a multiphase composition of the material and the possibility for cobalt clusters to be present in the TiO_2 matrix. At the same time, the $Ti_{0.92}Co_{0.08}O_{2-\delta}$ films deposited on $SrTiO_3$ substrates exhibit room-temperature ferromagnetism only in a limited range of carrier concentrations ($2 \cdot 10^{18}$—$5 \cdot 10^{22}$ cm^{-3}),[339]

* J. Kim, F. Ren, S. J. Pearton, C. R. Abernathy, M. E. Overberg, G. T. Thaler, and Y. D. Park, unpublished results.

* A. L. Buchachenko and R. Z. Sagdeev, *Perspektivnye Tekhnologii* [*Advanced Technologies*], **10**, Iss. 5, March 15, 2003 (in Russian).

which excludes clustering of cobalt. Clearly, further physicochemical studies of TiO_2:Co are required.

Iron-doped TiO_2 epitaxial films with the rutile structure possess ferromagnetism with nearly-room T_C,[340] while TiO_2:V thin films with the anatase structure, grown on a $LaAlO_3$ substrate are ferromagnets with $T_C > 400$ K, which was confirmed by anomalous Hall effect measurements.[341] It should be noted that the first studies of (In,Mn)As also revealed ferromagnetic inclusions similar to the MnAs phase with $T_C \approx 300$ K; homogeneous DMS were obtained later.[6,7]

It is important that interesting results were obtained in experiments with the multiphase and nonequilibrium transition metal pnictides. For instance, a material prepared by deposition of 3-nm MnSb islands on a GaAs matrix is characterized by an easy magnetization reversal and has a giant magnetoresistance in low fields (effect is as high as 880% in a magnetic field of 1 T and 320000% in a 2 T field at room temperature).[342] The formation of nanostructures (including ferromagnetic ones) in MnAs films (T_C = 310 K) deposited on GaAs(001) substrate was observed at 30 °C.[343]

Unstable compounds CrAs [209,344] and CrSb [345] with the zinc blende structure were prepared by deposition on GaAs substrates. These materials possess room-temperature ferromagnetism. Because of 100% spin polarization they can serve excellent sources of spins grown on technologically important semiconductor substrates.

Yet another example of inhomogeneous spintronic materials is provided by the materials based on ZnO, which is widely used in opto-electronics and cell phones. Smaller in size and faster optical modulators, detectors, lasers, *etc*. based on zinc oxide can be produced with ease. Zinc oxide crystallizes in the würtzite structure, possesses piezoelectric properties, and has a broad forbidden band (3.3 eV) and a high limit of transition metal solubility. From this, interest in doping ZnO with transition metals to obtain ZnO-based ferromagnetic semiconductors possessing piezoelectric properties is quite understandable. The doped material must not contain mobile carriers capable of screening electric fields induced in the material.

The Mn, Fe, or Co doped nanocrystalline ZnO thin films were obtained by sol-gel technique.[346—350] Recent studies of bulk and thin-film ZnO:M (M = Co,[351,352] Mn,[353,354] and V [355]) samples confirmed their room-temperature ferromagnetism (*e.g.*, T_C = 290—380 K for ZnO:Mn) in contrast to studies[356,*] where a spin glass behavior was assumed. At the same time, detailed measurements[357] of the magnetic properties of ZnO:M (M = Cr, Mn, Fe, Co, Ni, Cu) epitaxial films revealed no magnetic ordering down to 3 K. However, ferromagnetism with $T_C \approx 50$ K was observed in a study of diffusion doping of four-pod ZnO nanostructures with manganese at 873 and 1073 K.[358] The nickel-doped ZnO nanocrystals with $T_C > 350$ K were synthesized from solution.[359] The ZnO:Ni^{2+} nanocrystals with a characteristic size of the order of 6 nm exhibit paramagnetism but their aggregation gives rise to ferromagnetism, which is probably due to additional doping with nickel during the growth (Ni content in the material was about 1 at.%). The results of structural, magnetic, and optical measurements of $Zn_{0.9}Co_{0.1}O$ epitaxial films obtained by laser deposition on a sapphire substrate were reported;[360] the films exhibit ferromagnetism with T_C = 300 K (the presence of nanoclusters and inhomogeneities is excluded). The hysteresis loop was observed up to T = 350 K in the $Zn_{0.91}Co_{0.09}O$ films kept in Zn vapors* and up to T = 300 K in (Zn,Co)O nanocrystals.[361] However, in similar situations one must feel certain of homogeneity of the isoelectronically doped ZnO. In the case of ZnO one can not rule out the possibility of formation of noninteracting antiferromagnetic clusters comprising impurity atoms with an increase in the dopant concentration; this was confirmed in the studies of monophase (Zn,Mn)O and (Zn,Co)O samples possessing no ferromagnetism above 2 K.**

Oriented ZnO(110) films on sapphire substrates were doped*** with transition metals by laser deposition at 600 °C. Room-temperature ferromagnetism in the films was observed at Sc, Ti, V, Fe, Co, and Ni concentrations of about 5 at.%, whereas the films doped with Cr, Mn, and Cu possessed no ferromagnetism. Ferromagnetism was also observed in ZnO:Co [361] and CdSe:Co [362] quantum dots.

Additional doping of the transition metal-containing ZnO bulk phases with copper increases the density of current carriers that provide with indirect exchange interaction between magnetic impurities, which can cause ferromagnetism. For instance, a T_C of 550 K in a $Zn_{0.94}Fe_{0.05}Cu_{0.01}O$ sample was reported.[363]

Ferromagnetic nanocrystals CdSe:Mn,[364] ZnS:Mn,[365] ZnSe:Mn,[366] InAs:Mn,[367] and TiO_2:Co **** can be promising as ferromagnetic coatings for spintronics applications.

A novel ferromagnetic semiconductor material with $T_C > 400$ K and a structure comprised of alternating thin layers (a few atoms thick) of GaSb, GaMn, and their

* G. Lawes, A. S. Risbud, A. P. Ramirez, and R. Seshadri, http://arXiv.org/cond-mat/0403196.

* D. A. Schwartz and D. R. Gamelin, http://arXiv.org/cond-mat/0404518.

** G. Lawes, A. S. Risbud, A. P. Ramirez, and R. Seshadri, http://arXiv.org/cond-mat/0403196.

*** M. Venkatesan, C. B. Fitzgerald, J. G. Lunney, and J. M. D. Coey, http://arXiv.org/cond-mat/0406719.

**** J. D. Bryan, S. M. Heald, S. A. Chambers, and D. R. Gamelin, http://arXiv.org/cond-mat/0407451.

mixture was prepared by molecular epitaxy.[368] The authors believed that the material also retains the desired properties at higher temperatures, although a T_C of 400 K is sufficient for successful use of the material in spintronic devices at room temperature.

Doping of hosts with the rutile structure is also of interest. A transparent $Sn_{0.95}Co_{0.05}O_{2-\delta}$ film grown by laser deposition on a sapphire substrate exhibited high-temperature ferromagnetism with $T_C = 650$ K, but a very high magnetic moment (7.5 ± 0.5 μ_B per Co atom) can be indicative of inhomogeneous sample.[369] Early studies of (Ga,Mn)As [370] pointed to a low Mn solubility in the matrix and the formation of magnetic nanoclusters that complicate the determination of T_C. Therefore, criticism must be expressed when analyzing the results obtained in studies concerned with novel ferromagnetic semiconductors possessing nearly room-temperature T_C (see, *e.g.*, a review[44]). For instance, ferromagnetism in lanthanum-doped compound $Ca_{1-x}La_xB_6$ ($0.01 < x < 0.5$) with $T_C \approx$ 900 K was reported,[371—373] but the authors of study* found that in this case ferromagnetism is due to the presence of Fe and Ni impurities contaminated the material during synthesis.

DMS based on silicon hosts would also be of applied value. Unfortunately, (Si,Mn) samples obtained by deposition technique[374] or molecular bean epitaxy[375] have a two-phase composition; the ferromagnetic phase (tentatively, SiMn) has $T_C \approx 30$ K and the antiferromagnetic phase Si_3Mn_5 has the Neel temperature $T_N \approx 95$ K.[375] In this connection of considerable interest is a recent magnetic and structural study[376] of single-crystalline $Mn_{0.05}Si_{0.95}$ films obtained by heat treatment of amorphous films deposited on the Si(001) surface. SQUID-Measurements revealed ferromagnetism with $T_C > 400$ K; however, in this case multiphase composition of the material also cannot be ruled out.[376]

Investigations of light-induced ferromagnetism[251,377,378,**] or electric-field controlled ferromagnetism[151,152,154] allow one to distinguish between true ferromagnetism in magnetic semiconductors, which originates from indirect exchange interaction between impurity spins involving delocalized carriers and ferromagnetism induced by magnetic nanoclusters. A photo-induced phase transition to ferromagnetic state in (Ga,Mn)As films ($x = 0.011$, hole density less than 10^{20} cm^{-3}, $T_C = 30$ K) was realized at 60 K,[377] the magnetization being equal to 15% of the saturation magnetization.

* C. Bennett, J. van Lierop, E. M. Berkeley, J. F. Mansfield, C. Henderson, M. C. Aronson, D. P. Young, A. Bianchi, Z. Fisk, F. Balakirev, and A. Lacerda, http://arXiv.org/cond-mat/0306709.

** G. A. Khodaparast, J. Wang, J. Kono, A. Oiwa, and H. Munekata, http://arXiv.org/cond-mat/0305017.

4. Ferromagnetism in spintronic materials

4.1. Models of ferromagnetism in dilute magnetic semiconductors

DMS and HTFS exhibit a number of new properties of doped semiconductors, which are of importance for spintronics applications. These are a high degree of spin polarization, an injection of long-lived spins, an electrically and optically controllable ferromagnetism, and a possibility for DMS and HTFS of being embedded in the known semiconductor circuits. Although ferromagnetism in the best studied DMS (Ga,Mn)As was first observed as early as 1996 with $T_C = 60$K, the microscopic nature of ferromagnetism in the DMS based on type III—V hosts and in isoelectronic HTFS based on type II—IV—V_2 hosts, *etc.*, is not well theoretically understood as yet.

It is unclear how can magnetism in DMS and HTFS occur provided rather long distances between magnetic impurities and even greater separations between current carriers. The well-known models for exchange interactions (direct or double one) cannot give explanations. A characteristic feature of DMS and HTFS is the dependence of their magnetic, electric, and optical properties on the dopant concentration (x) or on current carrier density, but an empirical rule $T_C = (2000x\pm10)$ K [81] is invalid for $Ga_{1-x}Mn_xAs$. Ferromagnetism in DMS and HTFS belongs to the most interesting problems in basic research.

In contrast to cryoelectronics that employs the Bardeen—Cooper—Schrieffer—Bogolubov microscopic theory or the Ginzbirg—Landau phenomenological approach for calculations, no substantiated spintronics-oriented concepts of the mechanism of magnetic interaction between impurity spins and of the origin of high T_C in DMS and HTFS have been proposed so far. To make the DMS and HTFS real rather than hypothetical spintronic materials, one should answer the question as to the nature of ferromagnetism in and characteristics of the semiconductor matrix and the magnetic dopants responsible for high T_C.

Most theories of ferromagnetism in such DMS as (Ga,Mn)As, (Ga,Mn)P or (Ga,Mn)N are based on (semi)phenomenological models. There are three approaches, which can be followed to study magnetic states in DMS and HTFS. The first approach postulates the existence of local magnetic moments, a ferromagnetic exchange interaction of these moments with valence electrons (exchange parameter $J_{pd} < 0$), and an antiferromagnetic interaction of these moments with the conduction electrons of the semiconductor matrix. This approach is used for the description of ferromagnetism in such DMS as (Ga,Mn)As, (Ga,Mn)P, and (Ga,Mn)N (see a review[379] and Refs 79, 380—382). Some of these theories take into account the role of shallow acceptors[383] or deep

resonance levels.[384,385] Note that the expression[77,78] (see also Ref. 79) for T_C containing the phenomenological fitting parameter J_{pd} of the exchange interaction between localized and delocalized electrons, which was used in numerous studies of magnetic semiconductors (especially, DMS) coincides, correct to the change $J_{pd} \to J_{sd}$, with the Abrikosov—Gor´kov equation derived in the mean field approximation for the T_C of alloys of magnetic impurities with non-magnetic metals[386]:

$$T_C = \frac{4xS(S+1)J_{pd}^2}{3a}\frac{\chi_h}{g^2\mu_B^2},$$

where a is the lattice constant, S is the spin of the impurity whose concentration in the material is x, and $\chi_h = 0.5g^2\mu_B^2\rho(\varepsilon)$ is the magnetic susceptibility of holes in the valence band of the semiconductor or of the conduction electrons of the metal (Pauli susceptibility). The second term in this relation is proportional to $m^*k_F \propto p^{1/3}$ (k_F is the Fermi wave vector and p is the density of holes with the effective mass m^*); as applied to DMS, this means that $T_C \propto x \cdot p^{1/3}$, which contradicts experimental data. It should be emphasized that the Abrikosov—Gor´kov relation is applicable to the systems in which the concentration, x, of spin carriers (magnetic impurities) is much lower than the density, n, of charge carriers (*e.g.*, to dilute alloys Cu—Mn). But in the case of DMS and HTFS we deal with the reverse situation, namely, $x \gg n$ (hole density), which means that the distance between delocalized holes much exceeds the average distance between localized impurities and, hence, direct Heisenberg-type impurity exchange or indirect RKKY magnetic exchange is impossible. It is the condition $x >> n$ that is responsible for the fact that in the external magnetic field, which polarizes localized magnetic moments, the itinerant carriers "see" a large number of Mn^{2+} ions (strong effective magnetic field of these ions causes giant Zeeman splitting in DMS and semimetals and half-metals). At sufficiently high concentration of charge carriers, a reverse effect is possible, namely, magnetization of localized magnetic moments by the charge carriers.

As can be seen, the T_C value is independent of the sign of the parameter J_{pd}. But if for metals the exchange interaction between the conduction electrons and impurity can be treated as a contact interaction (this is more correct for the f rather than d impurity orbitals), this approximation is at least rough in the case of semiconductors. The case in point is that, unlike metals, replacement of atoms of the semiconductor matrix by a non-isoelectronic transition metal atom causes a strong disturbance and the localized atomic state is "pumped" from the heavy hole band. Owing to the character of the p—d chemical bond the impurity d-orbitals are mixed with p-orbitals and the degree of delocalization of d-orbitals strongly depends on the position of the d-level in the semiconductor band and on the concentration of magnetic impurities. These features of the electronic structure cannot be described using a single parameter of contact exchange interaction J_{pd}, though intra-atomic interactions of d-electrons, Hund exchange J_H, and the Anderson—Hubbard repulsion U undoubtedly remain among important factors.

Semiphenomenological models of DMS are also related to some versions of the density functional theory (see, *e.g.*, a review* and references cited therein). The Local Density Approximation (LDA) calculations of DMS ignore strong intra-impurity electron correlations that suppress fluctuations in the number of d-electrons. As a result, these calculations give unrealistically high d state density near the top of the valence band, underestimate the role of the 4p component of holes in the valence band, and overestimate the strength of sp—d-hybridization.[387,388] Other versions of the density functional approach (*e.g.* LDA+U [389]), which include the Coulomb repulsion between impurity 3d electrons (Anderson—Hubbard parameter U) allow a more realistic electron energy spectrum and the 4p-character of holes in the valence band to be obtained.

However, first-principle (*ab initio*) density functional calculations cannot[86] intrinsically to correctly allow for high-energy states induced in DMS and HTFS by magnetic impurities. Although application of this method led to some advances in the theory of simple metals, as applied to semiconductors, the approach has a fundamental drawback caused by energy variation over the electron density. This procedure cannot be correctly performed for DMS and HTFS because the minimum change in the electron density requires excitation of an electron-hole pair with a finite energy equal to the width of the band gap in semiconductor, which here is not infinitesimal, as required in the variational method.

First-principle calculations are employed in the second approach to studies of the magnetic properties of DMS and HTFS. It is based on a generalized cluster method; namely, a low magnetic impurity concentration is simulated using a cubic supercell with the magnetic ion at the center and then the cell is involved in calculations of the density of spin-polarized states in the entire homogeneously doped crystal.[80,390—396] Sometimes an exchange Hamiltonian is introduced phenomenologically, with the effective magnetic exchange constant playing the role of a fitting parameter in numerical calculations.[80,391] The cluster approach is based on the assumption of a local perturbation produced by an impurity in the matrix and treats the impurity region in the semiconductor crystal as a defect quasi-molecule in which the impurity ion is chemically bound to the neighboring matrix atoms.[397,398] The matrix elements of the potential for a substitutional impu-

* J. Sinova, T. Jungwirth, and J. Ñerne, http://arXiv.org/cond-mat/0402568.

rity are related to the "oxidative ability", *i.e.*, they are assumed to be proportional to the energy difference between the impurity orbital and the corresponding orbital of the atom to be replaced. Most methods used in the framework of the cluster approach are based on the tight-binding approximation in which the electron wave functions are represented by linear combinations of AO or MOs and provide some idea of the energy spectrum of a semiconductor containing one impurity. But these are mainly one-electron methods, which cannot correctly allow for the intra-impurity electron-electron interactions (electron correlations) inside the transition or rare-earth metal atoms, that are necessary for the description of the magnetic properties. Yet another problem of electronic structure calculations in the framework of the cluster approach is concerned with the outermost ("surface") atoms of the cluster, which have dangling bonds; localized energy levels of the surface atoms in the electron energy spectrum should be differentiated from the energy levels of the bulk atoms. If the supercell is a cluster whose size exceeds the localization radius of the impurity state, in a periodic structure comprised of such clusters the localized levels are broadened to create an impurity band.

In spite of drawbacks of the cluster approach, numerical calculations of DMS and HTFS show that differences between the physical and chemical nature of transition metal impurities and cations in the semiconductor cause significant changes in the electron energy spectrum. Heavy transition metal impurities in the crystal give rise to quite essential states that are few in the allowed energy bands. The electron-electron interactions and covalent effects governing the structure of chemical bonds play an important role in the formation of the properties of impurities with non-filled shells in the semiconductor hosts. The third strategy of studying the magnetic states in DMS and HTFS is presented in Sections 4.2 and 4.3.

4.2. Electronic structure of magnetic impurities in dilute magnetic semiconductors and high-temperature ferromagnetic semiconductors

A consistent theory of exchange interactions in DMS and HTFS, which explains the reasons for magnetic ordering must allow for the structure of chemical bonds between the impurity and the matrix as well as for the Coulomb and electron-electron exchange interactions in the 3d-shells (intra-atomic correlations).

Usually, the energy levels of simple isoelectronic substitutional impurities lie near the forbidden energy band, being comprised of the contributions of the valence electrons of the semiconductor matrix. At the same time, taking $Pb_{1-x}Sn_xTe$ as an example, it was proposed[399] that this rule can be violated for charged impurities of Group III elements in the type IV—VI hosts. This violation appeared to be logic for DMS and HTFS. Experimental data substantiating the existence of shallow impurity (Cr, Mn, and Fe) levels in narrow-gap type III—V semiconductors (InAs, InSb) were first reported in a monograph.[189]

According to the third approach, in studying the magnetic states and ferromagnetism in DMS and HTFS various interactions involving d-electrons are derived taking into account the chemical bonds and electronic structure of type III—V, II—IV—V_2, *etc.* semiconductors doped with transition metals. Such a theory permits the description of the electronic structure of these impurities, contains all ingredients for an accurate derivation of indirect magnetic exchange between impurities, and allows the properties of DMS and HTFS to be predicted. Peculiarities of the electronic structure of a semiconductor with one d-impurity were studied back in the mid-1970s [61,62] (see also monographs[400—402]).

A tetrahedral crystal field characteristic of semiconductors splits five-fold degenerate (with respect to the orbital momentum projection) impurity d-levels into three-fold degenerate t_2 and doubly degenerate e sublevels, the latter lying lower on the energy scale. In other words, the localized d-electrons of transition metal impurities possess t_2 and e symmetry of the semiconductor point symmetry group T_d, so the magnetic impurity ion replacing atoms of Group II(s^2) or III(s^2p) elements can have the $d^n(e^r t_2^{n-r})$ or $d^{n-1}(e^r t_2^{n-r-1})$ configuration. Covalent bonds involving the t_2-orbitals are nearly σ-type and strong, whereas the e-orbitals form weak π-bonds involving p-orbitals. The electronic configurations of the $4f^n6s^2$ REE impurities in the semiconductor hosts are similar to those of transition metal impurities. However, these apparent d- and f-configurations are violated in the case of the impurities with half-filled electron shells that retain its high-spin state in accord with the Hund rule. Namely, in the case of cationic replacement manganese ions in the GaAs and GaP hosts retain the $3d^5$ state while europium ions in InP retain the $4f^7$ state. In both cases these impurities give rise to acceptor levels in the forbidden energy band. Having determined positions of the acceptor levels relative to the top of the valence band from the optical absorption edge and the position of the bottom of the band gap from the photo-ionization energy of the semiconductor, one can determine the "absolute" positions of the bottom and top of the forbidden band and of the impurity levels relative to vacuum.[401,402] Thus it was established that the true reference point for the energies of the 3d-levels in type III—V (for impurities from V to Cu) and II—VI (for impurities from Sc to Zn) semiconductors is the photo-ionization threshold of free 3d-atom. In other words, the energy levels of magnetic impurities in semiconductors are not related to the top or bottom of the band gap or to other characteristics of the electronic structure of different hosts; rather, they are calculated relative to the absolute reference point, namely, the vacuum level. This means that as the forbidden band

of the semiconductor matrix is broadened (*i.e.*, with a decrease in the bond covalency in the matrix), the energy levels of magnetic impurities calculated with respect to the top of the valence band increase. Numerous experimental data indicate a significant redistribution of the electron and spin density in the region between the impurity and the neighboring atoms, the spin density perturbation near the impurity site extending up to the fifth coordination sphere; this was confirmed by analyzing double electron-nuclear resonance spectra.[400]

Typical of transition metal impurities in the semiconductor hosts of DMS and HTFS is tunneling of impurity d-electrons to heavy hole *p*-states and back, described by a very important hybridization parameter V that exceeds 1 eV (parameter of hybridization with light holes is small). Therefore, changes in the electron d states are due to the effect of the electronic states of the crystal environment. Unlike other impurities in semiconductors, transition metal ions can create impurity levels not only in the allowed energy band but also in the forbidden energy band. The bonding configurations of the p-orbitals of the valence band with d-orbitals, where the d-component dominates, are classified as the crystal field resonances (CFR). The antibonding configurations with predominant contribution of the p-component of the valence band are called the dangling bond hybrids (DBH). Manganese ions $Mn^{2+}(d^5)$ and $Mn^{3+}(d^4)$ involved in the exchange interaction in DMS and HTFS have populated electron configurations $d^4(e^2t^2)$ and $d^5(e^2t^3)$ in accord with the Hund rule. The $d^6(e^3t^3)$ charge state lies much higher than these configurations on the energy scale due to strong intra-atomic Coulomb repulsion (Anderson—Hubbard parameter U). Empty CFR levels (d^6/d^5) are pinned deep in the conduction band, while the antibonding e-orbitals should be excluded from consideration, which will be done in analyzing the Hamiltonian (see below). Empty CFR levels can be responsible for antiferromagnetic ordering of the impurity ions, which is rather weak in DMS and HTFS at optimum impurity concentrations.

The qualitative picture of the electronic structure of 3d-impurities presented above is confirmed by the results of rigorous calculations using the following Hamiltonian for magnetic impurities in the semiconductor matrix:

$$\hat{H} = \hat{H}_{\rm h} + \hat{H}_{\rm d} + \hat{H}_{\rm hd}. \qquad (1)$$

The first term in expression (1), the band Hamiltonian

$$\hat{H}_{\rm h} = \sum_{\vec{p},\sigma} \varepsilon_{\vec{p}{\rm h}} \hat{c}^{+}_{\vec{p}{\rm h}\sigma} \hat{c}_{\vec{p}{\rm h}\sigma},$$

includes only the heavy holes characterized by higher density of states compared to light holes and the greatest hybridization parameter, V, with impurity d-electrons. Here, $\hat{c}^{+}_{\vec{p}h\sigma}(\hat{c}_{\vec{p}h\sigma})$ is the creation (annihilation) operator of the hole with the momentum $\boldsymbol{p}$, the spin orientation σ, and the energy $\varepsilon_{\vec{p}h}$.

The next term in Hamiltonian (1),

$$\hat{H}_{\rm d} = \sum_{i} \left[E_{\rm d} \left(\hat{n}_{i\uparrow} + \hat{n}_{i\downarrow} \right) + U \hat{n}_{i\uparrow} \hat{n}_{i\downarrow} \right],$$

describes the subsystem of impurity d-electrons in the semiconductor matrix, where $E_{\rm d}$ is the initial non-renormalized level of the magnetic impurity in the semiconductor, and $\hat{n}_{i\sigma} = \hat{\rm d}^{+}_{i\sigma}\hat{\rm d}_{i\sigma}$ is the number operator for the d-electrons (with the spin orientation $\sigma = \uparrow,\downarrow$) of the impurity that randomly occupies the ith lattice site. The Anderson—Hubbard parameter U includes the Coulomb repulsion between d-electrons in the same orbital. If necessary, one can allow for the degeneracy of d-orbitals and include in the Hamiltonian the additional intra-atomic correlations, namely, the inter-orbital Coulomb and exchange interactions.

The last term in Hamiltonian (1) describes the resonant (r) and potential (p) scattering of heavy holes by impurities:

$$\hat{H}_{\rm hd} = \hat{H}^{(r)}_{\rm hd} + \hat{H}^{(p)}_{\rm hd},$$

$$\hat{H}^{(r)}_{\rm hd} = \sum_{j,\vec{p},\sigma} \left(V_{\vec{p}} \hat{c}^{+}_{\vec{p}{\rm h}\sigma} d_{j\sigma} \exp\left\{ i \frac{\vec{p}\vec{R}_j}{\hbar} \right\} + {\rm H.c.} \right),$$

$$\hat{H}^{(p)}_{\rm hd} = \sum_{j,\vec{p},\vec{q},\sigma} W_{\vec{p}\vec{q}} \hat{c}^{+}_{\vec{p}{\rm h}\sigma} \hat{c}_{\vec{p}{\rm h}\sigma} \exp\left\{ i \frac{(\vec{p} - \vec{q})\vec{R}_j}{\hbar} \right\}. \qquad (2)$$

Here, $V_{\vec{p}} \approx V$ and $W_{\vec{p}\vec{q}} \approx W$ are respectively the p—d-hybridization parameter and the scattering potential, both of them being only slightly dependent on the hole momenta, and H.c. stands for "Hermitian conjugation". The parameter W is the pseudopotential difference between the atom of the semiconductor host and the substituent magnetic impurity atom. Hamiltonian (1) proposed for DMS and HTFS includes magnetic impurities randomly distributed over the ith lattice sites (their coordinates are denoted as R_j in expression (2) of the Hamiltonian); the impurity concentration is specified by particular problems.

Impurity states in condensed matter can be best described using Green´s functions. The method is based on separation of the Hamiltonian into the unperturbed part and perturbation

$$\hat{H} = \hat{H}_0 + \hat{H}_1.$$

Green´s function of a particular problem (resolvent)

$$G(\varepsilon) = \left(\varepsilon - \hat{H}\right)^{-1} = \left(\varepsilon - \hat{H}_0 - \hat{H}_1\right)^{-1}$$

is found using the Dyson equation

$$G = G_0 + G_0\hat{H}_1 G,$$

where $G_0 = (\varepsilon - \hat{H}_0)^{-1}$ is the unperturbed Green´s function:

$$G(\varepsilon) = \left(\hat{I} - G_0\hat{H}_1\right)^{-1} G_0$$

($\hat{I}$ is the unity matrix). From the knowledge of Green´s function $G(\varepsilon)$ one can calculate the energy spectrum and any characteristics of an impurity crystal. The advantages of Green´s function technique are also that the perturbation $\hat{H}_1$ can not necessary be small, defects in the crystal can be taken into account, and systems from a perfect crystal to an impurity can be studied. The method was also used in studies of the effect of short-range impurity potentials (point impurities or defects in crystal) on the quantum states and vibrational spectra,[403] magnetically ordered crystals,[404] and electronic properties of semiconductors.[405,406] General properties of disordered systems were considered in a monograph.[407] Green´s function method was used to study the influence of an isolated magnetic impurity on the spectrum of semiconductor.[61,62]

Theory presented here also employs Green´s function formalism and treats the first two terms of Hamiltonian (1), $H_0 = H_h + H_d$, which describe noninteracting subsystems of heavy holes and impurity electrons, as the "major" terms. The interaction between these subsystems occurs by scattering of current carriers in the semiconductor by d-electrons with Hamiltonian (2) treated as perturbation:

$$\hat{H}_1 = \hat{H}_{hd} = \hat{H}_{hd}^{(r)} + \hat{H}_{hd}^{(p)}.$$

Computational details have been reported in Refs 408—416. All characteristic parameters of semiconductor hosts (widths of allowed and forbidden bands and masses of heavy holes) and magnetic impurities (energies of initial impurity levels E_d, Coulomb repulsion between d-electrons U, pd-hybridization parameter V, and potentials W) were taken from the literature and then used in calculations carried out with a realistic semi-elliptic density of states for itinerant carriers:

$$\rho(\varepsilon) = \frac{8}{\pi w^2}[-\varepsilon(\varepsilon + w)]^{1/2}\vartheta(-\varepsilon)\vartheta(\varepsilon + w) \approx \frac{8}{\pi w}(-\varepsilon/w)^{1/2},$$

where w is the width of the heavy-hole band (usually, $w \approx 2$—3 eV in DMS and HTFS) and ε is the heavy hole energy counted from the top of the valence band ($-\varepsilon \approx 10^2$ meV, *i.e.*, $-\varepsilon \ll w$).

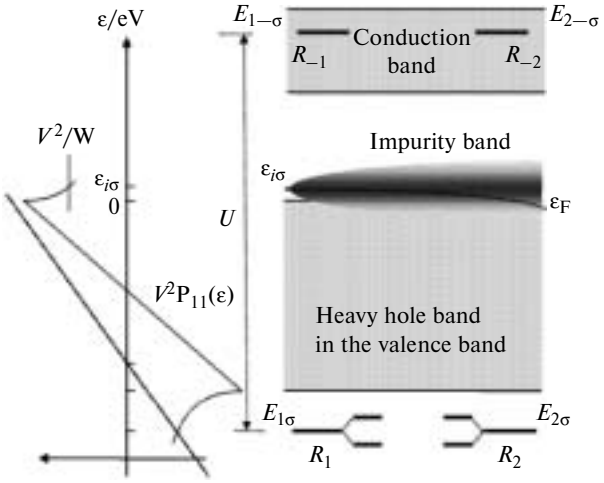

Fig. 2. Calculated scheme of energy levels in GaAs:Mn. The d^5/d^4 CFR levels ($E_{1\sigma}$, $E_{2\sigma}$) lie below the bottom of the heavy hole band, being 3.47 eV lower than the top of the valence band. The energy of the initial impurity d level is $E_d = -2.6$ eV. As the Mn content increases, the impurity band merges with the valence band. Shown is splitting of the CFR levels of two Mn impurities into bonding and antibonding energy levels.

The results of electronic structure calculations of manganese impurities in two DMS, (Ga,Mn)As and (Ga,Mn)N, are shown in Figs 2 and 3, respectively.

In GaAs:Mn with one impurity ($i = 1$ in Hamiltonian (1)), which corresponds to a very low impurity concentration in the real system, the appearance of the acceptor level is due to potential scattering of heavy holes from the band of width $w = 2.9$ eV [417] by manganese ions with the potential $W = 1.02$ eV. The energy of the accep-

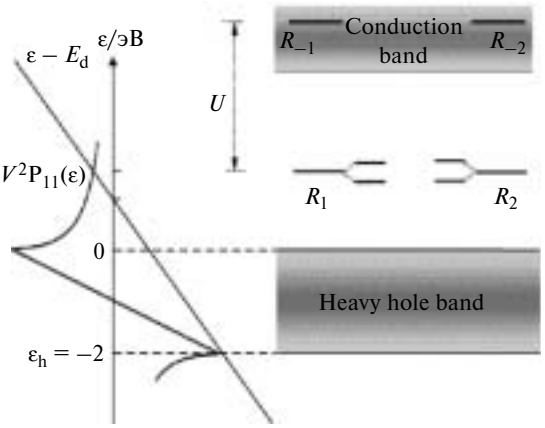

Fig. 3. Calculated scheme of energy levels in GaN:Mn. The d^5/d^4 CFR levels (denoted as $R_{1,2}$) of each Mn impurity lie deep in the forbidden energy band. Energies of the initial impurity d level ($E_d = 1.2$ eV) and of the bottom of the heavy hole band ($\varepsilon_h = -2$ eV) were calculated relative to the top of the valence band. Shown is splitting of the CFR levels of two Mn impurities into bonding and antibonding energy levels.

tor level (E_{acc}) counted from the top of the valence band is given by,

$$E_{acc} \equiv \varepsilon_i = W[1 - w/(4W)]^2, \quad (3)$$

being equal to 85 meV for GaAs:Mn. Position of the CFR d^5/d^4 level is determined from the self-consistent solution to the equation

$$E_{CFR} - E_d \equiv E_{i\sigma} - E_d = V^2 P_{11}(E_{i\sigma}), \quad (4)$$

where E_{CFR} is the energy of the CFR level,

$$P_{11}(\varepsilon) = \int_{-w}^{0} \frac{\rho(\omega)}{\varepsilon - \omega} d\omega =$$

$$= \begin{cases} \dfrac{2}{\varepsilon + w/2 + sign\varepsilon[\varepsilon(\varepsilon + w)]^{1/2}}, & \text{if } \varepsilon > 0 \text{ or } \varepsilon < -w \\ \dfrac{4}{w^2}(w + 2\varepsilon), & \text{if } -w \le \varepsilon \le 0 \end{cases}$$

is the real part of Green´s function of the holes in the valence band, which has the form $(\varepsilon - \hat{H}_h)^{-1}$ in the matrix representation, and integration in $P_{11}(\varepsilon)$ is performed over the interval from the bottom of the heavy hole band to the top of the overlapping impurity band. A graphical solution to Eq. (4) for GaAs:Mn is shown in Fig. 2, *a*. Resonant scattering with the hybridization parameter $V =$ 1.22 eV renormalizes position of the initial impurity d-level $E_d = -2.6$ eV in GaAs:Mn into position of the CFR level with $E_{i\sigma} = -3.47$ eV below the bottom of the heavy hole band. Coulomb repulsion between d-electrons with energy $\acute{U} \approx 4.5$ eV shifts the empty d^6/d^5 CFR to the conduction band of (Ga,Mn)As. Resonant scattering is insufficiently strong to form a DBH at $w = 2.9$ eV and the acceptor level in GaAs:Mn is due to potential scattering in accord with Eq. (3).

The results of electronic structure calculations of the system GaP:Mn are qualitatively similar to those shown in Fig. 2 for GaAs:Mn; they only differ in that the acceptor level originates from the DBH. In GaP:Mn, for the energy of the initial impurity d-level one has $E_d = -1.3$ eV; $w = 2.6$ eV, and the resonant scattering occurs with hybridization parameter $V = 1.31$ eV. Higher position of the impurity d-level in GaP:Mn compared to GaAs:Mn is due to broadening of the forbidden band (2.26 eV in GaP *vs.* 1.42 eV in GaAs), being also responsible for the CFR level with energy $E_{CFR} = -3.28$ eV and a DBH with $E_{DBH} \equiv \varepsilon_i = 400$ meV with respect to the top of the valence band, which are induced by resonant scattering of holes by the impurity. The crystal field resonances and dangling hybrid bonds are two solutions to Eqn. (4), which can also be represented graphically (similarly to the left side in Fig. 2). But in contrast to GaAs:Mn, in the case of GaP:Mn the straight line $E—E_d$ intersects both peaks of the real part of Green´s function $P_{11}(E)$ and give rise to the DBH and CFR.

In GaAs:Mn, the calculated position of the CFR level ($E_{CFR} = E_{i\sigma} = -3.47$ eV) nearly coincides with the measured value (−3.4 eV)[416b,418] and lies in the valence band below the bottom of the heavy hole band (−2.9 eV). The situation with the CFR in GaP:Mn is also similar. Therefore, the lowest d^5/d^4 CFR levels in (Ga,Mn)V (V = As, P) are always filled and, hence, Mn^{2+} ions retain the fifth electron in the 3d-shell and the neutral impurity state $A^0(3d^5\bar{p})$, where $\bar{p}$ denotes a loosely bound hole occupying the acceptor level in the forbidden energy bands of GaAs and GaP and A is the spectroscopic notation of the impurity state. Our assumptions of the chemical regularities of the electronic structure of impurities in DMS and the results of calculations are confirmed by the detection of the $3d^5\bar{p}$ complexes in GaAs:Mn by EPR [419] and IR spectroscopy.[420] Acceptor levels originate from resonant scattering (GaP:Mn) or potential scattering (GaAs:Mn) and lie 400 meV (GaP:Mn) or 100 meV (GaAs:Mn) above the top of the valence band. The last-mentioned value is much larger than a value of 30 meV obtained from calculations using the theory of effective mass.*

p—d-Hybridization (parameter V differs from zero only for the same spin states of a d-electron and a *p*-hole) is only possible if the localized spin and the spin of the itinerant hole have the same orientation during tunneling. Strong intra-atomic Coulomb interaction between d-electrons (parameter U) and the Hund coupling provide half-filled $3d^5$-shells of the manganese impurity ion in the lowest CFR levels. In the case of two impurity atoms ($i = 1, 2$ in Hamiltonian (1)) tunneling of d-electrons to empty states near the top of the valence band and back with the energy $\sim\rho V^2$ (dependence from the distance between impurities is omitted for simplicity) causes splitting of the acceptor and CFR levels into bonding and antibonding sublevels (see Fig. 2, lowest CFR). As the impurity concentration increases, the distance between impurities is shortened while the number of acceptor levels and the splitting value increases. As a result, the acceptor levels are broadened to give an impurity band, which is overlapped with the valence band in (Ga,Mn)As and in type (II—IV,Mn)V_2 HTFS. In $Ga_{1-x}Mn_xAs$, the overlap begins at $x < 1$ at.%, which was confirmed experimentally.[260,421] An IR spectroscopy study[421] of compounds (Ga,Mn)As with $T_C = 70$ K revealed energy levels of antisites As_{Ga} at 500 meV, which lie above the acceptor levels (~100 meV). The overlap of the impurity band and the valence band in (Ga,Mn)As with an increase in the Mn content is schematically shown in Fig. 2. In (Ga,Mn)P, the DBH levels lie deep in the forbidden energy band, so the impurity band remains isolated from the valence band with an increase in the Mn content.

* H. Åsklund, L. Ilver, and J. Kanski, http://arXiv.org/cond-mat/0112287.

Resonant nature of the manganese CFR t_2-level (d^5/d^4) near the middle of the band gap in (Ga,Mn)N was confirmed experimentally[422] and by numerical calculations.[391,390] The electronic structure of GaN:Mn (see Fig. 3) was calculated using the following parameters of the GaN matrix and the Mn impurity: position of initial impurity d-level $E_d = +1.2$ eV, the heavy hole band width $w = 2$ eV, and hybridization parameter $V = 1.2$ eV. Position of the only impurity CFR level d^5/d^4 was determined by graphical solution to the Eq. (4), which is presented on the left in Fig. 3. The CFR level is above the top of the valence band ($E_{CFR} = 1.7$ eV), lying nearly in the middle of the forbidden band (for GaN with the zinc blende structure the width of the forbidden band is 3.23—3.25 eV at 300 K and 3.3 eV at 0 K).

The manganese CFR t_2-levels (d^5/d^4) appear deep in the valence bands of the GaAs and GaP hosts (see Fig. 2) but deep in the forbidden band of GaN (see Fig. 3) due to the narrower band gaps, higher position of the valence bands in GaAs and GaP compared to GaN, and referencing to vacuum of the Mn 3d-level. In GaN:Mn, the CFR t_2-level is empty is the Ga^{3+} ion is replaced by $Mn^{3+}(d^4)$ impurity and becomes magnetically active only upon *n*-doping. The configuration $Mn^{3+}(d^4)$ corresponds to a neutral state; each Mn impurity ion introduced in GaN gives an empty CFR level near the middle of the band gap, this level playing the role of a deep acceptor. Therefore, in contrast to (Ga,Mn)As and (Ga,Mn)P, there is no need of binding a hole to retain electrical neutrality of (Ga,Mn)N. This behavior is also characteristic of the early transition metal ions (Sc, Ti, V) in all compounds of the III—V type.

Replacing Ga^{3+}, the Mn^{2+} impurity retains its high-spin state with a half-filled d-shell $3d^5$ due to strong intra-atomic Hund exchange. In other words, the manganese impurities in the (Ga,Mn)V systems create hole-attracting potentials, acting as acceptors in (Ga,Mn)As and (Ga,Mn)P, and increase the magnetic moments of the *p*-type (III,Mn)V compounds. On the contrary, a Mn impurity in the wide-gap *n*-type semiconductor GaN donates one d-electron to the valence band and thus undergoes transition to the $Mn^{3+}(d^4)$ state. The impurity band (not shown in Fig. 3) of *n*-type (Ga,Mn)N appears near this state inside the band gap.

It is important for the electronic structure of a semiconductor containing a magnetic impurity that the absolute position of the CFR level depends only slightly on the semiconductor matrix, because the CFR energy calculated relative to vacuum is compensated by the competing bonds with the electronic states in the valence band and in the conduction band. On the contrary, the DBH energies are closely related to the density of states in the heavy hole band, their positions being dependent on the strength of pd-hybridization.[408—416]

It should be noted that qualitative schemes of the energy levels of 3d-impurities calculated in an extended III—V supercell[390] are similar to the diagrams shown in Figs. 2 and 3 obtained[408—414,416b] using Green´s function formalism. According to calculations,[390] doping with manganese cations leads to the appearance of holes in the shallow acceptor levels of GaAs and GaSb and in the deep CFR level of GaN. Positions of the CFR and DBH levels of the 3d-impurity in type III—V compounds obtained using Green´s function technique[408—416] and from numerical calculations[390] (see also Refs 80 and 391) are similar because first-principle calculations in the supercell begin with calculations for a single impurity in a finite cluster. However, further use of the "supercell" approach to describe the magnetic state by buildup of a periodic cluster structure does not go beyond the Stoner phenomenological model of itinerant ferromagnetism. Therefore, it is quite reasonable that in similar studies the DMS and HTFS are analyzed and discussed in terms of the exchange splitting and the spin subbands corresponding to spin orientations "up" and "down" (see., *e.g.*, Refs 80, 390—396).

Below we present the third strategy of research into the nature of magnetism in DMS and HTFS. Here, the exchange interaction and the magnetic properties are analyzed with allowance for the electron states of transition metal impurities in different semiconductors. The electron energy spectrum is formed by the chemical bonds between the 3d-orbitals of the impurity ions and the p-orbitals electrons in the valence band, whereas the magnetic state is governed by the Coulomb and exchange interaction inside the atomic 3d shells (intra-atomic correlations electron).

4.3. Nature of ferromagnetism in dilute magnetic semiconductors and high-temperature ferromagnetic semiconductors

Consideration of the chemical bonds formed by magnetic impurities in semiconductors helps to clarify the nature of exchange interaction between electrons localized on distant magnetic impurities in the semiconductor. Owing to peculiarities of the electronic structure of transition metal impurities it is impossible to directly extrapolate the ferromagnetic properties of *p*-type (Ga,Mn)As with relatively narrow band gap to high-temperature DMS, *e.g.*, *n*-type (Ga,Mn)N with a broad forbidden band or *p*-type (Ga,Mn)P. However, this often occurs in phenomenological approaches (see, *e.g.*, Ref. 77).

Two Mn impurities in *p*-(Ga,Mn)As and *p*-(Ga,Mn)P have relatively shallow acceptor levels (see Fig. 2, levels R_1 and R_2) that are absent in *p*-(Ga,Mn)N and a deep CFR level in the allowed band. In the *n*-type (Ga,Mn)N, the localized states are deep CFR levels in the forbidden band (see Fig. 3, levels R_1 and R_2). In these two different cases indirect exchange interactions between electrons occupying the CFR levels R_1 and R_2 of two impurities are basically different. The nature of ferromagnetic exchange

in the *p*-type and *n*-type DMS and in the isoelectronic HTFS should be considered separately.[408—416]

Spin-selective electron transfer with the energy ρV^2 between impurities is governed by p—d-hybridization and strong intra-atomic electron correlations (Coulomb interactions and Hund exchange) (see Section 4.2). In other words, transfer is only possible if the electron spins $S_{i=1,2}$ of neighboring impurities (*e.g.*, Mn^{2+}) with the wave functions ψ_1 and ψ_2 have parallel orientations. In this case, tunneling removes the degeneracy of the initial impurity states $\psi_{1,2}$, their energy levels become split ($E_+ - E_- = 2\rho V^2$), and now one deals with a bonding and antibonding combinations of the wave functions of two impurities, namely, $\psi_+ = (\psi_1 + \psi_2)/\sqrt{2}$ and $\psi_- = (\psi_1 - \psi_2)/\sqrt{2}$ (spin triplet S = 1); the energy difference between these states is no more than the exchange energy $E_- - E_+ = -2J_{ex}\vec{S}_1\vec{S}_2$. Indeed, the Hamiltonian $\hat{H}$ of two impurities has the form

$$E_- - E_+ = \langle\psi_-|\hat{\hat{H}}|\psi_-\rangle - \langle\psi_+|\hat{\hat{H}}|\psi_+\rangle = -2\langle\psi_1|\hat{\hat{H}}|\psi_2\rangle, \qquad (5)$$

i.e., the exchange interaction J_{ex} of two isolated electrons formally coincides with the energy $\rho V^2 = \langle\psi_1|\hat{H}|\psi_2\rangle$ of electron tunneling between impurities due to p—d-hybridization. If the impurity spins have antiparallel orientations, no tunneling occurs and the impurity levels do not split. But splitting of the levels of two localized electrons does not provide an indirect magnetic exchange. In the semiconductor with the heavy hole band of width *w* the proportion of the holes involved in magnetic exchange between identical impurities with the CFR energy levels E_{CFR} is $[(w/E_{CFR})\cdot\rho V]^2$. As a result, an indirect exchange interaction occurs between electrons localized on impurities, which can be written as follows taking into account Eq. (5)

$$J'_{ex} \propto \rho V^2\cdot[(w/E_{CFR})\rho V]^2 = \rho^3 V^4 (w/E_{CFR})^2, \qquad (6)$$

We called it *kinematic exchange* interaction because it is due to tunneling, *i.e.*, electron transfer between impurities *via* the empty band and impurity states. Kinematic exchange is accompanied by a decrease in the kinetic energy of itinerant heavy holes owing to their hybridization with impurity d-electrons with the same spin orientation. Otherwise, in accord with the Hund rule an electron hopping to the impurity atom with a different spin orientation requires an additional energy. If the magnetic moments of impurities are not aligned, the Hund rule will block transfer of an electron with the spin orientation parallel to the angular momentum direction of the first impurity to the second impurity with the "wrong" angular momentum direction. Splitting of the initial impurity levels, not suppressed by the Hund rule, and the kinematic exchange occur only if not all available bands and impurity states are filled, that is $\rho(\varepsilon) \neq 0$ in Eq. (6). (Here, for qualitative description of kinematic exchange (6) the dependence of tunneling on the distance between impurities is left out of consideration).

Rigorous total energy calculations takes into account all changes in the energy spectrum and significant rearrangement of the impurity band and the heavy hole band with allowance for both resonant and potential scattering. The total energy of the system is given by the spur of the Hamiltonian, $E = Tr\hat{H}$, and the change in the total energy due to scattering of current carriers by impurities is given by

$$E_{FM} = \frac{1}{\pi}\cdot \mathrm{Im}\int_{-\infty}^{\infty}\varepsilon\cdot Tr\Delta G[\varepsilon - i\delta\cdot sign(\varepsilon-\varepsilon_F)]d\varepsilon - \sum_i Un_{i\uparrow}n_{i\downarrow},$$

where $\Delta G(\varepsilon) = G(\varepsilon) - G_0(\varepsilon)$ is the difference between the total and unperturbed Green´s functions (for computational details, see Refs 408—416). To calculate the pair exchange interaction, one should know the electron energy spectrum of the semiconductor with two magnetic impurities (*cf.* Section 4.2). Owing to indirect spin-dependent overlap of the impurity orbitals of two magnetic impurities in the semiconductor the change in the energy of the system is the ferromagnetic energy gain relative to the spin-disordered state, *i.e.*, the exchange energy

$$J'_{ex} = \frac{V^4}{\pi}\int_{\varepsilon_F}^{\varepsilon_t} d\varepsilon \frac{P_{12}(\varepsilon)\Gamma_{12}(\varepsilon)}{[\varepsilon - E_d - V^2P_{11}(\varepsilon)]^2 + (V^4/4)\pi^2\rho^2(\varepsilon)}, \qquad (7)$$

where

$$P_{12}(\varepsilon) = \int d\omega \frac{\sin[k(\omega)R]}{k(\omega)R}\frac{\rho(\omega)}{\varepsilon-\omega}$$

and

$$\Gamma_{12}(\varepsilon) = 2\pi\rho(\varepsilon)\frac{\sin[k(\varepsilon)R]}{k(\varepsilon)R}$$

are the real and imaginary parts of heavy-hole Green´s function:

$$P_{12}(\varepsilon) + (i/2)\Gamma_{12}(\varepsilon)$$

and integration in J'_{ex} is performed from the Fermi energy to the top of the valence band, ε_t. Here, $k = (2m\varepsilon)^{1/2}/\hbar$ is the wave vector of the hole with the mass *m* moving with the energy ε and *R* is the average distance between impurities whose concentration is $x = a^3/(4R^3)$, where *a* is the lattice constant. At $\varepsilon_t = 0$, the energy of exchange interaction (7) can be written in explicit form as

$$J'_{ex} = \frac{64}{\pi}\cdot\rho^3(\varepsilon_F)V^4\left(\frac{w}{E_{CFR}}\right)^2\left[1 + \frac{\sin k_bR}{k_bR} + \frac{1}{12}(k_bR)^2\right]\times$$
$$\times\frac{\sin k_FR - k_FR\cos k_FR}{(k_FR)^3}, \qquad (8)$$

where $k_F = \sqrt{-2\ m\varepsilon_F}/\hbar$ is the Fermi wave vector, E_{CFR} is the position of the CFR impurity level, $k_b = \sqrt{2mw}/\hbar$,

and $\rho(\varepsilon_F)$ is the density of hole states in the Fermi level $\varepsilon_F(x)$ (ε_F is counted from the top of the valence band and depends on the dopant concentration). In Eq. (8) the coefficient on the left side before the brackets coincides with the qualitative estimate (6).

Kinematic exchange interaction in *p*-type DMS and in HTFS involves virtual transitions of d-electrons to unoccupied valence and impurity states. It self-consistently allows for three important interrelated contributions to the magnetic energy, namely, d—p-tunneling (hybridization parameter V), CFR d-resonances, and DBH dangling p-bonds and can be reduced to none of the conventional exchange interactions. Unlike phenomenological models dealing with localized impurity spins and itinerant holes in the allowed band, the kinematic exchange takes into account a change in the hole density of states and therefore the magnetic response of holes owing to the resonant scattering and impurity band formation. From Eq. (8) it follows that only at unreally high concentrations of magnetic impurities ($k_bR \ll 1$) kinematic exchange changes its sign similarly to RKKY indirect exchange (see Section 3.3). At low impuriy concencentrations ($k_bR \gg 1$), as is typical of DMS and HTFS, the kinematic exchange is proportional to 1/R, being much stronger than the RKKY exchange. The kinematic exchange differs from the Vonsovsky—Zener double exchange mechanism[65,70—72] used[65] to explain ferromagnetism in manganites $(La,Sr^{2+})MnO_3$ (mixed-valence compounds with intrinsic Mn sublattice) by the exchange of different valence states ($Mn^{3+} \rightleftharpoons Mn^{4+}$) *via* oxygen anions. In *p*-type DMS and in HTFS, transition metal impurity ions have the same integer valence and occupy the CFR states identically (*cf.* the levels R_1 and R_2 in Fig. 2); therefore, no Zener exchange interaction[65] occurs in these substances. Nevertheless, density functional calculations[388,395] of *p*-type DMS (In,Mn)As and (Ga,Mn)As were performed with the Zener model in spite of the absence of mixed valence in the DMS and the experimental results mentioned above.*

In the molecular field approximation the spin Hamiltonian of the kinematic exchange interaction (7), (8) in DMS and HTFS has the form

$$\hat{H}_{MF} = -\frac{1}{2}\sum_i J'_{ex}(R)J_i\langle J\rangle. \qquad (9)$$

Here, summation is performed over all positions of the magnetic impurities with the orbital moment J_i in the semiconductor lattice. The coefficient 1/2 accounts for the fact that, by implication of kinematic exchange, the energy gain for two spins with parallel orientations *vs.* their antiparallel orientations is J'_{ex} (7), (8). In a conventional spin model ($J''\vec{S}_1\vec{S}_2$, see., *e.g.*, Ref. 423) this energy gain is $2J''$, where J'' is the direct Heisenberg exchange interaction. From Eq. (9) it follows that the Curie temperature of the ferromagnetic—paramagnetic phase transition is given by

$$T_C = z\frac{J'_{ex}}{k_B}\cdot\frac{J(J+1)}{6}, \qquad (10)$$

where J is the total spin of impurities (angular momentum) and z is the coordination number of the magnetically active impurities in a given DMS or HTFS.

An important feature of magnetic impurities in semiconductors, which was considered in the previous Section, is that the manganese ion retains their valence. When manganese replaces the higher-valence atoms in DMS and HTFS, the Pauling principle of electrical neutrality is obeyed owing to the formation of the Mn^{2+} complexes with heavy holes. The total "spin" of the complex appears to be lower than $S(Mn^{2+}) = 5/2$. For instance, in (Ga,Mn)As and (Ga,Mn)P the total momentum $\vec{J} = \vec{S} + \vec{j}$ of the complex $Mn(3d^5\bar{p})$ equals $J = S - j = 1$, because it is formed by the orbital momentum $j = 3/2$ of a loosely bound hole $\bar{p}$, involved in antiferromagnetic interaction with the spin of the Mn^{2+} ion ($S = 5/2$). The antiferromagnetic exchange constant of the complex $Mn(3d^5\bar{p})$ was measured by Raman scattering.[424] Coexistence of weakly and strongly localized states in (Ga,Mn)As was also confirmed by conductivity measurements.[281]

Ternary compounds, *e.g.*, HTFS based on manganese-doped type II—IV—V_2 hosts exhibit a more impressive picture of cation substitution compared to binary III—V compounds. Namely, Mn^{2+} ions replace both the atoms of Group II elements with retention of the spin $S = 5/2$ and the atoms of Group IV elements. For the same reason (antiferromagnetic exchange of holes and the local spin) the Mn_{Ge} ion in the HTFS $(ZnGe,Mn)P_2$ forms a complex with the momentum $J = 1/2$ with two holes, which was confirmed by ESR.[319] Replacement of the Ge^{4+} ion with the smaller radius by Mn^{2+} ion in the HTFS $(CdGe,Mn)As_2$ was confirmed by an increase in the lattice constant[329] and by estimates of the average angular momentum from magnetic measurements[413,415,416a] ($J < 5/2$ per formula unit of $(CdGe,Mn)As_2$).

The Fermi energy appeared in Eqns (7) and (8) depends on the magnetic impurity concentration x and is related to the volume density, $n(x)$, of charge carriers in the material:

$$\frac{a^3}{8}n(x) = 2\int_{\varepsilon_F(x)}^{0}\rho(\varepsilon)d\varepsilon$$

(coefficient 8 is due to the presence of four pairs of atoms of Group III—V or isoelectronic chemical elements in the unit cell of volume a^3). Usually, the parameter $n(x)$ is

* Y. H. Matsuda, G. A. Khodaparas, M. A. Zudov, J. Kono, Y. Sun, F. V. Kyrychenko, G. D. Sanders, C. J. Stanton, N. Miura, S. Ikeda, Y. Hashimoto, S. Katsumoto, H. Munekata, http://arXiv.org/cond-mat/0404635.

found from Hall effect measurements, by IR spectroscopy,[424] using an electrochemical cell, or other methods.

To calculate the $T_C(x)$ of a *p*-type DMS, one must substitute the total spin of impurities J and the coordination number z in Eq. (10). Calculations of the kinematic exchange (7) require substitution of the known characteristics of the material and magnetic impurities, namely, the mass and concentration of heavy holes, the heavy hole band width, hybridization parameter, and the energy of the impurity level. If the role of the impurity band is insignificant ($\varepsilon_t = 0$), one can use expression (8). Using the impurity content x and the corresponding hole concentration n in the samples of the material under study, an $n(x)$ extrapolation can be constructed. Studies[408—416] present the results of $T_C(x)$ calculations for various materials, carried out using the $n(x)$ dependences, that are in excellent agreement with experimental data.

For such DMS as (Ga,Mn)As or (Ga,Mn)P one must substitute the spin $J = 1$ in Eq. (10). The results obtained for a particular case of calculations are shown in Fig. 4. For comparison, Fig. 4 also presents the results of our calculations using the phenomenological theory of DMS,[78] which significantly differ from the experimental data due to ignoring the chemical bond of the Mn impurity in GaAs:Mn. The plots shown in Fig. 4 were calculated using relation (10) with the hole densities measured for seven (Ga,Mn)As samples with $T_C \le 140$ K.[425] As can be seen from Fig. 4, the kinematic theory predicts a maximum T_C of about 160 K for annealed samples. Later,

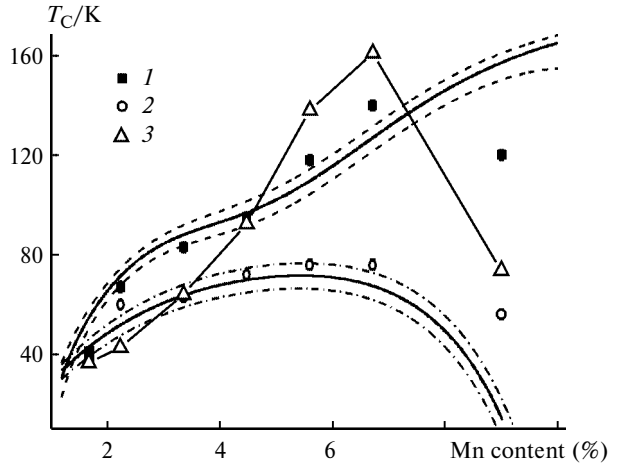

Fig. 4. Curie temperature T_C plotted *vs.* $Ga_{1-x}Mn_xAs$ composition. The solid curves represent the results obtained from $T_C(x)$ calculations[414] for kinematic exchange starting from the experimental hole density. The filled squares, open circles, and open triangles respectively denote the experimental T_C values of annealed (*1*) and as-grown (*2*) materials;[425] and the results obtained[425] for the as-grown samples (*3*) based on the phenomenological theory[78] (see Website*).

* http://ep2ds14.fzu.cz/ms/setparam.ausprg.php.

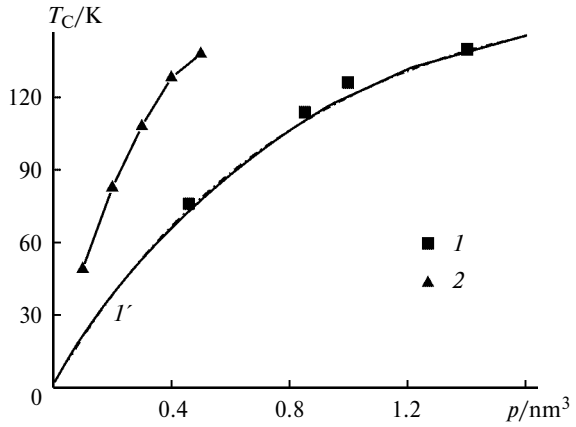

Fig. 5. Curie temperature plotted *vs.* hole concentration in $Ga_{0.94}Mn_{0.06}As$: experimental data[425] (*1*) and results of $T_C(p)$ calculations using phenomenological theory[78] (*1*). The smooth curve *1′* obtained from $T_C(p)$ calculations for kinematic exchange mechanism.

(Ga,Mn)As samples with $T_C = 150$—160 K were synthesized.[426—428,*]

In contrast to phenomenological models dealing with localized spins and free holes near the top of the valence band, the kinematic exchange (7) allows for the change in the hole density states and thus their magnetic "response" owing to resonant scattering and impurity band formation. As a result, one gets realistic $T_C(x)$ dependences that are consistent with the experimental data (see Fig. 4 and the $T_C(x)$ dependences reported for other DMS samples in Refs 408—412) rather than a linear plot of Curie temperature *vs.* impurity concentration ($T_C \propto x \cdot p^{1/3}$).

Phase transitions in DMS and HTFS from the paramagnetic to ferromagnetic state can be induced either by a decrease in the temperature at a constant density of current carriers or by an increase in the carrier density at constant temperature. The carrier density can be changed by doping, annealing, applying an electric field or by exposing the material to light. The dependence of T_C on the hole density p in (Ga,Mn)As containing 6 at.% of Mn calculated using Eqns (8) and (10) on the basis of the experimentally measured hole densities in the sample after four stages of annealing in different regimes is presented in Fig. 5. The $T_C(p)$ curve reaches a saturation point of 158 K at a hole density, p, of 3.0 nm^{-3} (not shown in Fig. 5), *i.e.*, the $T_C(p)$ dependence does not obey the relation $T_C \propto x \cdot p^{1/3}$ used in phenomenological theory[77—79] which predicts an infinite increase in T_C with increasing the hole concentration.

The results of $T_C(T_a)$ calculations using the measured hole density[429] for three annealing temperatures T_a are in

* K. W. Edmonds, P. Boguslawski, K. Y. Wang, R. P. Campion, N. R. S. Farley, B. L. Gallagher, C. T. Foxon, M. Sawicki, T. Dietl, M. B. Nardelli, and J. Bernholc, http://arXiv.org/cond-mat/0307140.

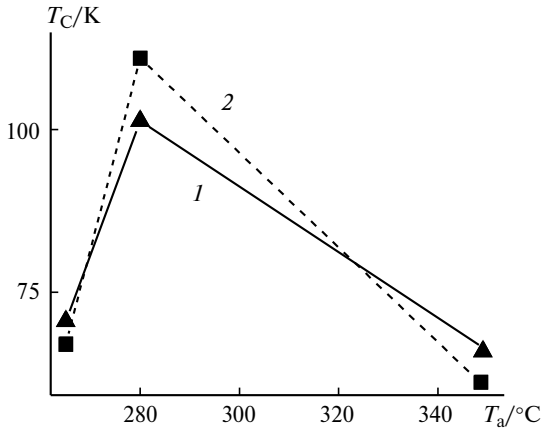

Fig. 6. Curie temperature plotted *vs*. annealing temperature of (Ga,Mn)As: results of calculations[413] (*1*) and experimental data[429] (*2*).

good agreement with the experimentally measured Curie temperatures (Fig. 6).

In the case of *p*-type (Ga,Mn)N the kinematic exchange theory should be slightly modified. Here, Mn remains a neutral isoelectronic substitutional defect with the configuration $Mn^{3+}(d^4)$, because the CFR level of $Mn^{2+/3+}$ falls in the middle of a broad forbidden energy band of GaN (see Fig. 3). If the hole concentration is higher than the Mn impurity content, ferromagnetism in *p*-type (Ga,Mn)N has a kinematic exchange mechanism, similarly to (Ga,Mn)As and *p*-(Ga,Mn)P, but with the localized moments of the $Mn^{3+}(e^2t^2)$ magnetic impurities $J = 2$.

If one deals with a doped DMS such as *n*-type (Ga,Mn)N, a fraction of Mn^{3+} impurities traps donor electrons and becomes charged ions $Mn^{2+}(d^5)$. As a result, the impurity band in (Ga,Mn)N, which appears near the CFR level, contains both Mn^{2+} and Mn^{3+} ions in contrast to (Ga,Mn)As, (Ga,Mn)P, and *p*-type (Ga,Mn)N. Here, a problem is posed of the magnetic exchange interaction in *n*-type (Ga,Mn)N with the impurity band in the deep CFR level, which remains separated from the allowed bands in the whole range of Mn concentrations. If other shallow acceptors do not create free holes near the top of the valence band, the Fermi level must lie in the impurity band and electron tunneling between the CFR levels must occur due to the heavy hole p-orbitals mixed with the d-orbitals owing to p—d-hybridization. In this case the role of the p-orbitals in (Ga,Mn)N is similar to that played by the oxygen p-orbitals in the double exchange in $(La,Sr)MnO_3$ [65] and the magnetic interaction in *n*-type (Ga,Mn)N is provided by the exchange of the valence states $Mn^{2+} \rightleftharpoons Mn^{3+}$. Here, the T_C value of *n*-type (Ga,Mn)N equals the half-width of the impurity band, averaged over positions of the impurity levels;[413,416b] that is, the highest T_C is achieved if the impurity band is half-filled and position of the Fermi level coincides with the CFR level. The Curie temperature calculated with the hybridization parameter $V = 1.2$ eV and the "spin" $J = 2$ varies from 100 K at $x = 0.01$ to 1000 K at $x = 0.05$, being in agreement with the experimental data ($T_C = 940$ K [303,430—433] in (Ga,Mn)N epitaxial films). If the Fermi level lies near the bottom of the conduction band, T_C is exponentially low with respect to the impurity concentration.[434]

In the H_d term of the Hamiltonian (1), the three-fold degeneracy of the d-orbitals with t_2 symmetry is significant when calculating the broadening of the impurity band with increasing the impurity concentration. The case in point is that the band p-states obey the Fermi statistics. But in the statistics of the atomic d-states hybridized with the band p-states the d-orbital cannot be filled with two electrons with (i) parallel spin orientations due to the Pauli exclusion principle and (ii) antiparallel spin orientations due to the Coulomb repulsion characterized by the Anderson—Hubbard parameter *U*. The description of the states of magnetic impurities is similar to the Heitler—London treatment of hydrogen molecule (1927). If the energy of the $Mn^{2+}(d^5)$ impurity is E_{CFR} and the energy of the $Mn^{3+}(d^4)$ impurity is μ (chemical potential), their statistical sum is $Z = \exp[-E_{CFR}/(k_BT)] + 3\exp[-\mu/(k_BT)]$. From here the occupation numbers of the impurity atomic shells differ from the Fermi distribution:

$$n(d^5) = -k_BT\frac{\partial \ln Z}{\partial E_{CFR}} = \frac{n_F(E_{CFR} - \mu)}{3 - 2n_F(E_{CFR} - \mu)},$$

$$n(d^4) = -\frac{1}{3}k_BT\frac{\partial \ln Z}{\partial \mu} = \frac{1 - n_F(E_{CFR} - \mu)}{3 - 2n_F(E_{CFR} - \mu)},$$

where $n_F(E_{CFR} - \mu) = (\exp\{(E_{CFR} - \mu)/(k_BT)\} + 1)^{-1}$ is the Fermi distribution. As can be seen, if $E_{CFR} - \mu > 0$ (chemical potential is lower than the CFR level of the fifth electron of the Mn^{2+} impurity), one has $n_F(E_{CFR} - \mu) = 0$ and the occupation numbers are $n(d^5) = 0$ and $n(d^4) = 1/3$ at low temperatures. If $\mu > E_{CFR}$, one has $n(d^5) = 1$ and $n(d^4) = 0$. The quantum statistics of magnetic impurities in semiconductors is derived on the basis of the Fermi statistics and the atomic statistics in such a way that the impurity states obey the atomic statistics that allows each impurity level to be occupied by one electron only (even in the case of degenerate t_2-states) and the impurity band to be filled with integer numbers of electrons.[408—412,414,416b,]

Density functional calculations of such HTFS as $(Cd,Mn)GeP_2$ and $(Zn,Mn)GeP_2$ using the Zener model predict ferromagnetism[326] while the supercell calculations[435,436] of the same compounds predict an antiferromagnetic ground state. The data,[392,393] according to which both CFR and DBH favor the ferromagnetic state of $(CdGe,Mn)P_2$, seem to be the best approximation to the

theory of the kinematic exchange in HTFS. In *p*-type $(CdGe,Mn)As_2$, ferromagnetic ordering is favored by the $(Cd,V_{Cd},Mn)GeAs_2$ vacancies and nonstoichiometry of the type $(CdGe,Mn)GeAs_2$, which increase the concentrations of the holes and empty states involved in kinematic exchange near the top of the valence band.[329] In type III—V DMS, the highest Curie temperatures correlate with the width of the forbidden band in spite of different exchange mechanisms in the *p*- and *n*-type compounds, Namely, T_C increases in the order (Ga,Mn)As, (Ga,Mn)P, (Ga,Mn)N. Consideration of type II—IV—V_2 compounds gives the following order of a decrease in the stability of the ferromagnetic phase of the manganese-doped hosts[198]:

$$GaN \Rightarrow GaP \Rightarrow GaAs \Rightarrow CuGaS_2 \Rightarrow$$
$$\Rightarrow CuGaSe_2 \Rightarrow GaSb \approx CuGaTe_2.$$

In fact, the theory of kinematic exchange interaction in DMS and HTFS has no fitting parameters; all quantities are expressed through the available characteristics of materials. For instance, the energy spectrum and the calculated curves $T_C(x)$ and $T(p)$ of annealed samples shown in Figs 2 and 4—6 were obtained using the same known parameters of the (Ga,Mn)As system, *viz.*, the heavy hole mass $m = 0.51m_0$, the width of the heavy hole band $w =$ 2.9 eV, pd-hybridization parameter $V = 1.22$ eV, coordination number $z = 4.0$, and the energy of the impurity d-level $E_d = -2.6$ eV. With these parameter values, the Curie temperatures were determined from the experimental hole concentrations. The calculated dependences of T_C on the impurity concentration, hole density, and annealing temperature (see also Refs 408—416b) are in good agreement with experimental data.

Greater hole density provides a higher conductivity, *i.e.*, the DMS and HTFS exhibiting the highest T_C must be good conductors.

Formally, the kinematic exchange interaction between magnetic impurities is given by the integral (7), which allows for reconstruction of the whole electron spectrum. This differs the mechanism of kinematic exchange from the double and other types of exchange mechanism involving a specific parameter of exchange interaction that is usually introduced phenomenologically. The effect of antisites (*e.g.*, As_{Ga}) or interstitial defects and possible clustering of impurities are included in this theory *via* the effective coordination number *z* and statistics. A simplified picture of the structure of the valence band (heavy hole band with a semi-elliptic density of states) does not present an obstacle to the development of this theory, which can be improved with allowance for, *e.g.*, the light hole band.

The theory is also suitable for the description of ferromagnetism in other DMS, *e.g.*, an elemental dilute semiconductor (Ge,Mn)[154,247,437,438] or a wide-gap ZnO matrix doped with Mn and Fe,[346,349] where magnetic impurities (Mn^{2+} and Fe^{2+}) isoelectronically replace Zn ions, and I—III—VI_2 based HTFS. Transition metal ions in Ge are usually interstitial impurities that are in some cases involved in complexation.

The empty impurity CFR levels (d^6/d^5) lie deep in the conduction band due to strong intra-atomic Coulomb repulsion (Anderson—Hubbard parameter *U*) and can be a reason for antiferromagnetic ordering in the impurity band. In zinc blende type crystals, indirect exchange involving empty electron states in the conduction band is weak because the hybridization V_{ds} between the impurity d and s electron states near the bottom of the conduction band is low from symmetry considerations.[401,402] In connection with the empty states in the electronic spectrum of a material the Blombergen—Rowland mechanism of indirect exchange[439] is worth noting, according to which interaction between the impurity spins in DMS involves virtual states in the allowed bands, created by electron transitions from the bands to the impurity acceptor levels. This mechanism was the subject of a few studies[383,443,*] (see also a discussion in Refs 440, 441) that postulated the existence of a contact dp or ds exchange interaction ignoring the chemical bonds of magnetic impurities in semiconductors. The properties of DMS were analyzed* using the Blombergen—Rowland mechanism and the Hamiltonian (1). However, the T_C of *n*-(Ga,Mn)N was found to be proportional to $|V_{dp}|^2|V_{ds}|^2$, *i.e.*, unrealistically low.* In the case of DMS and HTFS of particular theoretical interest is to allow for the distribution functions of random local magnetic fields over the lattice sites chaotically occupied by magnetic impurities[442,443] (at present, in the framework of the Ising model that can be solved exactly), which leads to unusual temperature dependences of the magnetization.

Conclusion

The review presents the state-of-the-art in the field of spintronics, a rapidly developing field of science and technology, which employs the experience, concepts, and ideas from different fields of knowledge of the condensed matter. Among them are the band theory of solids; microelectronics; magnetism and various versions of magnetic resonance; superconductivity in nanosystems including single-electron electronics, Josephson tunneling, Abrikosov vortices, all types of transport mechanisms (Boltzmann, ballistic, hole, tunneling); specific methods such as optical spin orientation and photo-EMF; materials science;[1] physical chemistry of materials and materials design; and strong electron interactions in condensed matter.

* V. Barzykin, http://arXiv.org/cond-mat/0311114.

Among the variety of spintronics-related aspects, in this review the emphasis was placed on the fundamentals of spintronics; formulation of criteria for spintronic materials; consideration of the first-generation spintronic materials (ferromagnetic metal alloys); characterization of the physicochemical properties of the second-generation spintronic materials, namely, concentrated magnetic semiconductors and semimetals and half-metals, semimagnetic semiconductors, dilute magnetic semiconductors (DMS), and high-temperature ferromagnetic semiconductors (HTFS). Research on inhomogeneous magnetic materials and high-T_C nanocrystals including organic materials suitable for spintronics applications was also outlined. (Semi)phenomenological and numerical cluster approaches used to explain the magnetic properties of novel spintronic materials (DMS and HTFS) were analyzed. The electronic structures of semiconductors doped with magnetic impurities were considered.[400—402] It is the structure of the chemical bonds formed by the magnetic impurity in the semiconductor matrix that is responsible for both the mechanism of exchange interaction and the nature of ferromagnetism[408—416] that occurs in the DMS and HTFS with an increase in the transition metal content.

It was not the authors´ goal to provide with exhaustive literature on the subject. Most of the studies selected from the rapidly growing body of information are concerned with the subject of this review, namely, spintronic materials and magnetic properties of DMS and HTFS. (for continuously renewable literature on DMS and HTFS, please visit the Website*.)

Without pretending to cover all aspects of spintronics, which has got a new impetus to development after the discovery of DMS and HTFS, in conclusion the authors of this review take the risk of making some prognoses. Currently, spintronic devices based on first-generation materials are increasingly used, whereas the DMS- and HTFS-based devices are still in the stage of test models or demonstration facilities. Spintronics serves as a generator of new ideas and methods in materials science, solid-state physics, and solid-state chemistry. Research and development in order to solve spintronics-related problems involves design of setups; elaboration of methods of synthesis of single crystals and nanocrystals, and heterostructures with alternating DMS and HTFS layers; synthesis of novel materials; improvement of methods of liquid-phase epitaxy, chemical vapor deposition, and low-temperature molecular beam epitaxy.

In studying the properties of spintronic materials researchers discover new types of magnetic interactions that cannot be described using the available concepts of magnetism. Probably, in the case of DMS and HTFS we deal with a novel type of indirect magnetic exchange, which does not occur in the transition metal oxides described by Zener theory of ferromagnetic insulators. Novel spintronic materials based on semiconductors seem to be quite promising because, according to theory, they can exhibit Curie temperatures much exceeding room temperature, high current carrier mobilities, and high degree of spin polarization.

At present, investigations in the field of spintronics are carried out at research institutes and in research laboratories at many universities and largest corporations. Great investments in the field are due to the fact that spintronics is among the top-priority research avenues in the nanotechnology programs. Since 2003, a research program on spin-dependent effects in solids and spintronics has been developed in the Russian Academy of Sciences (Division of Physical Sciences). The main avenues of basic research carried out at the Russian Academy of Sciences (Section "Chemical Sciences and Materials Science")* include synthesis and investigations of novel compounds, design of materials and nanomaterials including magnetic materials, which also covers the field of spintronics.

The aforesaid of course gives no assurances that spintronics, in its basic research aspects and as a novel technology, will always offer exclusive prospects and, similarly to electronics, will appear to be an irreplaceable applied discipline in the nearest decades. However, irrespective of how long will be the lifetime of hopeful technology assessment (by the way, this also concerns nanotechnology), investigations in the field of spintronics and spintronic materials undoubtedly belong to the topical avenues of research on condensed matter. This is of considerable importance for, *e.g.*, the development of new principles of interaction between distant magnetic impurities and creation of a new generation of HTFS and devices based on these materials. Probably, the most exciting aspects of spintronics will be related to the effects, devices, and materials that cannot be imagined as yet. Addressees of this review, that is, physicists, chemists, and materials scientists must be ready for future changes.

References

1. E. I. Rashba, *J. Superconductivity: Incorporating Novel Magnetism*, 2002, **15**, 13.
2. S. A. Wolf, D. D. Awschalom, R. A. Buhrman, J. M. Daughton, S. von Molnar, M. L. Roukes, A. Y. Chtchelkanova, and D. M. Treger, *Science*, 2001, **294**, 1488.
3. *Spin Electronics*, Eds M. Ziese and M. J. Thornton, Springer, Berlin, 2001, 500 pp.
4. M. N. Baibich, J. M. Broto, A. Fert, F. Nguyen Van Dau, and F. Petroff, *Phys. Rev. Lett.*, 1988, **61**, 2472.
5. G. Binasch, P. Grünberg, F. Saurenbach, and W. Zinn, *Phys. Rev., B*, 1989, **39**, 4828.

* http://unix12.fzu.cz/ms/allpubl.php.

* *Poisk* [*Poisk*], Iss. 35 (145), August 29, 2003 (in Russian).

6. H. Munekata, H. Ohno, S. von Molnar, A. Segmüller, L. L. Chang, and L. Esaki, *Phys. Rev. Lett.*, 1989, **63**, 1849.
7. H. Ohno, H. Munekata, S. von Molnar, and L. L. Chang, *J. Appl. Phys.*, 1991, **69**, 6103.
8. H. Ohno, H. Munekata, T. Penney, S. von Molnar, and L. L. Chang, *Phys. Rev. Lett.*, 1992, **68**, 2664.
9. H. Munekata, A. Zaslavsky, P. Fumagalli, and R. J. Gambino, *Appl. Phys. Lett.*, 1993, **63**, 2929.
10. M. I. Dyakonov, in *Future Trends in Microelectronics: The Nano, the Giga, and the Ultra*, Eds S. Luryi, J. Xu, and A. Zaslavsky, Wiley-IEEE Press, New York, 2004, p. 424.
11. K. E. Drexler, *Proc. Natl. Acad. Sci. USA*, *Chemistry Section*, 1981, **78**, 5275.
12. K. E. Drexler, *Nanosystems: Molecular Machinery, Manufacturing, and Computation*, Wiley, New York, 1992, 556 pp.
13. L. P. Gor´kov and G. M. Eliashberg, *Zh. Eksp. Teor. Fiz.*, 1965, **48**, 1407 [*Sov. Phys. J. Exp. Theor. Phys.*, 1965, **21**, 940 (Engl. Transl.)].
14. E. A. Shapoval, *Zh. Eksp. Teor. Fiz.*, 1964, **47**, 1007 [*Sov. Phys. J. Exp. Theor. Phys.*, 1964, **20**, 675 (Engl. Transl.)].
15. E. I. Rashba, *Fizika Tverdogo Tela*, 1960, **2**, 1224 [*Sov. Phys. Solid State*, 1960, **2**, 1109 (Engl. Transl.)].
16. E. I. Rashba, *Usp. Fiz. Nauk*, 1964, **84**, 557 [*Sov. Phys. Usp.*, 1965, **7**, 823 (Engl. Transl.)].
17. R. L. Bell, *Phys. Rev. Lett.*, 1962, **9**, 52.
18. V. V. Kveder, Yu. A. Osip´yan, and A. I. Shalynin, *Pis´ma v Zhurn. Eksp. Teor. Fiziki*, 1984, **40**, 10 [*Sov. Phys. JETP Lett.*, 1984, **40**, 729 (Engl. Transl.)].
19. V. V. Kveder, V. Ya. Kravchenko, T. R. Mchelidze, Yu. A. Osip´yan, and D. E. Khmel´nitskii, *Pis´ma v Zhurn. Eksp. Teor. Fiziki*, 1986, **43**, 202 [*Sov. Phys. JETP Lett.*, 1986, **43**, 255 (Engl. Transl.)].
20. Yu. A. Bychkov and E. I. Rashba, *Pis´ma v Zhurn. Eksp. Teor. Fiziki*, 1984, **39**, 66 [*Sov. Phys. JETP Lett.*, 1984, **39**, 78 (Engl. Transl.)].
21. V. K. Kalevich and V. L. Korenev, *Pis´ma v Zhurn. Eksp. Teor. Fiziki*, 1990, **52**, 859 [*Sov. Phys. JETP Lett.*, 1990, **52**, 230 (Engl. Transl.)].
22. A. V. Vedyayev, B. Dieny, and N. Ryzhanova, *Europhys. Lett.*, 1992, **19**, 329.
23. E. L. Frankevich and E. I. Balabanov, *Pis´ma v Zhurn. Eksp. Teor. Fiziki* [*Sov. Phys. JETP Lett.*], 1965, **1**, 33 (in Russian).
24. E. L. Frankevich, V. I. Lesin, and A. I. Pristupa, *Zhurn. Eksp. Teor. Fiziki*, 1978, **75**, 415 [*Sov. Phys. J. Exp. Theor. Phys.*, 1978, **48**, 208 (Engl. Transl.)].
25. I. A. Sokolik and E. L. Frankevich, *Usp. Fiz. Nauk*, 1973, **111**, 261 [*Sov. Phys. Usp.*, 1973, **111** (Engl. Transl.)].
26. A. L. Buchachenko, R. Z. Sagdeev, and K. M. Salikhov, *Magnitnye i spinovye effecty v khimicheskikh reaktsiyakh* [*Magnetic Field Induced and Spin Effects in Chemical Reactions*], Nauka, Novosibirsk, 1978, 296 pp. (in Russian).
27. A. L. Buchachenko, *Usp. Khim.*, 1999, **68**, 99 [*Russ. Chem. Rev.*, 1999, **68**, 85 (Engl. Transl.)].
28. V. A. Ivanov and K. Kanoda, *Molec. Cryst. Liq. Cryst.*, 1996, **285**, 211.
29. V. A. Ivanov and K. Kanoda, *Physica C*, 1996, **268**, 205.
30. V. A. Ivanov, E. A. Ugolkova, and M. Ye. Zhuravlev, *Zhurn. Eksp. Teor. Fiziki*, 1998, **113**, 715 [*J. Exp. Theor. Phys.*, 1998, **86**, 395 (Engl. Transl.)].
31. V. F. Gantmakher and M. V. Feigel´man, *Usp. Fiz. Nauk*, 1998, **168**, 113 [*Physics-Uspekhi*, 1998, **41**, 105 (Engl. Transl.)].
32. V. I. Ovcharenko and R. Z. Sagdeev, *Usp. Khim.*, 1999, **68**, 381 [*Russ. Chem. Rev.*, 1999, **68**, 345 (Engl. Transl.)].
33. A. L. Buchachenko, *Usp. Khim.*, 2003, **72**, 419 [*Russ. Chem. Rev.*, 2003, **72**, 375 (Engl. Transl.)].
34. M. Oestreich, M. Brender, J. Hubner, D. H. W. W. Rühle, T. H. P. J. Klar, W. Heimbrodt, M. Lampalzer, K. Voltz, and W. Stolz, *Semicond. Sci. Technol.*, 2002, **17**, 285.
35. I. Źutić, J. Fabian, and S. Das Sarma, *Rev. Mod. Phys.*, 2004, **76**, 323.
36. J.-P. Ansermet, *J. Phys.: Condens. Matter*, 1998,**10**, 6027.
37. J. Bass and W. P. Pratt, Jr., *J. Magn. Magn. Mater.*, 1999, **200**, 274.
38. J. M. Daughton, A. V. Pohm, R. T. Fayfield, and C. H. Smith, *J. Phys., D*, 1999, **32**, 169.
39. M. A. M. Gijs and G. E. W. Bauer, *Adv. Phys.*, 1997, **46**, 285.
40. G. Prinz, *Science*, 1998, **282**, 1660.
41. M. D. Stiles, in *Ultrathin Magnetic Structures III*, Eds B. Heinrich and J. A. C. Bland, Springer, New York, 2004.
42. P. M. Tedrow and R. Meservey, *Phys. Rep.*, 1994, **238**, 173.
43. H. Ohno, *Science*, 1998, **281**, 951.
44. S. J. Pearton, C. R. Abernathy, M. E. Overberg, G. T. Thaler, D. P. Norton, N. Theodoropoulou, A. F. Hebard, Y. D. Park, F. Ren, J. Kim, and L. A. Boatner, *J. Appl. Phys.*, 2003, **93**, 1.
45. A. J. Epstein, *MRS Bull.*, 2003, **28**, 492.
46. A. M. Goldman, V. Vas´ko, P. Kraus, K. Nikolaev, and V. A. Larkin, *J. Mag. Magn. Mater.*, 1999, **200**, 69.
47. K. Tsukagoshi, B. W. Alphenaar, and H. Ago, *Nature*, 1999, **401**, 572.
48. *Magnetic Interactions and Spin Transport*, Eds A. Chtchelkanova, S. A. Wolf, and Y. Idzerda, Kluwer Academic Dordrecht—Plenum, New York, 2003, 572 pp.
49. *Magnetic Multilayers and Giant Magnetoresistance. Fundamentals and Industrial Applications*, Ed. U. Hartman, Springer-Verlag, Berlin—Heidelberg—NewYork, 2000, 320 pp.
50. E. Hirota, H. Sakakima, and K. Inomata, *Giant Magneto-Resistance Devices*, Springer, Berlin, 2002, 177 pp.
51. P. M. Levy and I. Mertig, in *Spin Dependent Transport in Magnetic Nanostructures*, Eds S. Maekawa and T. Shinjo, Taylor and Francis, New York, 2002, 47 pp.
52. S. Maekawa, S. Takahashi, and H. Imamura, in *Spin Dependent Transport in Magnetic Nanostructures*, Eds S. Maekawa and T. Shinjo, Taylor and Francis, New York, 2002, p. 143.
53. S. S. P. Parkin, in *Spin Dependent Transport in Magnetic Nanostructures*, Eds S. Maekawa and T. Shinjo, Taylor and Francis, New York, 2002, p. 237.
54. T. Shinjo, in *Spin Dependent Transport in Magnetic Nanostructures*, Eds S. Maekawa and T. Shinjo, Taylor and Francis, New York, 2002, p. 1.
55. V. L. Ginzburg, *Usp. Fiz. Nauk*, 2002, **172**, 213 [*Physics-Uspekhi*, 2002, **45**, 205 (Engl. Transl.)].
56. Ya. K. Syrkin and M. E. Dyatkina, *Khimicheskaya svyaz´ i stroenie molekul* [*The Chemical Bonding and Molecular Struc-*

ture], Goskhimizdat, Moscow—Leningrad, 1946, 588 pp. (in Russian).
57. L. I. Koroleva, *Magnitnye poluprovodniki* [*Magnetic Semiconductors*], Izd-vo MGU, Moscow, 2003, 312 pp. (in Russian).
58. L. V. Keldysh, *Zhurn. Eksp. Teor. Fiziki*, 1963, **45**, 364 [*Sov. Phys. J. Exp. Theor. Phys.*, 1963, **18**, 253 (Engl. Transl.)].
59. V. N. Ryabokon´ and K. K. Svidzinskii, *Fizika tverdogo tela*, 1969, **11**, 585 [*Sov. Phys. Solid State*, 1969, **11**, 473 (Engl. Transl.)].
60. V. N. Ryabokon´ and K. K. Svidzinskii, *Fizika i Tekhnika Poluprovodnikov*, 1971, **5**, 1865 [*Sov. Phys. Semiconductors*, 1971, **5** (Engl. Transl.)].
61. V. N. Fleurov and K. A. Kikoin, *J. Phys. C*, 1976, **9**, 1673.
62. F. D. M. Haldane and P. W. Anderson, *Phys. Rev., B*, 1976, **13**, 2553.
63. P. W. Anderson, *Usp. Fiz. Nauk*, 1979, **127**, 19 [*Sov. Phys. Usp.*, 1979 (Engl. Transl.)].
64. E. L. Nagaev, *Fizika magnitnykh poluprovodnikov* [*Physics of Magnetic Semiconductors*], Nauka, Moscow, 1979, 432 pp. (in Russian).
65. C. Zener, *Phys. Rev.*, 1951, **82**, 403.
66. P. W. Anderson and H. Hasegawa, *Phys. Rev.*, 1955, **100**, 675.
67. P. G. de Gennes, *Phys. Rev.*, 1960, **118**, 141.
68. F. Fröhlich and F. R. N. Nabarro, *Proc. Roy. Soc. (London), A*, 1940, **275**, 382.
69. S. Schubin and S. Wonsowsky, *Sow. Phys.*, 1935, **7**, 292.
70. S. V. Vonsovsky, *Zhurn. Eksp. Teor. Fiziki*, 1946, **16**, 981 (in Russian).
71. S. Vonsovsky, *J. Phys.*, 1946, **10**, 486.
72. C. Zener, *Phys. Rev.*, 1951, **81**, 440.
73. Yu. P. Irkhin and E. A. Turov, *Fizika Metallov i Metallovedenie*, 1957, **4**, 9 [*Phys. Metals Metallography*, 1957, **4** (Engl. Transl.)].
74. Yu. P. Irkhin, *Fizika metallov i metallovedenie*, 1959, **7**, 3 [*Phys. Metals Metallography*, 1959, **7** (Engl. Transl.)].
75. E. A. Turov and Yu. P. Irkhin, *Fizika metallov i metallovedenie*, 1960, **9**, 488 [*Phys. Metals Metallography*, 1960, **9** (Engl. Transl.)].
76. H. Katayama-Yoshida and K. Sato, *Physica B*, 2003, **327**, 337.
77. T. Dietl, H. Ohno, F. Matsukura, J. Cibert, and D. Ferrand, *Science*, 1998, **287**, 139.
78. T. Jungwirth, W. A. Atkinson, B. H. Lee, and A. H. MacDonald, *Phys. Rev., B*, 1999, **59**, 9818.
79. T. Dietl, H. Ohno, and F. Matsukura, *Phys. Rev., B*, 2001, **63**, 195205.
80. S. Sanvito, P. Ordejon, and N. A. Hill, *Phys. Rev., B*, 2001, **63**, 165206.
81. F. Matsukura, H. Ohno, A. Shen, and Y. Sugawara, *Phys. Rev., B*, 1998, **57**, 2037
82. J. Szczytko, W. Mac, A. Stachow, A. Twardowski, P. Becla, and J. Tworzydlo, *Solid State Commun.*, 1996, **99**, 927.
83. J. Okabayashi, A. Kimura, O. Rader, T. Mizokawa, A. Fujimori, T. Hayashi, and M. Tanaka, *Phys. Rev., B*, 1998, **58**, 4211.
84. J. Szczytko, W. Bardyszewski, and A. Twardowski, *Phys. Rev., B*, 2001, **64**, 075306.
85. H. Ohno, N. Akiba, F. Matsukura, A. Shen, K. Ohtani, and Y. Ohno, *Appl. Phys. Lett.*, 1998, **73**, 363.
86. Z. V. Popović, V. A. Ivanov, M. J. Konstantinović, A. Cantarero, J. Martínez-Pastor, D. Olguín, M. I. Alonso, M. Garriga, O. P. Khuong, A. Vietkin, and V. V. Moshchalkov, *Phys. Rev., B*, 2001, **63**, 165105.
87. A. Overhauser, *Phys. Rev.*, 1953, **92**, 411.
88. A. Overhauser, *Phys. Rev.*, 1954, **94**, 768.
89. C. P. Slichter, *Principles of Magnetic Resonance*, 3rd ed., Springer-Verlag, Berlin, 1990, 655 pp.
90. M. I. Dyakonov and V. I. Perel, in *Modern Problems in Condensed Matter Science*, Vol. **8**, Eds F. Meier and B. P. Zakharchenya, North-Holland, Amsterdam, 1984, p. 11.
91. A. Berg, R. R. Gerhards, and K. von Klitzing, *Phys. Rev. Lett.*, 1990, **64**, 2563.
92. K. R. Wald, L. P. Kouwenhoven, and P. L. McEuen, *Phys. Rev. Lett.*, 1994, **73**, 1011.
93. S. E. Barrett, G. Dabbagh, L. N. Pfeiffer, K. W. West, and R. Tycko, *Phys. Rev. Lett.*, 1995, **74**, 5112.
94. M. I. Dyakonov and V. I. Perel, *Zhurn. Eksp. Teor. Fiziki*, 1971, **60**, 1954 [*Sov. Phys. J. Exp. Theor. Phys.*, 1971, **33**, 1053 (Engl. Transl.)].
95. M. I. Dyakonov and V. I. Perel, *Fizika Tverdogo Tela*, 1971, **13**, 3581 [*Sov. Phys. Sol. State*, 1971, **13**, 3023 (Engl. Transl.)].
96. M. I. Dyakonov and V. Yu. Kachorovsky, *Fizika i Tekhnika Poluprovodnikov*, 1986, **20**, 178 [*Sov. Phys. Semiconductors*, 1986, **20**, 100 (Engl. Transl.)].
97. R. W. Wood and A. Ellett, *Phys. Rev.*, 1924, **24**, 243.
98. W. Hanle, *Z. Physik*, 1924, **30**, 93.
99. J. Brossel and A. Kastler, *Compt. Rend. Hebd. Acad. Sci.*, 1949, **229**, 1213.
100. A. Kastler, *Science*, 1967, **158**, 214.
101. M. I. Dyakonov and V. I. Perel, *Pis´ma v Zhurn. Eksp. Teor. Fiziki*, 1971, **13**, 657 [*Sov. Phys. JETP Lett.*, 1971, **13**, 467 (Engl. Transl.)].
102. N. S. Averkiev and M. I. Dyakonov, *Fizika i Tekhnika Poluprovodnikov*, 1983, **17**, 629 [*Sov. Phys. Semiconductors*, 1983, **17**, 393 (Engl. Transl.)].
103. A. A. Bakun, B. P. Zakharchenya, A. A. Rogachev, N. N. Tkachuk, and V. G. Fleisher, *Pis´ma v Zhurn. Eksp. Teor. Fiziki*, 1984, **40**, 464 [*Sov. Phys. JETP Lett.*, 1984, **40**, 1293 (Engl. Transl.)].
104. M. I. Dyakonov and V. I. Perel, *Phys. Lett., A*, 1971, **35**, 459.
105. E. L. Ivchenko and G. E. Pikus, *Pis´ma v Zhurn. Eksp. Teor. Fiziki*, 1978, **27**, 604 [*Sov. Phys. JETP Lett.*, 1978, **27**, 604 (Engl. Transl.)].
106. V. I. Belinicher, *Phys. Lett., A*, 1978, **66**, 213.
107. V. M. Asnin, A. A. Bakun, A. M. Danishevskii, E. L. Ivchenko, G. E. Pikus, and A. A. Rogachev, *Solid State Commun.*, 1979, **30**, 565.
108. G. Lampel, *Phys. Rev. Lett.*, 1968, **20**, 491.
109. M. I. Dyakonov and V. I. Perel, *Zhurn. Eksp. Teor. Fiziki*, 1973, **65**, 362 [*Sov. Phys. J. Exp. Theor. Phys.*, 1973, **38** (Engl. Transl.)].
110. V. G. Fleisher and I. A. Merkulov, in *Optical Orientation*, Eds F. Maier and B. P. Zakharchenya, North-Holland, Amsterdam, 1984, p. 173.
111. A. I. Ekimov and V. I. Safarov, *Pis´ma v Zhurn. Eksp. Teor. Fiziki*, 1972, **15**, 453 [*Sov. Phys. JETP Lett.*, 1972, **15**, 179 (Engl. Transl.)].

112. P. Paget, G. Lampel, B. Shapoval, and V. I. Safarov, *Phys. Rev., B*, 1977, **15**, 5780.
113. J. M. Kikkawa and D. D. Awshalom, *Science*, 2000, **287**, 473.
114. V. G. Fleisher, R. I. Dzhioev, and B. P. Zakharchenya, *Pis´ma v Zhurn. Eksp. Teor. Fiziki*, 1976, **23**, 22 [*Sov. Phys. JETP Lett.*, 1976, **23**, 18 (Engl. Transl.)].
115. S. Kronmüller, W. Dietsche, J. Weis, K. von Klitzing, W. Wegscheider, and M. Bichler, *Phys. Rev. Lett.*, 1998, **81**, 2526.
116. S. F. Alvarado and P. Renaud, *Phys. Rev. Lett.*, 1992, **68**, 1387.
117. N. F. Mott, *Proc. R. Soc. London*, *Ser. A*, 1936, **153**, 699.
118. N. F. Mott, *Proc. R. Soc. London, Ser. A*, 1936, **156**, 368.
119. I. A. Campbell, A. Fert, and A. R. Pomeroy, *Phil. Mag.*, 1967, **15**, 977.
120. A. Fert and I. A. Campbell, *Phys. Rev. Lett.*, 1968, **21**, 1190.
121. T. Valet and A. Fert, *Phys. Rev., B*, 1993, **48**, 7099.
122. S. von Mo´lnar and T. Kasuya, *Phys. Rev. Lett.*, 1968, **21**, 1757.
123. M. Escorne, A. Ghazalli, and P. Leroux-Hugon, *Proc. 12th Intern. Conf. on the Physics of Semiconductors*, Ed. M. H. Pilkuhn, Teubner, Stuttgart, 1974, p. 915.
124. R. W. Cochrane, M. Plischke, and J. O. Ström-Olsen, *Phys. Rev., B*, 1974, **9**, 3013.
125. T. Story, R. R. Galazka, R. B. Frankel, and P. A. Wolff, *Phys. Rev. Lett.*, 1986, **56**, 777.
126. A. G. Aronov, *Zhurn. Eksp. Teor. Fiziki*, 1976, **24**, 37 [*Sov. Phys. JETP*, 1976, **24**, 32 (Engl. Transl.)].
127. M. Johnson and R. H. Silsbee, *Phys. Rev. Lett.*, 1985, **55**, 1790.
128. R. I. Dzhioev, B. P. Zakharchenya, and V. L. Korenev, *Phys. Solid. State*, 1995, **37**, 1929.
129. V. P. LaBella, D. W. Bullock, Z. Ding, C. Emery, A. Venkatesan, W. F. Oliver, G. J. Salamo, P. M. Thibado, and M. Mortazavi, *Science*, 2001, **292**, 1518.
130. W. F. Egelhoff, Jr., M. D. Stiles, D. P. Pappas, D. T. Pierce, J. M. Byers, B. Johnson, B. T. Jonker, S. F. Alvarado, J. F. Gregg, J. A. C. Bland, and R. A. Buhrman, *Science*, 2002, **296**, 1195.
131. W. F. Egelhoff, Jr., M. D. Stiles, D. P. Pappas, D. T. Pierce, J. M. Byers, B. Johnson, B. T. Jonker, S. F. Alvarado, J. F. Gregg, J. A. C. Bland, and R. A. Buhrman, *Science*, 2002, **296**, 5571.
132. P. R. Hammar, B. R. Bennet, M. J. Yang, and M. Johnson, *Phys. Rev. Lett.*, 1999, **83**, 203.
133. G. Schmidt, D. Ferrand, L. W. Molenkamp, A. T. Filip, and B. J. van Wees, *Phys. Rev., B*, 2000, **62**, 4790.
134. H. J. Zhu, M. Ramsteiner, H. Kostial, M. Wassermeier, H.-P. Schonherr, and K. H. Ploog, *Phys. Rev. Lett.*, 2001, **87**, 016601.
135. *Semiconductors and Semimetals*, Eds J. K. Furdyna and J. Kossut, Vol. **25**, Academic Press, New York, 1988, 496 pp.
136. B. T. Jonker, Y. D. Park, B. R. Bennett, H. D. Cheong, G. Kioseoglou, and A. Petrou, *Phys. Rev., B*, 2000, **62**, 8180.
137. M. Oestreich, J. Hubner, D. Hagele, P. J. Klar, W. Heimbrodt, W. W. Ruhle, D. E. Ashenford, and B. Lunn, *Appl. Phys. Lett.*, 1999, **74**, 1251.
138. R. Fiederling, M. Keim, G. Reuscher, W. Ossau, G. Schmidt, A. Waag, and L. W. Molenkamp, *Nature*, 1999, **402**, 787.
139. Y. Ohno, D. K. Young, B. Beschoten, F. Matsukura, H. Ohno, and D. D. Awschalom, *Nature*, 1999, **402**, 790.
140. H. Ohno, *J. Magn. Magn. Mater.*, 1999, **200**, 110.
141. P. Van Dorpe, Z. Liu, W. Van Roy, V. F. Motsnyi, M. Sawicki, G. Borghs, and J. De Boeck, *Appl. Phys. Lett.*, 2004, **84**, 3495.
142. X. Jiang, R. Wang, S. van Dijken, R. Shelby, R. Macfarlane, G. S. Solomon, J. Harris, and S. S. P. Parkin, *Phys. Rev. Lett.*, 2003, **90**, 256603.
143. E. I. Rashba, *Phys. Rev., B*, 2003, **68**, 241310(R).
144. J. Stephens, J. Berezovsky, J. P. McGuire, L. J. Sham, A. C. Gossard, and D. D. Awschalom, *March Meeting of the APS (Montreal, 22—26 March 2004)*, Montreal, 2004.
145. A. G. Aronov and G. E. Pikus, *Fizika i Tekhnika Poluprovodnikov*, 1976, **10**, 1177 [*Sov. Phys. Semiconductors*, 1976, **10**, 698 (Engl. Transl.)].
146. J. M. Kikkawa and D. D. Awschalom, *Nature*, 1999, **397**, 139.
147. J. M. Kikkawa and D. D. Awschalom, *Phys. Rev. Lett.*, 1998, **80**, 4313.
148. R. I. Dzhioev, V. L. Korenev, I. A. Merkulov, B. P. Zakharchenya, D. Gammon, Al. L. Efros, and D. S. Katzer, *Phys. Rev. Lett.*, 2002, **88**, 256801.
149. I. Malajovich, J. J. Berry, N. Samarth, D. D. Awschalom, *Nature*, 2001, **411**, 770.
150. J. A. Gupta, X. Peng, A. P. Alivisatos, and D. D. Awschalom, *Phys. Rev., B*, 1999, **59**, 10421.
151. H. Ohno, D. Chiba, F. Matsukura, T. Omiya, E. Abe, T. Dietl, Y. Ohno, and K. Ohtani, *Nature*, 2000, **408**, 944.
152. D. Chiba, M. Yamanouchi, F. Matsukura, and H. Ohno, *Science*, 2003, **301**, 943.
153. D. D. Awshalom and R. K. Kawakami, *Nature*, 2000, **408**, 923.
154. Y. D. Park, A. T. Hanbicki, S. C. Erwin, C. S. Hellberg, J. M. Sullivan, J. E. Mattson, T. F. Ambrose, A. Wilson, G. Spanos, and B. T. Jonker, *Science*, 2002, **295**, 651.
155. Y. Kato, R. C. Myers, A. C. Gossard, and D. D. Awschalom, *Nature*, 2004, **427**, 50.
156. L. I. Magarill, A. V. Chaplik, and M. V. Entin, *Fizika i Tekhnika Poluprovodnikov*, 2001, **35**, 1128 [*Semiconductors*, 2001, **35**, 1081 (Engl. Transl.)].
157. S. Datta and B. Das, *Appl. Phys. Lett.*, 1990, **56**, 665.
158. Yu. A. Bychkov, E. I. Rashba, *J. Phys. C*, 1984, **17**, 6039.
159. J. Schliemann, J. C. Egues, and D. Loss, *Phys. Rev. Lett.*, 2003, **90**, 146801.
160. J. C. Egues, G. Burkard, and D. Loss, *Appl. Phys. Lett.*, 2003, **82**, 2658.
161. M. E. Flatte and G. Vignale, *Appl. Phys. Lett.*, 2001, **78**, 1273.
162. B. König, U. Zehnder, D. R. Yakovlev, W. Ossau, T. Gerhard, M. Keim, A. Waag, and G. Landwehr, *Phys. Rev., B*, 1999, **60**, 2653.
163. W. L. Ng, M. A. Lourenco, R. M. Gwilliam, S. Ledain, G. Shao, and K. P. Homewood, *Nature*, 2001, **410**, 192.
164. Z. H. Xiong, Di Wu, Z. Valy Vardeny, and J. Shi, *Nature*, 2004, **427**, 821.
165. J. Appelbaum, K. J. Russell, D. J. Monsma, V. Narayanamurti, C. M. Marcus, M. P. Hanson, and A. C. Gossard, *Appl. Phys. Lett.*, 2003, **83**, 4571.

166. S. D. Ganichev, E. L. Ivchenko, S. N. Danilov, J. Eroms, W. Wegscheider, D. Weiss, and W. Prettl, *Phys. Rev. Lett.*, 2001, **86**, 4358.
167. R. D. R. Bhat and J. E. Sipe, *Phys. Rev. Lett.*, 2000, **85**, 5432.
168. R. K. Kawakami, Y. Kato, M. Hanson, I. Malajovich, J. M. Stephens, E. Johnston-Halperin, G. Salis, A. C. Gossard, and D. D. Awschalom, *Science*, 2001, **294**, 131.
169. S. I. Kiselev, J. C. Sankey, I. N. Krivotorov, N. C. Emley, R. J. Schoelkopf, R. A. Buhrman, and D. C. Ralph, *Nature*, 2003, **425**, 380.
170. S. Murakami, N. Nagaosa, and S. Zhang, *Science*, 2003, **301**, 1348.
171. E. I. Rashba, *Phys. Rev., B*, 2003, **68**, 241315-R.
172. A. G. Mal´shukov, C. S. Tang, C. S. Chu, and K. A. Chao, *Phys. Rev., B*, 2003, **68**, 233307.
173. H. X. Tang, R. K. Kawakami, D. D. Awschalom, and M. L. Roukes, *Phys. Rev. Lett.*, 2003, **90**, 107201.
174. H. D. Chopra and S. Z. Hua, *Phys. Rev., B*, 2002, **66**, 020403-R.
175. D. Chiba, F. Matsukura, and H. Ohno, *Physica E,* 2004, **21**, 966.
176. M. Tanaka and Y. Higo, *Phys. Rev. Lett.*, 2001, **87**, 026602.
177. W. Weber, S. Riesen, and H. C. Siegmann, *Science*, 2001, **291** 1015.
178. A. Kiselev and K. W. Kim, *Appl. Phys. Lett.*, 2001, **78**, 775.
179. M. Ciorga, A. Wensauer, M. Pioro-Ladriere, M. Korkusinski, J. Kyriakidis, A. S. Sachrajda, and P. Hawrylak, *Phys. Rev. Lett.*, 2002, **88**, 56804.
180. D. Loss and D. P.. DiVincenzo, *Phys. Rev. A*, 1998, **57**, 120.
181. S. J. Tans, A. R. M. Verschueren, and C. Dekker, *Nature*, 1998, **393**, 49.
182. A. A. Jensen, J. R. Hauptmann, J. Nygerd, J. Sadowski, and P. E. Lindelof, *Nano Lett.*, 2004, **4**, 349.
183. V. Fleurov, V. A. Ivanov, F. M. Peeters, and I. D. Vagner, *Physica E*, 2002, **14**, 361.
184. M. Poggio, G. M. Steeves, R. C. Myers, Y. Kato, A. C. Gossard, and D. D. Awschalom, *Phys. Rev. Lett.*, 2003, **91**, 207602.
185. Yu. I. Manin, *Vychislimoe i nevychislimoe* [*Computable and Non-Computable*], Sov. Radio, Moscow, 1980, 128 pp. (in Russian).
186. R. P. Feinman, *Foundations Phys.*, 1986, **16**, 507.
187. P. W. Shor, *Proc. 35th Annual Symposium on Foundations of Computer Science (IEEE Press)*, 1994, p. 124.
188. K. A. Valiev, *Vestnik RAN* [*Herold of the Russian Academy of Sciences*],К.А.Валиев. *Вестник РАН*, 2000, **70**, 688 (in Russian).
189. E. M. Omel´yanovskii and V. I. Fistul´, *Primesi perekhodnykh metallov v polyprovodnikakh* [*Transition Metal Impurities in Semiconductors*], Metallurgiya, Moscow, 1983 (in Russian).
190. B. E. Kane, *Nature*, 1998, **393**, 133.
191. R. Vrijen and D. Di Vincenzo, *Phys. Rev., A*, 2000, **62**, 012306.
192. J. Beille, J. Voiron, and M. Roth, *Solid State Commun.*, 1983, **47**, 399.
193. N. Manyala, Y. Sidis, J. F. DiTusa, G. Aeppli, D. P. Young, and Z. Y. Fisk, *Nature Materials*, 2004, **3**, 255.
194. S. Krupicka, *Physics of Ferrites and Related Magnetic Oxides*, Academia, NCSAV, Prague, 1969 (in Czech).
195. V. A. Ivanov and R. O. Zaitsev, *J. Magn. Magnetic Mater.*, 1989, **81**, 331.
196. J. J. Versluijs, M. A. Bari, and J. M. D. Coey, *Phys. Rev. Lett.*, 2001, **87**, 026601-1.
197. S. K. Sampath and F. Cordaro, *J. Am. Ceram. Soc.*, 1998, **81** 649.
198. V. A. Ivanov, in *Sovremennye problemy i dostizheniya obshchei i neorganicheskoi khimii* [*Advances and Modern Problems in General and Inorganic Chemistry*], Ed. N. T. Kuznetsov, Nauka, Moscow, 2004, p. 150 (in Russian).
199. I. Tsubokawa, *J. Phys. Soc. Jpn*, 1960, **15**, 1664.
200. S. Methfessel and D. C. Mattis, *Handb. Phys.*, 1968, **18**, 389.
201. P. Wachter, *CRC Crit. Rev. Solid State Sci.*, 1972, **13**, 189.
202. F. Holtzberg, S. von Molnar, and J. M. D. Coey, *The Handbook on Semiconductors*, 1980, **3**, 815.
203. L. Esaki, P. J. Stiles, and S. von Molnar, *Phys. Rev. Lett.*, 1967, **19**, 852.
204. M. Penicaud, B. Siberchicot, C. B. Sommers, and J. Kübler, *J. Magn. Magn. Mater.*, 1992, **103**, 212.
205. S. M. Watts, S. Wirth, S. von Molnár, A. Barry, and J. M. D. Coey, *Phys. Rev., B*, 2000, **61**, 9621.
206. J. M. D. Coey, in *Spin Electronics*, Eds M. Ziese and M. J. Thornton, Springer, Berlin, 2001, p. 277.
207. C. P. Beam and D. S. Rodbell, *Phys. Rev.*, 1962, **126**, 104.
208. H. Akinaga, M. Mizuguchi, K. Ono, and M. Oshima, *J. Magn. Soc. Jpn*, 2000, **22**, 451.
209. H. Akinaga, T. Manago, and M. Shirai, *Jpn J. Appl. Phys., Part 2-Letters*, 2000, **39**, L1118.
210. J. H. Zhao, F. Matsukura, K. Takamura, E. Abe, D. Chiba, and H. Ohno, *Appl. Phys. Lett.*, 2001, **79**, 2776.
211. J. W. Dong, L. C. Chen, and C. J. Palmstrom, *Appl. Phys. Lett.*, 1999, **75**, 1443.
212. C. T. Tanaka, J. Nowak, and J. S. Moodera, *J. Appl. Phys.*, 1999, **86**, 6239.
213. H. Chiba, T. Atou, and Y. Syono, *J. Solid State Chem.*, 1997, **132**, 139.
214. K. Kohn, K. Inoue, O. Horie, and S.-I. Akimoto, *J. Solid State Chem.*, 1976, **18**, 27.
215. J. D. Garrett, J. E. Greedan, and D. A. MacLean, *Mater. Res. Bull.*, 1981, **16**, 145.
216. B. T. Matthias, R. M. Bozorth, and J. H. V. Vleck, *Phys. Rev. Lett.*, 1961, **7**, 160.
217. S. G. Yang, T. Li, B. X. Gu, Y. W. Du, H. Y. Sung, S. T. Hung, C. Y. Wong, and A. B. Pakhomov, *Appl. Phys. Lett.*, 2003, **83**, 3746.
218. C. M. Fang, G. A. de Wijs, and R. A. de Groot, *J. Appl. Phys.*, 2002, **91**, 8340.
219. K. Schwarz, *J. Phys.*, 1986, **16**, 211.
220. R. J. Soulen, Jr., J. M. Byers, M. S. Osofsky, B. Nadgorny, T. Ambrose, S. F. Cheng, P. R. Broussard, C. T. Tanaka, J. Nowak, J. S. Moodera, A. Barry, and J. M. D. Coey, *Science*, 1998, **282**, 85.
221. B. L. Chamberland, *CRC Crit. Rev. Solid State Sci.*, 1977, **7**, 1.
222. S. Ishibashi, T. Namikawa, and M. Satou, *Jpn J. Appl. Phys.*, 1978, **17**, 249.
223. M. S. Laad, L. Craco, and E. Müller-Hartmann, *Phys. Rev., B*, 2001, **64**, 214421.
224. Y. Ji, G. J. Strijkers, F. Y. Yang, C. L. Chien, J. M. Byers, A. Anguelouch, G. Xiao, and A. Gupta, *Phys. Rev. Lett.*, 2001, **86**, 5585.

225. J. S. Parker, S. M. Watts, P. G. Ivanov, and P. Xiong, *Phys. Rev. Lett.*, 2002, **88**, 196601.
226. K.-I. Kobayashi, T. Kimura, H. Sawada, K. Terakura, and Y. Tokura, *Nature*, 1998, **395**, 677.
227. C. Ritter, M. R. Ibarra, L. Morellon, J. Blasco, J. Garcia, and J. M. De Teresa, *J. Phys.: Condens. Matter*, 2000, **12**, 8295.
228. H. Asano, N. Kozuka, A. Tsuzuki, and M. Matsui, *Appl. Phys. Lett.*, 2004, **85**, 263.
229. M. Retuerto, J. A. Alonso, M. J. Martinez-Lope, J. L. Martinez, and M. Garcia-Hernandez, *Appl. Phys. Lett.*, 2004, **85**, 266.
230. Y. Sui, X. J. Wang, Z. N. Qian, J. G. Cheng, Z. G. Liu, J. P. Miao, Y. Li, and W. H. Su, *Appl. Phys. Lett.*, 2004, **85**, 269.
231. A. Hauri, A. Wasiela, A. Arnoult, J. Cibert, S. Tatarenko, T. Dietl, and Y. M. d´Aubigné, *Phys. Rev. Lett.*, 1997, **79**, 511.
232. S.-H. Wei and S. B. Zhang, *Phys. Rev., B*, 2002, **66**, 155211.
233. L. Hansen, D. Ferrand, G. Richter, M. Thierley, V. Hock, N. Schwarz, G. Reuscher, G. Scmidt, A. Waag, and L. W. Molenkamp, *Appl. Phys. Lett.*, 2001, **79**, 3125.
234. Y. Murayama, *Mesoscopic Systems: Fundamentals and Applications*, Wiley-VCH, Berlin, 2001.
235. M. A. Ruderman and C. Kittel, *Phys. Rev.*, 1954, **96**, 99.
236. T. Kasuya, *Prog. Theor. Phys.*, 1956, **16**, 45.
237. K. Yosida, *Phys. Rev.*, 1957, **106**, 893.
238. E. I. Kondorskii, *Zonnaya teoriya magnetizma (chast´ 2)* [*Band Theory of Magnetism* (*Chapter 2*)], Izd-vo MGU, Moscow, 1977, 95 pp. (in Russian).
239. A. T. Hindmarch and B. J. Hickey, *Phys. Rev. Lett.*, 2003, **91**, 116601.
240. S. M. Ryabchenko and Yu. G. Semenov, *Spektroskopiya kristallov* [*Spectroscopy of Crystals*], Fizmatlit, Leningrad, 1983, 432 pp. (in Russian).
241. I. I. Lyapilin and I. M. Tsidil´kovskii, *Usp.* F*iz. Nauk*, 1985, **146**, 35 [*Sov. Phys. Usp.*, 1985, **28**, 349 (Engl. Transl.)].
242. I. M. Tsidil´kovskii, *Usp.* F*iz. Nauk*, 1992, **162**, 63 [*Sov. Phys. Usp.*, 1992, **35**, 85 (Engl. Transl.)].
243. C. Gould, G. Schmidt, G. Richter, R. Fiederling, P. Grabs, and L. W. Molenkamp, *Appl. Surf. Science*, 2002, **190**, 395.
244. D. Ferrand, J. Cibert, A. Wasiela, C. Bourgognon, S. Tatarenko, G. Fishman, T. Andrearczyk, J. Jaroszyn´ski, S. Koles´nik, T. Dietl, B. Barbara, and D. Dufeu, *Phys. Rev., B*, 2001, **63**, 085201.
245. H. Saito, V. Zayets, S. Yamagata, Y. Suzuki, and K. Ando, *J. Appl. Phys.*, 2002, **91**, 8085.
246. H. Saito, V. Zayets, S. Yamagata, and K. Ando, *Phys. Rev. Lett.*, 2003, **90**, 207202.
247. F. Tsui, L. He, L. Ma, A. Tkachuk, Y. S. Chu, K. Nakajima, and T. Chikyow, *Phys. Rev. Lett.*, 2003, **91**, 177203.
248. M. Holub, S. Chakrabarti, S. Fathpour, P. Bhattacharyaa, Y. Lei, and S. Ghosh, *Appl. Phys. Lett.*, 2004, **85**, 973.
249. Y. L. Soo, S. W. Huang, Z. H. Ming, Y. H. Kao, and H. Munekata, *Phys. Rev., B*, 1996, **53**, 4905.
250. Y. Nishikawa, A. Tackeuchi, M. Yamaguchi, S. Muto, and O. Wada, *IEEE J. Sel. Topics Quantum Electron.*, 1996, **2**, 661.
251. S. Koshihara, A. Oiwa, M. Hirasawa, S. Katsumoto, Y. Iye, C. Urano, H. Takagi, and H. Munekata, *Phys. Rev. Lett.*, 1997, **78**, 4617.
252. A. Oiwa, T. Slupinski, and H. Munekata, *Appl. Phys. Lett.*, 2001, **78**, 518.
253. H. Ohno, *J. Cryst. Growth*, 2003, **251**, 285.
254. Y. Shon, W. C. Lee, Y. S. Park, Y. H. Kwon, S. J. Lee, K. J. Chung, H. S. Kim, D. Y. Kim, D. J. Fu, T. W. Kang, X. J. Fan, Y. J. Park, and H. T. Oh, *Appl. Phys. Lett.*, 2004, **84**, 2310.
255. R. Shioda, K. Ando, T. Hayashi, and M. Tanaka, *Phys. Rev., B*, 1998, **58**, 1100.
256. H. Ohno, A. Shen, F. Matsukura, A. Oiwa, A. Endo, S. Katsumoto, and Y. Iye, *Appl. Phys. Lett.*, 1996, **69**, 396.
257. J. Sadowski, P. Mathieu, P. Svedlindh, J. Z. Domagala, J. Bak-Misiuk, K. Swiatek, M. Karlsteen, J. Kanski, L. Ilver, H. Åsklund, and U. Sodervall, *Appl. Phys. Lett.*, 2001, **78**, 3271.
258. T. Kuroiwa, F. Matsukura, A. Shen, Y. Ohno, H. Ohno, T. Yasuda, and Y. Segawa, *Electronic Lett.*, 1998, **34**, 190.
259. H. Munekata, *Intern. Conf. on Crystal Growth-13, ICCG-13 (Kyoto, Japan, August, 2001)*, 2001.
260. A. van Esch, L. van Bockstal, J. de Boeck, G. Verbanck, A. S. vas Steenbergen, R. J. Wellman, G. Grietens, R. Bogaerts, F. Herlach, and G. Borghs, *Phys. Rev., B*, 1997, **56**, 13103.
261. S. J. Potashnik, K. C. Ku, R. Mahendiran, S. H. Chun, R. F. Wang, N. Samarth, and P. Schiffer, *Phys. Rev., B*, 2002, **66**, 012408.
262. H. Shimizu, T. Hayashi, T. Nishinaga, and M. Tanaka, *Appl. Phys. Lett.*, 1999,**74**, 398.
263. T. Hayashi, Y. Hashimoto, S. Katsumoto, and Y. Iye, *Appl. Phys. Lett.*, 2001, **78**, 1691.
264. D. V. Baxter, D. Ruzmetov, J. Scherschligt, Y. Sasaki, X. Liu, J. K. Furdyna, and C. H. Mielke, *Phys. Rev., B*, 2002, **65**, 212407.
265. T. Hayashi, M. Tanaka, T. Nishinaga, H. Shimoda, H. Tsuchiya, and Y. Otsuka, *J. Cryst. Growth*, 1997, **175**, 1063.
266. Y. Satoh, N. Inoue, Y. Nishikawa, and J. Yoshino, *Proc. 3rd Symp. Physics and Applications of Spin-Related Phenomena in Semiconductors (Sendai, Japan, November 1997)*, Eds H. Ohno, J. Yoshino, and Y. Oka, 1997, p. 23.
267. T. Hayashi, M. Tanaka, T. Nishinaga, and H. Shimada, *J. Appl. Phys.*, 1997, **81**, 4865.
268. T. Hayashi, M. Tanaka, K. Seto, T. Nishinaga, and K. Ando, *Appl. Phys. Lett.*, 1997, **71**, 1825.
269. M. Tanaka, *J. Vac. Sci. Technol. B*, 1998, **16**, 2267.
270. H. Ohno, *J. Magn. Magn. Mater.*, 2004, 272—276, 1.
271. K. Ando, T. Hayashi, M. Tanaka, and A. Twardowski, *J. Appl. Phys.*, 1998, **83**, 65481.
272. H. Ohno, F. Matsukura, T. Owiya, and N. Akiba, *J. Appl. Phys.*, 1999, **85**, 4277.
273. B. Beschoten, P. A. Crowell, I. Malajovich, D. D. Awschalom, F. Matsukura, A. Shen, and H. Ohno, *Phys. Rev. Lett.*, 1999, **83**, 3073.
274. A. Shen, F. Matsukura, S. P. Guo, Y. Sugawara, H. Ohno, M. Tani, A. Abe, and H. C. Liu, *J. Cryst. Growth*, 1999, **201/202**, 379.
275. A. Twardowski, *Mat. Sci. Eng., B*, 1999, **63**, 96.

276. B. Grandidier, J. P. Hys, C. Delerue, D. Stievenard, Y. Higo, and M. Tanaka, *Appl. Phys. Lett.*, 2000, **77**, 4001.
277. R. K. Kawakami, E. Johnson-Halperin, L. F. Chen, M. Hanson, N. Guebels, J. S. Speck, A. C. Gossard, and D. D. Awschalom, *Appl. Phys. Lett.*, 2000, **77**, 2379.
278. D. Chiba, N. Akiba, F. Matsukura, Y. Ohno, and H. Ohno, *Appl. Phys. Lett.*, 2000, **77**, 1873.
279. T. Hayashi, M. Tanaka, and A. Asamitsu, *J. Appl. Phys.*, 2000, **87**, 4673.
280. N. Akiba, D. Chiba, K. Natata, F. Matsukura, Y. Ohno, and H. Ohno, *J. App. Phys.*, 2000, **87**, 6436.
281. Y. Nagai, T. Kurimoto, K. Nagasaka, H. Nojiri, M. Motokawa, F. Matsukura, T. Dietl, and H. Ohno, *Jpn J. Appl. Phys.*, 2001, **40**, 6231.
282. S. J. Potashnik, K. C. Ku, S. H. Chun, J. J. Berry, N. Samarth, and P. Schiffer, *Appl. Phys. Lett.*, 2001, **79**, 1495.
283. G. M. Schott, W. Faschinger, and L. W. Molenkamp, *Appl. Phys. Lett.*, 2001, **79**, 1807.
284. K. M. Yu, W. Walukiewicz, T. Wojtowicz, I. Kuryliszyn, X. Liu, Y. Sasaki, and J. K. Furdyna, *Phys. Rev., B*, 2002, **65**, 201303.
285. J. Masek, J. Kudrnovsky, and F. Maca, *Phys. Rev., B*, 2003, **67**, 153203.
286. T. B. Goennenwein, T. A. Wassner, H. Huebl, M. S. Brandt, J. B. Philipp, M. Opel, R. Gross, A. Koeder, W. Schoch, and A. Waag, *Phys. Rev. Lett.*, 2004, **92**, 227202.
287. E. Ohya, H. Shimizu, Y. Higo, J. Sun, and M. Tanaka, *Jpn J. Appl. Phys.*, 2002, **41**, 24.
288. T. Slupinski, H. Munekata, and A. Oiwa, *Appl. Phys. Lett.*, 2002, **80**, 1592.
289. Th. Hartmann, M. Lampalzer, W. Stolz, K. Megges, L. Lorberth, P. J. Klar, and W. Heimbrodt, *Thin Solid Films*, 2000, **364**, 209.
290. W. Heimbrodt, Th. Hartmann, P. J. Klar, M. Lampalzer, W. Stolz, K. Volz, A. Schaper, W. Treutmann, H.-A. Krug von Nidda, A. Loidl, T. Ruf, and V. F. Sapega, *Physica E*, 2001, **10**, 175.
291. D. Chiba, K. Takamura, F. Matsukura, and H. Ohno, *Appl. Phys. Lett.*, 2003, **82**, 3020.
292. A. M. Nazmul, S. Sugahara, and M. Tanaka, *Phys. Rev., B*, 2003, **67**, 241308.
293. S. Haneda, M. Yamaura, Y. Takatani, K. Hara, S. Harigae, and H. Munekata, *Jpn J. Appl. Phys.*, 2000, **39**, L9.
294. Y. L. Soo, G. Kioseoglou, S. Huang, S. Kim, Y. H. Kao, Y. Takatani, S. Haneda, and H. Munekata, *Phys. Rev., B*, 2001, **63**, 195209.
295. T. Shono, T. Hasegawa, T. Fukumura, F. Matsukura, and H. Ohno, *Appl. Phys. Lett.*, 2000, 77, 1363.
296. N. Theodoropoulou, A. F. Hebard, S. N. G. Chu, M. E. Overgerg, C. R. Abernathy, S. J. Pearton, R. G. Wilson, and J. M. Zavada, *J. Appl. Phys.*, 2002, **91**, 7499.
297. M. E. Overberg, B. P. Gila, G. T. Thaler, C. R. Abernathy, S. J. Pearton, N. Theodoropoulou, K. T. McCarthy, S. B. Arneson, A. F. Hebard, S. N. G. Chu, R. G. Wilson, J. M. Zavada, and Y. D. Park, *J. Vac. Sci. Technol. B*, 2002, **20**, 969.
298. N. Theodoropoulou, A. F. Hebard, M. E. Overberg, C. R. Abernathy, S. J. Pearton, S. N. G. Chu, and R. G. Wilson, *Phys. Rev. Lett.*, 2002, **89**, 107203.
299. M. Zajac, J. Gosk, M. Kaminska, A. Twardowski, T. Szyszko, and S. Podliasko, *Appl. Phys. Lett.*, 2001, **79**, 2432.
300. M. L. Reed, M. K. Ritums, H. H. Stadelmaier, M. J. Reed, C. A. Parker, S. M. Bedair, and N. A. El-Masry, *Mater. Lett.*, 2001, **51**, 500.
301. M. L. Reed, N. A. El-Masry, H. Stadelmaier, M. E. Ritums, N. J. Reed, C. A. Parker, J. C. Roberts, and S. M. Bedair, *Appl. Phys. Lett.*, 2001, **79**, 3473.
302. N. Theodoropoulou, A. F. Hebard, M. E. Overberg, C. R. Abernathy, S. J. Pearton, S. N. G. Chu, R. G. and Wilson, *Appl. Phys. Lett.*, 2001, **78**, 3475.
303. S. Sonoda, S. Shimizu, T. Sasaki, Y. Yamamoto, and H. Hoi, *J. Crystal. Growth*, 2002, **237**, 1358.
304. T. A. Bither and W. H. Cloud, *J. Appl. Phys.*, 1965, **36**, 1501.
305. G. T. Thaler, M. E. Overberg, B. Gila, R. Frazier, C. R. Abernathy, S. J. Pearton, J. S. Lee, S. Y. Lee, Y. D. Park, Z. G. Khim, J. Kim, and F. Ren, *Appl. Phys. Lett.*, 2002, **80**, 3964.
306. Y. L. Soo, G. Kioseouglou, S. Kim, S. Huang, Y. H. Kaa, S. Kubarawa, S. Owa, T. Kondo, and H. Munekata, *Appl. Phys. Lett.*, 2001, **79**, 3926.
307. N. A. Theodoropoulou, A. F. Hebard, S. N. G. Chu, M. E. Overberg, C. R. Abernathy, S. J. Pearton, R. G. Wilson, and J. M. Zavada, *Appl. Phys. Lett.*, 2001, **79**, 3452.
308. S. J. Pearton, M. E. Overberg, G. Thaler, C. R. Abernathy, N. Theodoropoulou, A. F. Hebard, S. N. G. Chu, R. G. Wilson, J. M. Zavada, A. Y. Polyakov, A. Osinsky, and Y. D. Park, *J. Vac. Sci. Technol. A*, 2002, **20**, 583.
309. H. Akinaga, S. Nemeth, J. De Boeck, L. Nistor, H. Bender, G. Borghs, H. Ofuchi, and M. Oshima, *Appl. Phys. Lett.*, 2000, **77**, 4377.
310. M. Hashimoto, Y. K. Zhou, M. Kanamura, and H. Asahi, *Solid State Commun.*, 2002, **122**, 37.
311. S. E. Park, H.-J. Lee, Y. C. Cho, Se-Y. Jeong, C. R. Cho, and S. Cho, *Appl. Phys. Lett.*, 2002, **80**, 4187.
312. T. Endo, T. Slupi´nski, S. Yanagi, A. Oiwa, and H. Munekata, *Extended Abstracts, 7-th Symp. on the Physics and Application of Spin-Related Phenomena in Semiconductors (Yokohama, Japan, December 17—18, 2001)*, 2001, p. 33.
313. M. Yamanouchi, D. Chiba, F. Matsukura, and H. Ohno, *Nature*, 2004, **428**, 539.
314. S. G. Yang, A. B. Pakhomov, S. T. Hung, and C. Y. Wong, *Appl. Phys. Lett.*, 2002, **81**, 2418.
315. S. Y. Wu, H. X. Liu, Lin Gu, R. K. Singh, L. Budd, M. van Schilfgaarde, M. R. McCartney, D. J. Smith, and N. Newman, *Appl. Phys. Lett.*, 2003, **82**, 3047.
316. S. Yanagi, K. Kuga, T. Slupinski, and H. Munekata, *Physica E*, 2004, **20**, 333.
317. G. A. Medvedkin, T. Ishibashi, T. Nishi, and K. Hiyata, *Jpn J. Appl. Phys.*, 2000, **39**, L949.
318. G. A. Medvedkin, K. Hirose, T. Ishibashi, T. Nishi, V. G. Voevodin, and K. Sato, *J. Cryst. Growth*, 2002, **236**, 609.
319. P. G. Baranov, S. I. Goloshchapov, G. A. Medvedkin, and V. G. Voevodin, *Pis´ma v Zhurn. Eksp. Teor. Fiziki*, 2003, **77**, 686 [*JETP Lett.*, 2003, **77**, 582 (Engl. Transl.)].

320. P. G. Baranov, S. I. Goloshchapov, G. A. Medvedkin, S. B. Orlinskii, and V. G. Voevodin, *Physica B*, 2003, **340—342**, 878.
321. S. Cho, S. Choi, G.-B. Cha, S. C. Hong, Y. Kim, Y.-J. Zhao, A. J. Freeman, J. B. Ketterson, B. J. Kim, Y. C. Kim, and B.-C. Choi, *Phys. Rev. Lett*., 2002, **88**, 257203.
322. S. Choi, G. B. Cha, S. C. Hong, S. Cho, Y. Kim, J. B. Ketterson, S.-Y. Jeong, and G. C. Yi, *Solid State Commun*., 2002, **122**, 165.
323. S. J. Pearton, C. R. Abernathy, G. T. Thaler, R. Frazier, F. Ren, A. F. Hebard, Y. D. Park, D. P. Norton, W. Tang, M. Stavola, J. M. Zavada, and R. G. Wilson, *Physica B*, 2003, **340—342**, 39.
324. S. J. Pearton, M. E. Overberg, C. R. Abernathy, N. A. Theodoropoulou, A. F. Hebard, S. N. G. Chu, A. Osinsky, V. Zuflyigin, L. D. Zhu, A. Y. Polyakov, and R. G. Wilson, *J. Appl. Phys*., 2002, **92**, 2047.
325. S. Cho, S. Choi, G.-B. Cha, S. C. Hong, Y. Kim, A. J. Freeman, J. B. Ketterson, Y. Park, and H.-M. Park, *Solid State Commun*., 2004, **129**, 609.
326. K. Sato, G. A. Medvedkin, T. Ishibashi, S. Mitani, K. Takanashi, Y. Ishida, D. D. Sarma, J. Okabayashi, A. Fujimori, T. Kamatani, and H. Akai, *J. Phys. Chem. Solids*, 2003, **64**, 1461.
327. Y. Ishida, D. D. Sarma, K. Okazaki, J. Okabayashi, J. I. Hwang, H. Ott, A. Fujimori, G. A. Medvedkin, T. Ishibashi, and K. Sato, *Phys. Rev. Lett*., 2003, **91**, 107202.
328. T. Hwang, J. H. Shim, and S. Lee, *Appl. Phys. Lett*., 2003, **83**, 1809.
329. V. M. Novotortsev, V. T. Kalinnikov, L. I. Koroleva, R. V. Demin, S. F. Marenkin, T. G. Aminov, G. G. Shabunina, S. V. Boichuk, and V. A. Ivanov, *Zh. Neorg. Khim*., 2005, **50**, Iss. 4 [*Russ. J. Inorg. Chem*., 2005, **50**, Iss. 4 (Engl. Transl.)].
330. S. J. Pearton, Y. D. Park, C. R. Abernathy, M. E. Overberg, G. T. Thaler, J. Kim, F. Ren, J. M. Zavada, and R. G. Wilson, *Thin Solid Films*, 2004, **447—448**, 493.
331. V. N. Prigodin, N. P. Raju, K. I. Pokhodnya, and J. S. Miller, A.J.Epstein *Adv. Mater*., 2002, **14**, 1230.
332. M. A. Reed, C. Zhou, C. J. Muller, T. P. Burgin, and J. M. Tour, *Science*, 1997, **278**, 252.
333. E. G. Emberley and G. Kirczenow, *Chem. Phys*., 2002, **281**, 311.
334. Y. Masumoto, M. Murakami, T. Shono, T. Hasegawa, T. Fukumura, M. Kawasaki, P. Ahmet, T. Chikyow, S. Koshihara, and H. Koinuma, *Science*, 2001, **291**, 854.
335. I.-B. Shim, S.-Y. An, C.-S. Kim, S.-Y. Choi, and Y.-W. Park, *J. Appl. Phys*., 2002, **91**, 7914.
336. S. A. Chambers, S. Thevuthasan, R. F. C. Farrow, R. F. Marks, J. Thiele, L. Folks, M. G. Samant, A. J. Kellock, N. Ruzycki, D. L. Ederer, and U. Diebold, *Appl. Phys. Lett*., 2001, **79**, 3467.
337. R. J. Kennedy and P. Stampe, *Proc. Amer. Phys. Soc. Meeting*, March 18—22, 2002.
338. R. J. Kennedy, P. A. Stampe, E. Hu, P. Xiong, S. von Molnár, and Y. Xin, *Appl. Phys. Lett*., 2004, **84**, 2832.
339. L. A. Balagurov, S. O. Klimonskii, S. P. Kobeleva, A. F. Orlov, N. S. Perov, and D. G. Yarkin, *Pis´ma v Zhurn. Eksp. Teor. Fiziki*, 2004, **79**, 111 [*JETP Lett*., 2004, **79**, 98 (Engl. Transl.)].
340. Z. Wang, W. Wang, J. Tang, L. D. Tung, L. Spinu, and W. Zhou, *Appl. Phys. Lett*., 2003, **83**, 518.
341. N. H. Hong, J. Sakai, and A. Hassini, *Appl. Phys. Lett*., 2004, **84**, 2602.
342. H. Akinaga, M. Mizuguchi, K. Ono, and M. Oshima, *Appl. Phys. Lett*., 2000, **76**, 357.
343. R. Engel-Herbert, J. Mohanty, A. Ney, T. Hesjedal, L. Dãweritz, and K. H. Ploog, *Appl. Phys. Lett*., 2004, **84**, 1132.
344. K. Morita, K. M. Itoh, J. Muto, K. Mizoguchi, N. Usami, Y. Shiraki, and E. E. Haller, *Thin Solid Films*, 2000, **369**, 405.
345. N. R. S. Farley, C. R. Staddon, L. Zhao, K. W. Edmonds, B. L. Gallagher, and D. H. Gregory, *J. Mater. Chem*., 2004, **14**, 1087.
346. K. Ueda, H. Tabata, and T. Kawai, *Appl. Phys. Lett*., 2001, **79**, 988.
347. J. H. Kim, H. Kim, D. Kim, Y. E. Ihm, and W. K. Choo, *Physica B*, 2003, **327**, 304.
348. S. W. Lim, D. K. Hwang, and J. M. Myoung, *Solid State Commun*., 2003, **125**, 231.
349. D. P. Norton, S. J. Pearton, A. F. Hebard, N. Theodoropoulou, L. A. Boatner, and R. G. Wilson, *Appl. Phys. Lett*., 2003, **82**, 239.
350. S. G. Yang, A. B. Pakhomov, S. T. Hung, and C. Y. Wong, *IEEE Trans. Magn*., 2002, **38**, 2877.
351. P. Sharma, A. Gupta, F. J. Owens, K. V. Rao, R. Sharma, R. Ahuja, J. M. O. Guillen, B. Johannson, and G. A. Gehring, *Nature Mater*., 2003, **2**, 673.
352. Y. W. Heo, M. P. Ivill, K. Ip, D. P. Norton, S. J. Pearton, J. G. Kelly, R. Rairigh, A. F. Hubard, and T. Steiner, *Appl. Phys. Lett*., 2004, **84**, 2292.
353. T. Fukumura, Z. Jin, M. Kawasaki, T. Shono, T. Hasegawa, S. Koshihara, and H. Koinuma, *Appl. Phys. Lett*., 2001, **78**, 958.
354. S. Koles´nik, B. Dabrowski, and J. Mais, *J. Supercond*., 2002, **15**, 251.
355. H. Saeki, H. Tabata, and T. Kawai, *Solid State Commun*., 2001, **120**, 439.
356. A. S. Risbud, N. A. Spaldin, Z. Q. Chen, S. Stemmer, and R. Seshadri, *Phys. Rev., B*, 2003, **68**, 205202.
357. Z. Jin, T. Fukumura, M. Kawasaki, K. Ando, H. Saito, T. Sekiguchi, Y. Z. Yoo, M. Murakami, Y. Matsumoto, T. Hasegawa, and H. Koinuma, *Appl. Phys. Lett*., 2001, **78**, 3824.
358. V. A. L. Roy, A. B. Djurišić, H. Liu, X. X. Zvang, Y. H. Leung. M. H. Xie, J. Gao, H. F. Lui, and C. Surya, *Appl. Phys. Lett*., 2004, **84**, 756.
359. P. V. Radovanovic and D. R. Gamelin, *Phys. Rev. Lett*., 2003, **91**,157202.
360. S. Ramachandran, A. Tiwari, and J. Narayan, *Appl. Phys. Lett*., 2004, **84**, 5255.
361. D. A. Schwartz, N. S. Norberg, Q. P. Nguyen, J. M. Parker, and D. R. Gamelin, *J. Am. Chem. Soc*., 2003, **125**, 13205.
362. K. M. Hanif, R. W. Meulenberg, and G. F. Strouse, *J. Am. Chem. Soc*., 2002, **124**, 11495.
363. Y. H. Jeong, S.-J. Han, J.-H. Park, and Y. H. Lee, *J. Magn. Magn. Mater*., 2004, **272—276**, 1976.
364. F. V. Mikulec, M. Kuno, M. Bennati, D. A. Hall, R. G. Griffin, and M. G. Bawendi, *J. Am. Chem. Soc*., 2000, **122**, 2532.

365. J. F. Suyver, S. F. Wuister, J. J. Kelly, and A. Meijerink, *Nano Lett.*, 2001, **1**, 429.
366. D. J. Norris, N. Yao, F. T. Charnock, and T. A. Kennedy, *Nano Lett.*, 2001, **1**, 3.
367. C. A. Stowell, R. J. Wiacek, A. E. Saunders, and B. A. Korgel, *Nano Lett.*, 2003, **3**, 1441.
368. X. Chen, M. Na, M. Cheon, S. Wang, H. Luo, B. D. McCombe, X. Liu, Y. Sasaki, T. Wojtowicz, J. K. Furdyna, S. J. Potashnik, and P. Schiffer, *Appl. Phys. Lett.*, 2002, **81**, 511.
369. S. B. Ogale, R. J. Choudhary, J. P. Buban, S. E. Lofland, S. R. Shinde, S. N. Kale, V. N. Kulkarni, J. Higgins, C. Lanci, J. R. Simpson, N. D. Browning, S. Das Sarma, H. D. Drew, R. L. Greene, and T. Venkatesan, *Phys. Rev. Lett.*, 2003, **91**, 077205.
370. J. De Boeck, W. van Roy, J. Das, V. F. Motsnyi, Z. Liu, L. Lagae, H. Boeve, K. Dessein, and G. Borghs, *Semicond. Sci. Technol.*, 2002, **17**, 342.
371. D. P. Young, D. Hall, M. E. Torelli, Z. Fisk, J. L. Sarrao, J. D. Thompson, H.-R. Ott, S. B. Oseroff, R. G. Goodrich, and R. Zysler, *Nature*, 1999, **397**, 412.
372. H. R. Ott, J. L. Gavilano, B. Ambrosini, P. Vonlanthen, E. Felder, L. Degiorgi, D. P. Young, Z. Fisk, and R. Zysler, *Physica B*, 2000, **281/282**, 423.
373. H. J. Tromp, P. van Gelderen, P. J. Kelly, G. Brocks, and P. A. Bobbert, *Phys. Rev. Lett.*, 2001, **87**, 016401.
374. F. M. Zhang, Y. Zeng, J. Gao, X. C. Liu, X. S. Wu, and Y. W. Du, *J. Magn. Magn. Mater.*, 2004, **282**, 216.
375. H. K. Kim, D. Kwon, J. H. Kim, Y. E. Ihm, D. Kim, H. Kim, J. S. Baek, C. S. Kim, and W. K. Choo, *J. Magn. Magn. Mater.*, 2004, **282**, 244.
376. F. M. Zhang, X. C. Liu, J. Gao, X. S. Wu, Y. W. Du, H. Zhu, J. Q. Xiao, and P. Chen, *Appl. Phys. Lett.*, 2004, **85**, 786.
377. A. Oiwa, Y. Mitsumori, R. Moriya, T. Supinski, and H. Munekata, *Phys. Rev. Lett.*, 2002, **88**, 137202.
378. J. Wang, G. A. Khodaparast, J. Kono, T. Slupinski, A. Oiwa, and H. Munekata, *J. Supercond: Incorporating Novel Magnetism*, 2003, **16**, 373.
379. J. Konig, J. Schlieman, T. Jungwirth, and A. H. MacDonald, in *Electronic Structure and Magnetism of Complex Materials*, Springer Verlag, Berlin, 2002.
380. T. Dietl, F. Matsukura, and H. Ohno, *Phys. Rev., B*, 2002, **66**, 033203.
381. M. Berciu and R. N. Bhatt, *Phys. Rev. Lett.*, 2001, **87**, 107203.
382. Yu. G. Semenov and S. M. Ryabchenko, *Fizika Nizkikh Temperatur*, 2000, **26**, 1197 [Low Temp. Phys., 2000, **26**, 1886 (Engl. Transl.)].
383. V. K. Dugaev, V. I. Litvinov, J. Barnas, and M. Vieira, *Phys. Rev., B*, 2003, **67**, 033201.
384. J. Inoue, S. Nonoyama, and H. Itoh, *Phys. Rev. Lett.*, 2000, **85**, 4610.
385. J. Inoue, S. Nonoyama, and H. Itoh, *Physica E*, 2001, **10**, 170.
386. A. A. Abrikosov and L. P. Gor´kov, *Zhurn. Eksp. Teor. Fiziki*, 1963, **16**, 1575 [*Sov. Phys. J. Exp. Theor. Phys.*, 1963, **16**, 1575 (Engl. Transl.)].
387. S. Sanvito, G. Theurich, and N. Hill, *J. Superconductivity*, 2002, **15**, 85.
388. H. Akai, *Phys. Rev. Lett.*, 1998, **81**, 3002.
389. J. Park, S. Kwon, and B. Min, *Physica B*, 2000, **281/282**, 703.
390. P. Mahadevan and A. Zunger, *Phys. Rev., B*, 2004, **69**, 115211.
391. K. Sato and H. Katayama-Yoshida, *Jpn J. Appl. Phys.*, 2001, **40**, L485.
392. P. Mahadevan and A. Zunger, *Phys. Rev. Lett.*, 2002, **88**, 047205.
393. P. Mahadevan and A. Zunger, *Phys. Rev. Lett.*, 2002, **88**, 159904 — erratum.
394. L. Kronik, M. Jain, and J. R. Chelikowsky, *Phys. Rev., B*, 2002, **66**, 041203-R.
395. M. van Schilfgaarde and O. N. Mryasov, *Phys. Rev., B*, 2001, **63**, 233205.
396. E. Kulatov, H. Nakayama, H. Mariette, H. Ohta, and Y. A. Uspenskii, *Phys. Rev., B*, 2002, **66**, 045203.
397. V. A. Telezhkin and K. B. Tolpygo, *Fizika i Tekhnika Poluprovodnikov*, 1983, **16**, 1137 [*Sov. Phys. Semiconductors*, 1983, **16**, 857 (Engl. Transl.)].
398. S. Fujinaga, *Molecular Orbitals Method*, Ivanami Setan, Tokyo, 1980 (in Japanese) [*Metod molekulyarnykh orbitalej*, Mir, Moscow, 1983, 461 pp. (translated from Japanese)].
399. Yu. M. Kagan and K. A. Kikoin, *Pis´ma v Zhurn. Eksp. Teor. Fiziki*, 1980, **31**, 367 [*Sov. Phys. JETP Lett.*, 1980, **31**, 335 (Engl. Transl.)].
400. A. Zunger, in *Solid State Physics*, Vol. **39**, Eds H. Ehrenreich and D. Turnbull, Academic, Orlando, 1986, p. 276.
401. K. A. Kikoin, *Elektronnye svoistva primesei perekhodnykh metallov v poluprovodnikakh* [*Electronic Properties of Transition Metal Impurities in Semiconductors*], Energoatomizdat, Moscow, 1991, 304 pp. (in Russian).
402. K. A. Kikoin and V. N. Fleurov, *Transition Metal Impurities in Semiconductors*, World Scientific, Singapore, 1994, 360 pp.
403. I. M. Lifshits, *Usp. Fiz. Nauk*, 1963, **83**, 617 [*Sov. Phys. Usp.*, 1963, **6** (Engl. Transl.)].
404. Yu. A. Izyumov and M. V. Medvedev, *Teoriya magnitouporyadochennykh kristallov s primesyami* [*Theory of Magnetically Ordered Doped Crystals*], Nauka, Moscow, 1970, 271 pp. (in Russian).
405. B. I. Shklovskii and A. L. Efros, *Elektronnye svoystva legirovannykh poluprovodnikov* [*Electronic Properties of Doped Semiconductors*], Nauka, Moscow, 1979, 416 pp. (in Russian).
406. I. M. Lifshits, S. A. Gredeskul, and L. A. Pastur, *Vvedenie v teoriyu neuporyadochennykh sistem* [*Introduction to Theory of Disordered Systems*], Nauka, Moscow, 1982, 358 pp. (in Russian).
407. M. Lannoo and J. Bourgoin, *Point Defects in Semiconductors*, Springer-Verlag, Berlin—Heidelberg—New York, 1981.
408. V. A. Ivanov, P. M. Krstajić, F. M. Peeters, V. N. Fleurov, and K. Kikoin, *J. Magn. Magn. Mater.*, 2003, **258—259**, 237.
409. P. M. Krstajić, V. A. Ivanov, F. M. Peeters, V. N. Fleurov, and K. Kikoin, *Europhysics Lett.*, 2003, **61**, 235.
410. P. M. Krstajić, V. A. Ivanov, F. M. Peeters, V. Fleurov, and K. Kikoin, *J. Superconductivity: Incorporating Novel Magnetism*, 2003, **16**, 111.
411. V. A. Ivanov, P. M. Krstajić, F. M. Peeters, V. Fleurov, and K. Kikoin, *Physica B*, 2003, **329**, 1282.

412. V. Fleurov, K. Kikoin, V. A. Ivanov, P. M. Krstajić, and F. M. Peeters, *J. Magn. Magn. Mater.*, 2004, **272—276**, 1967.
413. V. A. Ivanov, V. Fleurov, and K Kikoin; V. M. Novotortsev, T. G. Aminov, S. F. Marenkin, G. G. Shabunina, L. I. Koroleva, and V. T. Kalinnikov; B. A. Aronzon, V. V. Ryl´kov, and S. V. Gudenko, *Proc. 16th National Symp. on Condensed Matter Physics*, SFKM-2004, Eds R. Zikic, Z. V. Popović, M. Damjanović, Z. Radović, Sokobanja (Serbia and Montenegro), September 20—23, 2004, p. 224—227.
414. P. M. Krstajić, F. M. Peeters, V. A. Ivanov, V. Fleurov, and K. Kikoin, *Phys. Rev. B*, 2004, **70**, 195215.
415. B. A. Aronzon, V. V. Ryl´kov, S. V. Gudenko, S. G. Mikhailov, V. Fleurov, K. Kikoin, and V. A. Ivanov, *Materialy nauchnoi konf. ISFTT* [*Proc. Annual ISSSP Scientific Conference*] (*Russian Scientific Center "Kurchatov Institute", Moscow, Russia, March 16—18, 2004*), Moscow, 2004, p. 70 (in Russian).
416. a) S. F. Marenkin, V. M. Novotortsev, T. G. Aminov, V. A. Ivanov; V. Fleurov, K. Kikoin; L. I. Koroleva, V. A. Morozova, R. V. Temin, and R. Szymczak, *14th Intern. Conf. on Crystal Growth ICCG-14, Session "Growth of Magnetic Semiconductors for Spintronics", Book of Abstr.* (*0655*) (*Grenoble, France, 9—13 August 2004*), Grenoble (France), 2004; b) V. Fleurov, V. A. Ivanov, and K. Kikoin, *Frontiers in Condensed Matter, Russia-Israel Conference* (*Shoresh* (*near Jerusalem*), *Tel Aviv, October 19—27, 2003*), p. 110, http://arXiv.org/cond-mat/0311525.
417. *Data in Science and Technology — Semiconductors: Group IV Elements and III-V Compounds*, Ed. O. Madelung, Springer-Verlag, Berlin, 1991, 164 pp.
418. H. Åsklund, L. Ilver, J. Kanski, J. Sadowski, and R. Mathieu, *Phys. Rev., B*, 2002, **66**, 115319.
419. J. Schneider, U. Kaufmann, W. Wilkening, M. Baeumler, and F. Köhl, *Phys. Rev. Lett.*, 1987, **59**, 240.
420. M. Linnarsson, E. Janzen, B. Monemar, M. Kleverman, and A. Thilderkvist, *Phys. Rev., B*, 1997, **55**, 6938.
421. E. J. Singley, K. S. Burch, R. Kawakami, J. Stephens, D. D. Awschalom, and D. N. Basov, *Phys. Rev., B*, 2003, **68**, 165204.
422. T. Graf, M. Gjukic, L. Görgens, O. Ambacher, M. S. Brandt, and M. Stutzmann, *Appl. Phys. Lett.*, 2002, **81**, 5159.
423. V. T. Kalinnikov, Yu. V. Rakitin, and V. M. Novotortsev, *Usp. Khim.*, 2003, **72**, 1123 [*Russ. Chem. Rev.*, 2003, **72**, 995 (Engl. Transl.)].
424. V. F. Sapega, T. Ruf, and M. Cardona, *Phys. Stat. Solidi (b)*, 2001, 226.
425. K. W. Edmonds, K. Y. Wang, R. P. Campion, A. C. Neumann, C. T. Foxon, B. L. Gallagher, and P. C. Main, *Appl. Phys. Lett.*, 2002, **81**, 3010.
426. I. Kuryliszyn, T. Wojtowicz, X. Liu, J. K. Furdyna, W. Dobrowolski, J.-M. Broto, M. Goiran, O. Portugal, H. Rakoto, and B. I. Raquet, *Acta Phys. Pol. A*, 2002, **102**, 659.
427. K. C. Ku, S. J. Potashnik, R. F. Wang, S. H. Chun, P. Schiffer, N. Samarth, M. J. Seong, A. Mascarenhas, E. Johnston-Halperin, R. C. Myers, A. C. Gossard, and D. D. Awschalom, *Appl. Phys. Lett.*, 2003, **82**, 2302.
428. B. Gallagher, *CECAM Workshop: Diluted Magnetic Semiconductors (Lyon, June 12—14 2003)*, Lyon, 2003.
429. K. M. Yu, W. Walukiewicz, T. Wojtowicz, W. L. Lim, X. Liu, Y. Sasaki, M. Dobrowolska, and J. K. Furdyna, *Appl. Phys. Lett.*, 2002, **81**, 5.
430. S. Sonoda, S. Shimizu, T. Sasaki, Y. Yamamoto, and H. Hori, *J. Appl. Phys.*, 2002, **91**, 7911.
431. T. Okuno, T. Fujino, M. Shindo, M. Katayama, K. Oura, S. Sonoda, and S. Shimizu, *Jpn J. Appl. Phys.*, 2002, **41**, L415.
432. M. Sato, H. Tanida, K. Kato, T. Sasaki, Y. Yamamoto, S. Sonoda, S. Shimizu, and H. Hori, *Jpn J. Appl. Phys.*, 2002, **41**, 4513
433. H. Hori, S. Sonoda, T. Sasaki, Y. Yamamoto, S. Shimizu, K. Suga, and K. Kindo, *Physica B*, 2002, **324**, 142.
434. I. Ya. Korenblit and E. F. Shender, *Usp. Fiz. Nauk*, 1978, **126**, 233 [*Sov. Phys. Usp.*, 1978, **21**, 832 (Engl. Transl.)].
435. Y.-J. Zhao, W. T. Geng, A. J. Freeman, and T. Oguchi, *Phys. Rev. B*, 2001, **63**, 201202.
436. Y.-J. Zhao, S. Picozzi, A. Continenza, W. T. Geng, and A. J. Freeman, *Phys. Rev., B*, 2002, **65**, 094415.
437. S. Cho, S. Choi, S.-C. Hong, Y. Kim, J. B. Ketterson, B.-J. Kim, Y. C. Kim, and J.-H. Jung, *Phys. Rev., B*, 2002, **66**, 033303.
438. A. Stroppa, S. Picozzi, A. Continenza, and A. J. Freeman, *Phys. Rev., B*, 2003, **68**, 155203.
439. N. Bloembergen and T. J. Rowland, *Phys. Rev.*, 1955, **97**, 1679.
440. G. Bouzerar, *Phys. Rev. Lett.*, 2004, **92**, 069701.
441. V. I. Litvinov and V. K. Dugaev, *Phys. Rev. Lett.*, 2004, **92**, 069702.
442. E. Z. Meilikhov, *Zhurn. Eksp. Teor. Fiziki*, 2003, **124**, 650 [*J. Exp. Theor. Phys.*, 2003, **97**, 587 (Engl. Transl.)].
443. E. Z. Meilikhov and R. Z. Farzetdinova, *Zhurn. Eksp. Teor. Fiziki*, 2004, **125**, 1367 [*J. Exp. Theor. Phys.*, 2004, **98**, 1198 (Engl. Transl.)].

Received August 30th, 2004